

REGULATION OF GLUCOSE HOMEOSTASIS BY DOC2B AND MUNC18  
PROTEINS

Latha Ramalingam

Submitted to the faculty of the University Graduate School  
in partial fulfillment of the requirements  
for the degree  
Doctor of Philosophy  
in the Department of Biochemistry & Molecular Biology,  
Indiana University

January 2014

Accepted by the Graduate Faculty, of Indiana University, in partial fulfillment of the requirements for the degree of Doctor of Philosophy.

Doctoral Committee

---

Debbie C. Thurmond, Ph.D., Chair

---

Jeffrey S. Elmendorf, Ph.D.

November 22, 2013

---

Raghavendra G. Mirmira, M.D., Ph.D.

---

Peter J. Roach, Ph.D.

## **DEDICATION**

I dedicate this dissertation to my parents. Without their love and encouragement I would never have reached this point.

## ACKNOWLEDGEMENTS

I would first like to thank my advisor, Dr. Debbie Thurmond, for providing a conducive research environment that enabled me to carry out and successfully complete my dissertation with critical thinking. It has been an absolute pleasure working in her laboratory. She is a great role model for women mentors. I thank all the current and former members of the Thurmond lab. In particular, I would like to thank Dr Jenna Jewell, Dr Erica Daniel and Dr Mike Kalwat for their mentoring and friendship. I would also like to thank Dr Eunjin Oh, Dr Zhanxiang Wang and Dr Stephanie Yoder for their help with my project, cheerful and engaging conversations in the laboratory and supporting me throughout my graduate work. They were great wonderful colleagues to work with. I would also like to thank Deepthi for her immense support both inside and outside of the lab and for being there for me at all times.

I thank the members of my thesis committee, Dr Jeffrey Elmendorf, Dr Raghu Mirmira and Dr Peter Roach. They have provided useful suggestions and ideas that benefited my project greatly. I am also incredibly grateful to all the members of the Wells Diabetic Center for all the fun conversations and reagents, in particular Yi-Chun Chen. I would like to thank the islet isolation core for their meticulous work to isolate islets. I would take many great memories from my time in graduate school.

I consider myself fortunate to have made good friends in Indianapolis who have supported me through the ups and downs of this journey. Chandra, Rakesh and Vinay

have been like a family to me, here in Indianapolis. They have helped me mould my character during my stay. Abhirami, Jyothi, Halesha and Aarthi were of great support and I will miss all the happier times spent together and I will cherish their friendships and these memories lifelong. I would like to thank my mom and dad who have always given me unrelenting encouragement and love. I owe my success to them. They have always pushed me to reach my full potential. I would also thank my brother for still not disowning me. Finally, I would also like to thank my husband, Naveen for his help with editing my manuscripts and I am excited to embark on the next chapter of my life together.

Latha Ramalingam

REGULATION OF GLUCOSE HOMEOSTASIS BY DOC2B AND MUNC18  
PROTEINS

Glucose homeostasis is maintained through the coordinated actions of insulin secretion from pancreatic beta cells and insulin action in peripheral tissues. Dysfunction of insulin action yields insulin resistance, and when coupled with altered insulin secretion, results in type 2 diabetes (T2D). Exocytosis of intracellular vesicles, such as insulin granules and glucose transporter (GLUT4) vesicles is carried out by similar SNARE (soluble NSF attachment receptor) protein isoforms and Munc18 proteins. An additional regulatory protein, Doc2b, was implicated in the regulation of these particular exocytosis events in clonal cell lines, but relevance of Doc2b in the maintenance of whole body glucose homeostasis *in vivo* remained unknown. The objective of my doctoral work was to delineate the mechanisms underlying regulation of insulin secretion and glucose uptake by Doc2b in effort to identify new therapeutic targets within these processes for the prevention and/or treatment of T2D. Towards this, mice deficient in Doc2b (Doc2b<sup>-/-</sup> knockout mice) were assessed for *in vivo* alterations in glucose homeostasis. Doc2b knockout mice were highly susceptible to preclinical T2D, exhibiting significant whole-body glucose intolerance related to insulin secretion insufficiency as well as peripheral insulin resistance. These phenotypic defects were accounted for by defects in assembly of SNARE complexes. Having determined that Doc2b was required in the control over whole body glycemia *in vivo*, whether Doc2b is also limiting for these mechanisms *in vivo* was examined. To study this, novel Doc2b transgenic (Tg) mice were engineered to express ~3 fold more Doc2b exclusively in pancreas, skeletal muscle and fat tissues.

Compared to normal littermate mice, Doc2b Tg mice had improved glucose tolerance, related to concurrent enhancements in insulin secretion from beta cells and insulin-stimulated glucose uptake in the skeletal muscle. At the molecular level, Doc2b overexpression promoted SNARE complex assembly, increasing exocytotic capacities in both cellular processes. These results unveiled the concept that intentional elevation of Doc2b could provide a means of mitigating two primary aberrations underlying T2D development.

Debbie C. Thurmond, PhD, Chair

## TABLE OF CONTENTS

<b>LIST OF TABLES</b>	x
<b>LIST OF FIGURES</b>	xi
<b>LIST OF ABBREVIATIONS</b>	xiv
<b>CHAPTER 1. INTRODUCTION</b>	1
1.1 SUMMARY	2
1.2 OVERVIEW OF DIABETES	2
1.2.1 The Physiology of Glucose Homeostasis	4
1.3 INSULIN GRANULE EXOCYTOSIS	7
1.3.1 Pancreatic Islets	7
1.3.2 Biphasic Insulin Secretion	8
1.3.3 Stimulus-Secretion Coupling and Insulin Exocytosis in the Beta Cell	9
1.4 GLUT4 VESICLE EXOCYTOSIS	11
1.4.1 The Insulin Receptor	11
1.4.2 Insulin Receptor Substrates and Signalling in Fat and Skeletal Muscle	12
1.5 SNARE PROTEINS INVOLVED IN EXOCYTOSIS	16
1.5.1 SNARE Protein Abundances and Diabetes	18
1.5.2 SNARE Core Complex Assembly	18
1.5.3 Syntaxins	20
1.5.4 Syntaxin 1	21
1.5.5 Syntaxins 2 and 3	22
1.5.6 Syntaxin 4	22
1.5.7 SNAP	24
1.5.8 VAMP2	24
1.6 SNARE ACCESSORY PROTEINS	25
1.6.1 Munc18 proteins	25
1.6.2 Munc18-1	26
1.6.3 Munc18c	27
1.6.4 Munc13	29
1.6.5 Doc2 proteins	31
1.6.6 Doc2b	33
1.7 RATIONALE	35
<b>CHAPTER 2. MATERIALS AND METHODS</b>	36
2.1 MATERIALS	37
2.2 ANIMALS	37
2.3 METHODS	42
2.3.1 Tissue Homogenization	42
2.3.2 Islet RNA Isolation and Quantitative-PCR	43
2.3.3 Intraperitoneal Glucose Tolerance Test and Insulin Tolerance Test	43
2.3.4 Skeletal Muscle Subcellular Fractionation	44
2.3.5 <i>In Vitro</i> Skeletal Muscle Glucose Uptake	45
2.3.6 Isolation, Culture and Perfusion of Mouse Islets	45
2.3.7 Cell Culture and Transient Transfection	46



2.3.8 Subcellular Fractionation of MIN6 Beta Cells	47
2.3.9 Co-immunoprecipitation	48
2.3.10 Recombinant Proteins and Interaction Assays	48
2.3.11 Statistical Analysis	49
<b>CHAPTER 3. DOC2B IS A KEY EFFECTOR OF INSULIN SECRETION AND SKELETAL MUSCLE INSULIN SENSITIVITY</b>	50
3.1 INTRODUCTION	51
3.2 RESULTS	52
3.2.1 Doc2b Knockout Mice are Glucose Intolerant	52
3.2.2 Impaired Biphasic Insulin Secretion in Islets Isolated from Doc2b Knockout Mice	61
3.2.3 Impaired Insulin Sensitivity, and Skeletal Muscle Glucose Uptake and GLUT4 Translocation in Doc2b Knockout Mice	67
3.2.4 Altered SM and SNARE Complex Formations in Skeletal Muscle of the Doc2b Knockout Mice	71
3.3 DISCUSSION	79
3.3.1 Mechanism(s) of Doc2b-Dependent Insulin Granule and GLUT4 vesicle fusion events	81
3.4 CONCLUSIONS	84
<b>CHAPTER 4. DOC2B ENRICHMENT ENHANCES GLUCOSE HOMEOSTASIS VIA POTENTIATION OF INSULIN SECRETION AND PERIPHERAL INSULIN SENSITIVITY</b>	85
4.1 INTRODUCTION	86
4.2 RESULTS	87
4.2.1 Improved Glucose Tolerance in Doc2b Enriched Mice	90
4.2.2 Doc2b Enrichment Potentiates Biphasic GSIS.	94
4.2.3 Doc2b Tg Mice have Enhanced Insulin Sensitivity and cell Surface GLUT4 accumulation in Skeletal Muscle	94
4.2.4 Doc2b Enrichment Promotes SNARE Complex Formation in Beta Cells and Skeletal Myoblasts.	98
4.3 DISCUSSION	103
<b>CHAPTER 5. CONCLUDING REMARKS</b>	109
5.1 FUTURE STUDIES	113
5.1.1 Post-translational modifications and SNARE complex formation	113
5.1.2 Regulation of Doc2b by calcium	116
5.1.3 Abundances of Doc2b and SNARE proteins.	118
5.1.4 Doc2b in whole body physiology and SNARE proteins as therapies	119
5.2 CONCLUSION	121
<b>APPENDIX: PERMISSION TO REPRODUCE PREVIOUSLY PUBLISHED MATERIAL</b>	122
<b>REFERENCES</b>	125
<b>CURRICULUM VITAE</b>	

## LIST OF TABLES

Table 2-1	List of antibodies used	38
Table 3-1	Fasting serum analytes of Doc2b <sup>+/+</sup> , Doc2b <sup>+/-</sup> and Doc2b <sup>-/-</sup> mice	59
Table 3-2	Tissue weights normalized to body weight of Doc2b <sup>+/+</sup> , Doc2b <sup>+/-</sup> and Doc2b <sup>-/-</sup> mice	60
Table 3-3	Tissue weights of Doc2b <sup>+/+</sup> , Doc2b <sup>+/-</sup> and Doc2b <sup>-/-</sup> mice	66
Table 4-1	Tissue weights of Doc2b Tg and Wt mice	93

## LIST OF FIGURES

Figure 1-1	Stimulus-secretion coupling in the beta cell	10
Figure 1-2	Schematic representation of the major features of IR	13
Figure 1-3	GLUT4 translocation in muscle/adipose	15
Figure 1-4	The switch hypothesis model	30
Figure 1-5	Doc2b functions as a scaffold for Munc18-1 and Munc18c	32
Figure 2-1	Linear sequence schematic of Doc2b myc his and genotyping analysis of Doc2b Transgenic mice	41
Figure 3-1	mRNA expression in glucose homeostatic tissues from Doc2b <sup>+/-</sup> and Doc2b <sup>-/-</sup> knockout mice	53
Figure 3-2	Protein expression in islets from Doc2b <sup>+/-</sup> and Doc2b <sup>-/-</sup> knockout mice	55
Figure 3-3	Protein expression in glucose homeostatic tissues from Doc2b <sup>+/-</sup> and Doc2b <sup>-/-</sup> knockout mice	56
Figure 3-4	Doc2b <sup>+/-</sup> and Doc2b <sup>-/-</sup> knockout mice are glucose intolerant	57
Figure 3-5	Doc2b <sup>+/-</sup> and Doc2b <sup>-/-</sup> knockout mice are glucose intolerant after 6 hours fast.	58
Figure 3-6	Doc2b <sup>+/-</sup> and Doc2b <sup>-/-</sup> knockout mice have reduced serum insulin concentration post-glucose injection	62
Figure 3-7	Doc2b <sup>+/-</sup> and Doc2b <sup>-/-</sup> knockout mouse islets show reduced biphasic insulin release	63
Figure 3-8	Doc2b <sup>+/-</sup> and Doc2b <sup>-/-</sup> knockout mouse islets show reduced	

	Insulin release in response to Kcl stimulation	65
Figure 3-9	Impaired insulin sensitivity in Doc2b-deficient mice	68
Figure 3-10	Impaired insulin stimulated GLUT4 translocation in skeletal muscle of Doc2b-deficient mice	69
Figure 3-11	Impaired glucose uptake in Doc2b deficient mice	70
Figure 3-12	No alterations in proximal insulin signaling in Doc2b deficient mice	72
Figure 3-13	Insulin-dependent but calcium-independent Doc2b-Munc18c association in mouse skeletal muscle	73
Figure 3-14	Glucose-dependent but calcium-independent Doc2b-Munc18c association in MIN6 beta cells	74
Figure 3-15	Calcium-independent SNARE-Munc18c association in mouse skeletal muscle	75
Figure 3-16	Absence of Syntaxin 4-Doc2b association in mouse skeletal muscle	77
Figure 3-17	Munc18c-Syntaxin 4 binding is increased in Doc2b <sup>-/-</sup> mouse skeletal muscle	78
Figure 3-18	Munc18c-Syntaxin 4 binding is increased in Doc2b <sup>-/-</sup> mouse skeletal muscle	80
Figure 4-1	Protein expression in tissues of Doc2b transgenic mice	88
Figure 4-2	Protein expression in islets and tissues of Doc2b transgenic mice	89
Figure 4-3	Doc2b Tg mice have enhanced glucose tolerance	91

Figure 4-4	Tetracycline-mediated repression of the Doc2b transgene reduces glucose tolerance to that of the Wt mice	92
Figure 4-5	Islets from Doc2b Tg mice exhibit potentiated biphasic insulin release	95
Figure 4-6	Doc2b Tg mice exhibit enhanced insulin sensitivity	96
Figure 4-7	Doc2b Tg mice show increased insulin-stimulated GLUT4 accumulation at the plasma membrane of skeletal muscle	98
Figure 4-8	Overexpression of Doc2b increases the abundance of SNARE complexes in the PM of MIN6 beta cells	100
Figure 4-9	Overexpression of Doc2b co-ordinately decreases Munc18c-Syntaxin 4 binding while increasing Syntaxin 4 activation in L6 GLUT4-myc myoblasts	101

## LIST OF ABBREVIATIONS

ADA	American Diabetes Association
ADP	Adenosine Diphosphate
APS	Associated Protein Substrate
AS160	Akt Substrate of 160 kDa
ATP	Adenosine Triphosphate
BSA	Bovine Serum Albumin
CAP	Cbl Adapter Protein
CDK	Cyclin Dependent Kinase
Doc2a	Double C2 Domain Protein alpha
Doc2b	Double C2 Domain Protein beta
Doc2g	Double C2 Domain Protein gamma
DMEM	Dulbecco's Modified Eagle's Medium
ECL	Enhanced Chemiluminescence
EGFP	Enhanced Green Fluorescent Protein
ER	Endoplasmic Reticulum
FBS	Fetal Bovine Serum
FRET	Fluorescence resonance energy transfer
GK	Goto-Kakizaki Rats
GLUT	Glucose Transporter
GSIS	Glucose-Stimulated Insulin Secretion
GST	Glutathione S-transferase Fusion Protein

GSV	GLUT4 Storage Vesicle
GWAS	Genome-Wide Association study
HFD	High Fat Study
HGO	Hepatic glucose transport
IB	Immunoblot
IGT	Impaired Glucose Tolerance
IP	Immunoprecipitation
IPGTT	Intraperitoneal Glucose Tolerance Test
IR	Insulin Receptor
IRS	Insulin Receptor Substrate
ITT	Insulin Tolerance Test
K <sub>ATP</sub>	ATP-Dependent Potassium
MIN6	Mouse Insulinoma Cell Line
MKRBB	Modified Kreb's Ringer Bicarbonate Buffer
MODY	Maturity onset diabetes of the youth
NEFA	Non-esterified Fatty Acids
NP40	Non-ionic P-40 Detergent
PBS	Phosphate Buffer Saline
PCR	Polymerase Chain Reaction
PDK-1	Phosphoinositide-dependent kinase-1 (PDK-1)
PI3K	Phosphatidylinositide Kinase
PKB	Protein Kinase B
PM	Plasma Membrane

PMSF	Phenylmethylsulfonylfluoride
PVDF	Polyvinylidene difluoride
RIA	Radioimmunoassay
RRP	Readily Releasable Pool
SDS-PAGE	Sodium Dodecylsulfate Polyacrylamide Gel Electrophoresis
Ser	Serine
SG	Secretory Granule
SH2	Src Homology 2 Domains
SM	Sec-1/Munc
SNAP	Synaptosome Associated Protein
SNARE	Soluble N-ethylmaleimide Sensitive Factor Attachment Protein Receptor
Syn 1	Syntaxin 1 Protein
Syn 3	Syntaxin 1 Protein
Syn 4	Syntaxin 4 Protein
T2D	Type 2 Diabetes
Tet	Tetracycline
Tg	Transgenic
Thr	Threonine
TIRF	Total Internal Reflection Fluorescence
Tyr	Tyrosine
t-SNARE	Target SNARE
VAMP	Vesicle Associated Membrane Protein
VDCC	Voltage-Dependent Calcium Channel



v-SNARE      Vesicle SNARE

Wt            Wild Type

## CHAPTER 1. INTRODUCTION

**Portion of the text in this chapter is reproduced from:**

Ramalingam L., Oh E., and Thurmond DC. (2013) Novel roles for insulin receptor (IR) in adipocytes and skeletal muscle cells via new and unexpected substrates. *Cell Mol Life Sci* 70, 2815-2834.

## **1.1 SUMMARY**

This introductory chapter presents an overview of insulin secretion and insulin action at the physiological level, and then progresses to an explain them at the cellular level within the pancreatic beta cells and insulin responsive cells. The SNARE and their accessory proteins involved in the exocytotic processes are discussed in detail. Towards the end of the chapter, Doc2b is emphasized, along with the context for the rationale of my dissertation work. Chapter 2 provides a detailed description of the materials and methods. Chapter 3 discusses the data generated from the Doc2b knockout mouse model. Chapter 4 addresses the role of Doc2b as a limiting factor in glucose homeostasis using Doc2b over-expressing transgenic model. Finally, chapter 5 summarizes these studies and suggests ideas for the future course of research. The overall goal of this dissertation is to improve our understanding of the molecular mechanisms by which Doc2b facilitate regulated exocytosis in insulin-secreting and insulin-responsive cell types to control glucose homeostasis.

## **1.2 OVERVIEW OF DIABETES**

Diabetes is a worldwide epidemic, with prevalence of diabetes mellitus growing at an exponential rate. The American Diabetes Association (ADA) estimates around 25 million Americans to be afflicted with diabetes currently, with type 2 diabetes (T2D) accounting for 85-90% of the cases; an additional 56 million have pre-type 2 diabetes. The remaining 15% of diabetes cases is split into type 1 diabetes (5-10%), gestational (1-2%) and other types of diabetes resulting from specific genetic conditions, such as maturity-onset diabetes of young (MODY); pancreatic disease; and other illness (1-5%).

The World Health Organization (WHO) estimates that the diabetic population is likely to reach 366 million by 2030 (1). The total annual cost of diabetes to the United States of America is estimated to be around \$245 billion, with 1 out of every 5 dollars spent on healthcare being spent on diabetes care (ADA 2012). Data released by the WHO indicates diabetes to be most prevalent in India, China, and United States of America, highlighting that diabetes is a worldwide health crisis.

Diabetes is classified into three types: type 1, type 2 and gestational diabetes. Type 1 diabetes, also known as insulin-dependent or juvenile diabetes, is an autoimmune disorder where pancreatic beta cells are destroyed, and therefore the affected individual is unable to produce insulin. T2D is a complex polygenic disease that occurs when a combination of defects in insulin secretion and insulin action occur. T2D is one of the leading causes of cardiovascular disease, renal failure, blindness, and peripheral nerve damage. When left untreated or poorly controlled, T2D eventually leads to life-threatening complications (UKPDS 2003). Pre-type 2 diabetes (hereafter referred to as 'prediabetes') is characterized by impaired glucose tolerance, which is a metabolic condition in which an individual's blood glucose values are elevated above normal levels, but are less than that of the established levels for diagnosing T2D. This is the intermediate state in the transition of glucose tolerance between normal glucose homeostasis and overt T2D. Prediabetes is associated with insulin resistance and progressive failure in beta cell secretory function, which over time results in the development of T2D. Prediabetic patients are at a high risk of progressing to T2D, with 11% of people with prediabetes progressing to T2D every year. About 50% people with

prediabetes develop T2D within 10 years if no lifestyle changes or pharmaceutical interventions are incorporated (HHS 2003). The third major form of diabetes mellitus, gestational diabetes, occurs during pregnancy. The precise mechanism is unknown; it is believed that the hormones produced during pregnancy interfere with the action of insulin as it binds the insulin receptor (IR). The interference probably occurs at the level of the cell signaling downstream of the IR. Mothers who are diagnosed with gestational diabetes have a 35 to 60% chance of developing T2D later in life (CDC 2011). Several other forms of diabetes are associated with specific genetic defects in beta cell function; MODY is characterized by impaired insulin secretion with minimal or no defects in insulin action. Unusual cases of diabetes result from genetically determined abnormalities of insulin action. Leprechaunism and Rabson-Mendenhall syndrome are two pediatric syndromes that have mutations in the insulin receptor gene with subsequent alterations in insulin receptor function. Excess glucagon causes glucagonoma, excess norepinephrine causes pheochromocytoma can cause diabetes. Any process that diffusely injures the pancreas can cause diabetes. Acquired processes include pancreatitis, trauma, infection and pancreatic carcinoma.

### **1.2.1 The Physiology of Glucose Homeostasis**

The regulation of blood glucose is achieved predominantly by the counter regulation of two hormones, insulin and glucagon. Insulin and glucagon are secreted by the beta and alpha cells, respectively, of the pancreatic islets which respond to glucose either through release or inhibition of the respective hormones. In the fasting state, when blood glucose levels are low, the insulin to glucagon ratio is low. The low glucose and

insulin levels cause glucagon release, which in turn promotes gluconeogenesis and glycogenolysis in the liver, leading to glucose release from the liver. The liver produces glucose by utilizing amino acids and this maintains endogenous blood glucose levels to prevent hypoglycemia during fasting. In the fed state, when the blood glucose levels are high, the insulin to glucagon ratio is high, because elevated glucose stimulates insulin secretion from the beta cells, and also inhibits glucagon secretion from the alpha cells. Insulin secreted from the pancreas travels first to the liver through the hepatic portal vein, thereby impeding hepatic glucose production/output (HGO) by inhibiting gluconeogenesis and glycogenolysis (2). During this process, the liver takes up or degrades nearly half of the secreted insulin (3). Insulin also inhibits HGO indirectly by inhibiting lipolysis in adipose tissue and amino acid release from muscle. The secreted insulin that survives degradation in the liver promotes glucose uptake in the peripheral tissues, including muscle and adipose. Glucose disappearance from the blood following glucose challenge or meal is the result of the combination of glucose uptake into the peripheral tissues and suppression of HGO in the liver.

The underlying cause of T2D is still under debate; it is not clear whether deficits in insulin secretion and increased insulin resistance occur in parallel or if one is the primary cause of the other. The general assumption in the field for many years has been that insulin resistance develops first, preceding the manifestation of T2D, given that the majority of the individuals are obese and highly insulin resistant. This rise in insulin resistance requires the beta cells to compensate by increasing their mass and insulin secretion to maintain normoglycemia. Eventually, the beta cells fail, leading to decreased

insulin secretion and loss of beta cell mass, thereby resulting in T2D. In T2D, the response of alpha cells to glucose (inhibition of glucagon secretion) is blunted, which likely contributes to elevated blood glucose levels in the disease (4). A dominant theory in the field has specified that the ability of the beta cells to mount a compensatory response determines if an individual will progress to T2D (5). However, only ~one-third of obese and insulin resistant individuals develop diabetes (6). In addition, approximately 12% of individuals developing T2D are lean, not obese, having no prior history of insulin resistance (7). Even individuals with genetic risk factors that are linked to beta cell dysfunction can avoid developing diabetes as long as they remain metabolically healthy (5). Thus, while it is clear that beta cell dysfunction is both necessary and sufficient to cause T2D, even in the absence of insulin resistance (8), there is evidence that insulin resistance is necessary but not sufficient to cause diabetes.

Substantial beta cell failure occurs at an early stage in disease progression, even before the disease is diagnosed (9). Both beta cell mass and function start to decline before the onset of hyperglycemia, and decrease by 40-65% by the time patients are diagnosed with T2D (10). Beta cell dysfunction occurs in genetically predisposed individuals with normal glucose tolerance well before the emergence of T2D (11). For example, glucose-stimulated insulin release was reduced among first degree relatives of Caucasian diabetic patients when compared to control individuals matched for age, sex, weight and insulin sensitivity (12). Some of these individuals are reportedly hyperinsulinemic prior to presenting with insulin resistance (12-13). Such hypersecretion of insulin in the absence of stimulatory fuel prompts hypoglycemia, and is counteracted

by increased food consumption. The increased food intake promotes increased fat storage and insulin resistance. Alternatively, systemic hyperinsulinemia reportedly reduces the number and sensitivity of IR present in liver and adipocytes, leading to insulin resistance (14). Moreover, transgenic mice over-expressing the insulin gene developed insulin resistance secondary to hyperinsulinemia. Also supporting the argument that beta cell dysfunction may precede insulin resistance, gene expression analyses of T2D islets identified changes in expression of genes that are important for beta cell function (15). Importantly, subsequent genome wide association studies linked a majority of the genes associated with T2D to beta cell function (16). As such, accumulating evidence suggests beta cell hyperinsulinemia to be a likely initiating event in the development of T2D, and that efforts to determining the cause(s) and mechanism of basal hyperinsulinemia could help identify a possible cure (8).

### **1.3 INSULIN GRANULE EXOCYTOSIS**

#### **1.3.1 Pancreatic Islets**

The pancreas is composed of an exocrine component, which releases digestive enzymes, and an endocrine component, representing 1-5% of the total pancreatic mass and consisting of highly structured clusters of cells, named the Islets of Langerhans (17). Islets contain different groups of cells of which the beta cells, which secrete insulin, comprise the majority, ~70-80%, of the total islet mass. Islets are composed of 15-20% of alpha cells that secrete glucagon to oppose the actions of insulin (18). Delta, epsilon, and PP cells make up the remaining 5-15%, secreting somatostatin, ghrelin, and pancreatic



polypeptide, respectively (19). The majority of this dissertation will focus on the insulin secreting beta cells.

### **1.3.2 Biphasic Insulin Secretion**

Under experimental *in vivo* conditions with administration of glucose intravenously, a biphasic insulin release profile is observed with a rapid acute phase followed by a slow sustained phase similar to the *in vitro* profile (20-21). Physiologically, first-phase insulin release inhibits gluconeogenesis and glycogenolysis, thereby suppressing hepatic glucose output from the liver (2). The sustained second-phase of insulin secretion plays a predominant role in glucose uptake in the peripheral tissues.

The beta cell contains around 10,000 insulin secretory granules, purported to exist as two separate pools: the readily releasable pool (RRP), and the reserve pool. These distinct pools are suggested to underlie the separable two different phases of biphasic insulin secretion, as first described in 1960 (22-24). The RRP accounts for less than 5% of the total number of insulin granules and until very recently was assumed to be responsible for the first-phase insulin release, given corroborating data suggesting these granules to be morphologically docked. However, results obtained using total internal reflection fluorescence (TIRF) microscopy in the last few years suggests that granules not necessarily predocked can contribute to the insulin release during the first-phase (25). First-phase insulin release is elicited by glucose, arginine and non-fuel secretagogues such as potassium chloride peaking within 2-5 minutes and completed within 10 minutes from the time of initiation. The rate of insulin release is approximated at ~15 granules per

minute, accounting for a total of 60–120 granules released during the first-phase (26). The reserve pool accounts for 95% of the mass of mature insulin granules, is located deeper within the cell (>50-100 microns from the PM), and is responsible for sustaining insulin release during the more prolonged second-phase. Only fuel secretagogues such as glucose can elicit second-phase insulin release (27), which is less robust than first-phase but persists as long as the glucose stimulus is present. The rate of insulin release during the second-phase is ~5 granules per minute, such that ~600 granules are utilized from the reserve pool when the second-phase persists over 120 minutes (25, 28-29); notably, this is still less than 10% of the total 10,000 granules predicted to be in a given beta cell, showing that each beta cell has an extensive capacity to secrete insulin.

### **1.3.3 Stimulus-Secretion Coupling and Insulin Exocytosis in the Beta Cell**

The beta cell is an electrically excitable cell type that has both glucose sensing and insulin exocytosis functions, allowing it to sense changes in blood glucose and appropriately respond by releasing insulin. As depicted in Fig. 1-1, glucose sensing arises from the presence of glucose transporter 2 (GLUT2) receptors present on the PM (30), increasing the flux of glucose into the beta cell by passive diffusion through these cell surface receptors; recent study suggests that human islet beta cells also use GLUT1 transporters (31). GLUT2 has a relatively low affinity ( $K_m \sim 30$  mM) for glucose and is constitutively active and the principal isoform in rodents. Glucose transporter 1 (GLUT1) is the predominant glucose transporter present in human beta cells ( $k_m \sim 6$  mM), given the glucose levels in humans are maintained between 3.6 mM (after a prolonged fast) to 7 mM (after a meal).

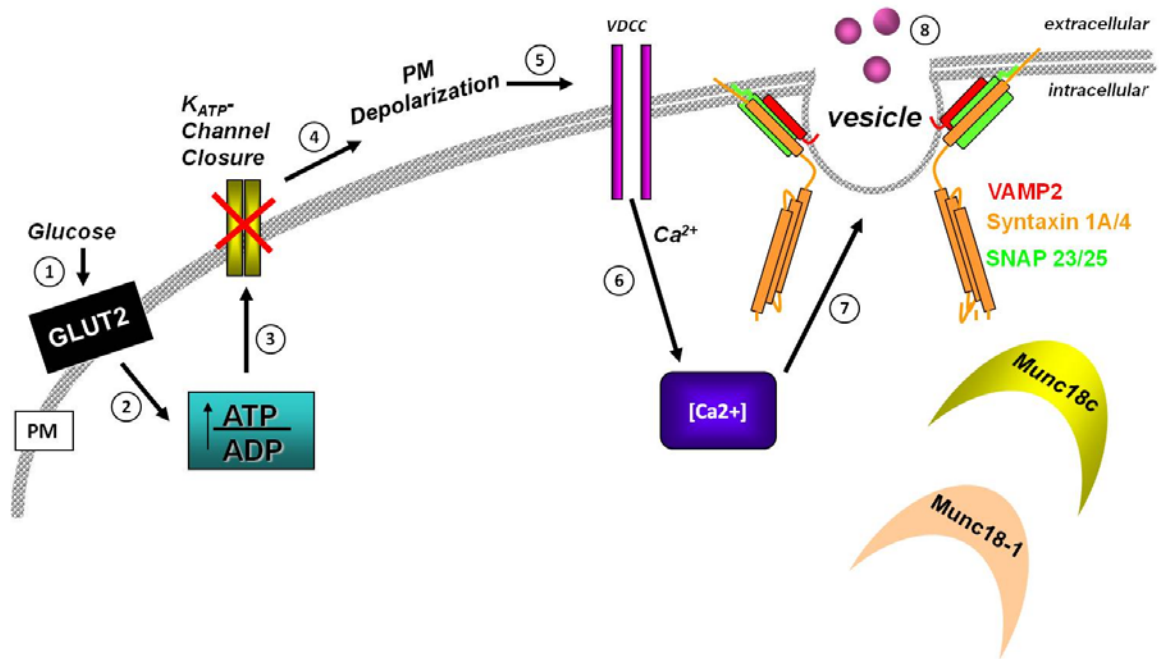


**Figure 1-1. Stimulus-secretion coupling in the beta cell.** Steps 1-3) Glucose enters the cell through the GLUT2 transporter and is metabolized, which increases the ATP: ADP ratio, resulting in closure of the KATP sensitive channels. Steps 4-6) Channel closure leads to PM depolarization, voltage dependent calcium channel (VDCC) opening and influx of calcium into the cell. Step 7) Through an incompletely understood mechanism(s), calcium entry triggers SNARE protein mediated vesicle fusion to facilitate insulin release. [Adapted from (32)].

Upon entry into the cell, glucose is rapidly phosphorylated by the enzyme glucokinase, yielding glucose-6-phosphate (G6P); this phosphorylation is a rate limiting step in glycolysis (33). The production of G6P drives energy into glycolysis and the tricarboxylic acid cycle leading to an increase in the ATP to ADP ratio (34). This increase in the ATP:ADP ratio causes closure of ATP-dependent ( $K_{ATP}$ ) potassium channels that results in an increase of the resting membrane potential, leading to PM depolarization (35). PM depolarization causes opening of L-type voltage dependent calcium channels (VDCC), thereby increasing the intracellular cytosolic calcium concentration  $[Ca^{2+}]_i$  (36). The elevated intracellular calcium causes immediate release of insulin granules already primed at the PM, particularly those adjacent to the VDCC (37). Granules are coordinately mobilized to the PM from the reserve pool, although the signals required for this remains under investigation. Once insulin granules arrive at the PM they undergo 'exocytosis', involving the docking and fusion of granules with the PM. The exocytosis of the insulin granules is mediated by Soluble N-ethylmaleimide-sensitive attachment receptor factor attachment protein receptor (SNARE) proteins, a complicated process requiring multiple types of complexes operating within the distinct phases, as will be discussed in Section 1.4.

## **1.4 GLUT4 VESICLE EXOCYTOSIS**

### **1.4.1 The Insulin Receptor**

The peripheral insulin responsive tissues, namely skeletal muscle and adipose strive to clear the excess glucose, thereby restoring glucose homeostasis. Approximately ~80% of the glucose is cleared by the skeletal muscle, with the remainder being utilized

by brain (25%) and rest cleared by liver and fat. These tissues are insulin responsive because their cells harbor insulin receptors (IR) on their surface membranes. IR is comprised of an extracellular  $\alpha$  subunit and a transmembrane-spanning  $\beta$  subunit linked by disulfide bonds (38). Upon insulin binding, a conformational change to the intracellular portion of the IR protein occurs, resulting in activation of the  $\beta$  subunit's tyrosine kinase activity and autophosphorylation of the kinase regulatory domain, leading to phosphorylation of the juxtamembrane tyrosine residues that function as docking sites for a wide range of substrates (39-40). These events are followed by an additional conformational change within the  $\beta$  subunit, unmasking important substrate binding sites and thus, stabilizing the receptor in an active conformation.

#### **1.4.2 Insulin Receptor Substrates and Signalling in Fat and Skeletal Muscle**

As depicted in Fig. 1-2, extracellular insulin binding to the IR triggers a cascade of intracellular signals to multiple substrates in skeletal muscle and fat cells: IRS proteins, APS/Cbl/CAP complexes, and most recently, Munc18c, a non-classical signaling component of the SNARE machinery (41). IR signaling through these substrates is coordinated in multiple cascades to evoke the main event required for glucose uptake by these cell types: the mobilization of insulin-responsive GLUT4-laden vesicles from intracellular storage pools to the cell surface (42-44). Once at the surface, GLUT4 proteins are incorporated into the PM to facilitate entry of glucose into the cells and out of circulation. The IRS proteins signal downstream to elicit a PI3 kinase-dependent signaling cascade, whilst APS/CAP/Cbl-signaling is purportedly an IRS and PI3 kinase-independent signaling cascade (45). Use of PI3K inhibitors has implicated an

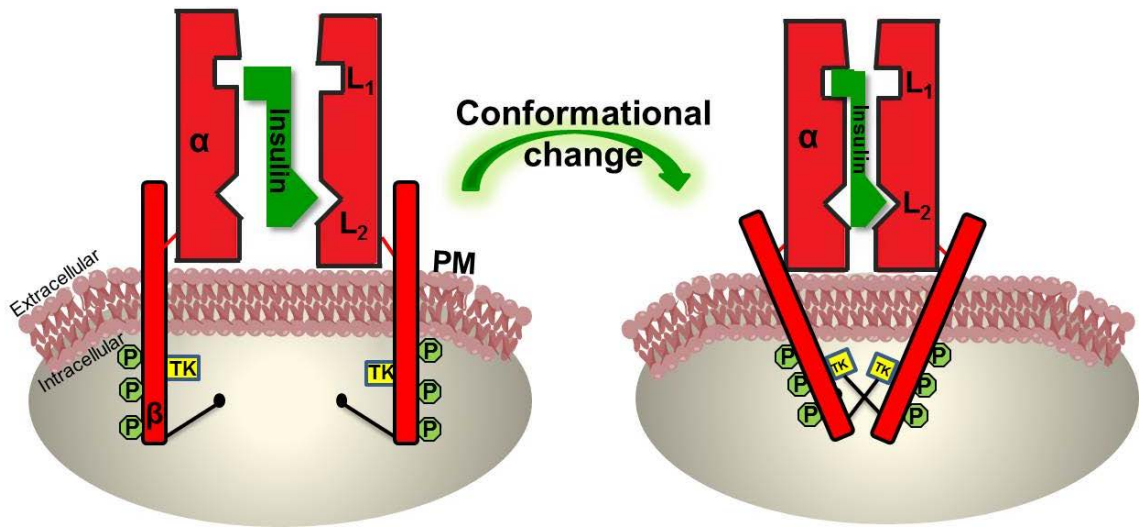


**Figure 1-2. Schematic representation of the major features of IR.** IR is a heteromeric structure comprised of two extracellular  $\alpha$  subunits that bind insulin, and two intracellular transmembrane  $\beta$  subunits. The intracellular domains contain the tyrosine kinase (TK) activity. Insulin binding to the extracellular domain of IR induces a conformational change to the intracellular domain, such that the receptor undergoes autophosphorylation.

IR-dependent but PI3K-independent signaling pathway. One well described PI3K independent pathway involves the APS/Cbl/CAP complex (46), which provides a second signal cascade that functions in parallel with PI3K to evoke GLUT4 translocation and glucose uptake in response to the insulin-IR signal. As depicted in Fig. 1-3, this pathway is initiated by recruiting Cbl (a proto-onco protein) to the activated IR via adapter proteins CAP (c-Cbl associated protein) and APS (Adapter protein with PH and SH2 domain) (47-48). APS is phosphorylated by IR, which in turn phosphorylates Cbl, leading to Cbl association with CAP and CrkII (49). This complex then translocates to the caveolar rich region of the PM with the help of flotillin, a lipid raft protein (50-52), and along with guanine nucleotide exchange factor C3G, activates TC10 in lipid rafts (53-54). TC10 binds to a number of downstream effectors such as CIP4, Exocyst, N-Wasp and Arp-2/3, which have roles in actin dynamics (55). Actin cytoskeleton re-organization is vital in insulin sensitive tissues to form a mesh which is critical for GLUT4 vesicle tracking and translocation to the PM. Actin depolymerization with latrunculin prevents GLUT4 translocation, suggesting a requirement for intact F-actin structure in insulin-stimulated GLUT4 translocation (56-57). Studies using jasplakinolide, an F-actin nucleating and stabilizing agent, inhibits GLUT4 translocation, further substantiating the role for actin re-organization in glucose transport (58-59).

In 2011 IR was found to utilize Munc18c, a regulatory protein of the SNARE machinery required to dock and fuse GLUT4 vesicles at the PM, as a substrate. As IRS-1 failed to bind Munc18c and no binding differences were seen in the presence of a PI3K inhibitor, it was concluded that IR signaling to Munc18c was independent of GLUT4

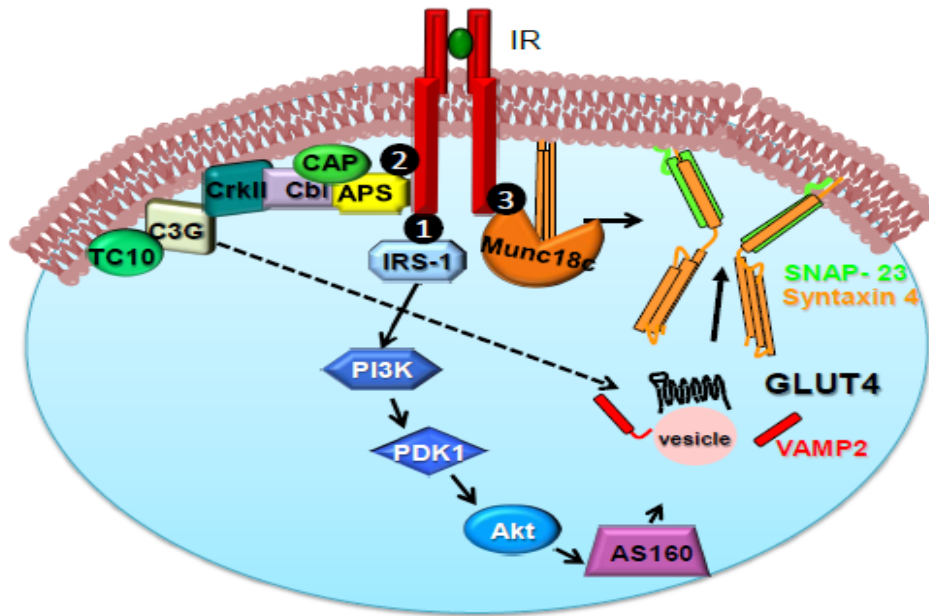


**Figure 1-3. GLUT4 translocation in muscle/adipose.** Three signaling pathways are required for the GLUT4 vesicle translocation in muscle and fat: 1) Phosphorylated IR binds and phosphorylates IRS-1 which activates PI3K. This further leads to PDK1 activation and subsequently Akt1/2 phosphorylation. AKT activates AS160, and AS160 which through, as of yet, undefined steps results in GLUT4 translocation, facilitates glucose uptake. 2) IR also phosphorylates APS which in turn phosphorylates Cbl. Cbl constitutively interacts with CAP, which associates with flotillin to stabilize the recruitment of this complex in caveolae. Phosphorylated Cbl in the caveolar lipid raft recruits CrkII, and CrkII constitutively binds to the nucleotide exchange factor C3G. C3G catalyzes the exchange of GTP for GDP on the lipid raft-associated protein TC10, a downstream effector important in GLUT4 translocation. 3) IR phosphorylates Munc18c.



which relays signal to the SNARE machinery to coordinate SNARE complex formation and vesicle fusion.

IR/IRS/PI3K signaling and that IR signaling to Munc18c occurred in parallel to that of the PI3K pathway in the mechanism of insulin-stimulated glucose uptake (41). IR required Munc18c residue Tyr 521 for binding and phosphorylation, although a second residue, Tyr 219, was also found to be essential in insulin-stimulated Munc18c phosphorylation and GLUT4 vesicle translocation in 3T3-L1 adipocytes, perhaps as a sequential phosphorylation event following Tyr 521 modification (41). By orchestrating these three substrate activation events, IR can propagate the insulin signal within minutes to coordinate both the mobilization and docking/fusion of GLUT4 vesicles with the help of SNARE proteins to achieve a 3 to 5-fold increase in cellular glucose uptake (41, 60-62).

### **1.5 SNARE PROTEINS INVOLVED IN EXOCYTOSIS**

SNAREs belong to a superfamily of proteins with more than 35 members that mediate fusion between vesicle and target membrane in various secretory pathways, including insulin granule exocytosis, neurotransmitter release, and insulin-stimulated GLUT4 vesicle exocytosis. To date, 6 vesicle SNARE (v-SNAREs) isoforms and 11 target-membrane SNARE proteins (called 't-SNAREs') have been identified that are involved in insulin granule and GLUT4 vesicle exocytosis events (63-67). The characterization of mammalian SNARE proteins began in the late 1980's, when the first synaptic vesicle protein Synaptophysin was cloned. Within a decade, key elements of

membrane fusion were identified (68-69). The first SNARE complexes, characterized in neuroendocrine cells, consisted of Syntaxin 1 (70), SNAP25 (71) and VAMP2 (72). They are classified based on the central amino acid residue in the zero layer of a helical bundle present in each protein. R SNAREs contribute arginine at this residue and are usually vesicle associated. Q SNAREs are target membrane associated (t-SNAREs) and contain glutamine at the central position. Q SNAREs are further classified into Q<sub>a</sub>, representing the syntaxin subfamily, and Q<sub>b</sub> or Q<sub>c</sub>, representing the SNAP family. The helical domain in each of these SNAREs, referred to as the 'SNARE' motif, contains a conserved stretch of 60–70 amino acids containing heptad repeats (73). Most SNARE proteins contain one SNARE motif, although SNAP23/25 consists of two SNARE motifs (74). Isolated SNARE motifs are unstructured, only gaining structure as they interact during the formation of the four alpha-helical bundle; this bundle is called the 'SNARE core complex'. SNARE proteins confer specificity and directionality for the vesicle to dock and fuse with the PM. Different SNARE proteins play a role in each phase of biphasic insulin release. Of the exocytotic SNAREs, Syntaxin 1 is required for first-phase, while Syntaxin 4 has a role in biphasic insulin secretion. Recently, Syntaxin 3 was found to regulate biphasic insulin release by mediating new comer granules to the PM. Both the phases require SNAP25 or SNAP23 to bind with v-SNARE VAMP2. Syntaxin 2/3 was also identified to bind VAMP8 to regulate biphasic insulin secretion (28, 75-77). GLUT4 mediated glucose uptake occurs in one phase and involves a smaller subset of SNARE components including t-SNAREs Syntaxin 4 and SNAP23, and v-SNARE VAMP2 (78-79). Accessory proteins like Munc18c and others (Doc2b and Munc13) further regulate the SNARE proteins during complex formation.

### **1.5.1 SNARE Protein Abundances and Diabetes**

Down-regulation of proteins involved in exocytosis is correlated with impaired beta cell function in T2D patients and rodent models (80-82). Islets of obese Zucker and diabetic GK rats show decreased levels of Syntaxin 1, Syntaxin 4, VAMP2 and SNAP25 (83). Similarly, islets from T2D patients have decreased Syntaxin 1, with a concomitant reduction in its Munc18 regulatory factor, Munc18-1 (80). Syntaxin 4 and its regulatory factor Munc18c are also reduced in T2D human and diabetic mouse skeletal muscle (80, 84). Attenuated expression of SNARE proteins has been proposed to impair insulin secretion, since restoration of Syntaxin 1 and SNAP25 protein levels in islets from the diabetic GK rat was sufficient to restore first-phase insulin release and normoglycemia (83).

### **1.5.2 SNARE Core Complex Assembly**

The SNARE hypothesis initially postulated that preassembled SNARE complexes formed at the site of vesicle docking were acted upon by N-ethylmaleimide sensitive factor (NSF) and alpha-SNAP to drive membrane fusion. Later, it was discovered that NSF and alpha-SNAP play a role in the disassembly of SNARE complexes (85), and the hypothesis was altered to its current state, which establishes that the SNARE proteins are the key elements for membrane fusion and SNARE core complex assembly involves the exquisite rearrangement of lipid bilayers to cause fusion (69). The vast majority of detailed structural assembly information described below involves the isoforms syntaxin 1A, SNAP25 and VAMP2, as these are the primary isoforms involved in presynaptic exocytosis (86). In beta cells, these isoforms of syntaxin and SNAP are operative in the

first phase of insulin secretion whereas, Syntaxin 4 and SNAP23 are involved in GLUT4 vesicle exocytosis and the second phase insulin secretion with VAMP2 playing a role in both the processes.

SNARE assembly begins by the formation of a binary cognate receptor complex at the target membrane composed of SNAP25 and syntaxins in a stoichiometric ratio of either 1: 1 or 2: 1 (74). It is believed that 50–70 clusters composed of Syntaxin 1 and SNAP25 together are associated with one docked granule at the PM (87-88). VAMP2 joins the binary complex to form a heterotrimeric complex in a 1:1:1 stoichiometric ratio (76, 89-91). These three SNARE proteins form a stable four helical bundle by the contribution of four  $\alpha$ -helices: one from VAMP, one from Syntaxin, and the remaining two from SNAP25 (92-95). The SNARE cycle starts with the amino- to carboxyl-terminal zippering to form a tight complex through hydrophobic interactions (96). SNARE core complexes are highly stable and resistant to extreme conditions like exposure to SDS, urea, and high temperatures (97). The assembly of SNARE proteins releases free energy, and this energy is used to overcome the repulsive forces of the opposing barriers to initiate fusion between the vesicle and the PM (95). The luminal pore is formed during the fusion by interactions between the transmembrane domains of Syntaxin 1 and VAMP2, which initiate the vesicle exocytosis. However, recent data suggest that the transmembrane domain is not required for the pore formation (98). The trans-SNARE complexes, present in the opposing membranes during fusion, merge to form cis-SNARE complexes, which are dissociated by the subsequent binding of NSF and SNAP proteins. SNAP recruits NSF, which, owing to its ATPase activity, disassembles

the SNARE core complex, making SNAREs available for another round of fusion. The t-SNAREs are redistributed along the PM, while the v-SNARE is endocytosed for future incorporation into cargo-loaded vesicles.

Based on fluorescence resonance energy transfer (FRET) and TIRF studies, it was shown that the assembly of SNARE complexes is locally regulated and varies from region to region in beta cells. Regions with preassembled SNAREs show faster exocytosis in response to calcium compared to regions without preassembled SNAREs (37). A few studies have demonstrated that around 3–15 SNARE complexes participate in the exocytosis event; controlled FRET experiments have elucidated that one SNARE complex is sufficient for fusion *in vitro* (99-100). However, it is difficult to rely on the above mentioned data as energy formed from one SNARE complex is insufficient for full fusion pore formation, and additional radiant force may be necessary to prevent the pore from resealing during release (101).

### **1.5.3 Syntaxins**

Syntaxins are t-SNAREs that are localized to the PM, the cytosolic face of endosomal, golgi, and endoplasmic reticulum membranes. Each isoform is specific in terms of its cellular localization, and some isoforms are further specified to apical versus basement membrane localizations within polarized cell types. Syntaxins are attached to the membrane through a characteristic hydrophobic C-terminal transmembrane domain, while the N-terminus remains in the cytosol. Syntaxins are characterized by a highly conserved SNARE motif present in the short carboxyl terminus, which is connected by a

short linker to three additional alpha helical domains (termed H<sub>a</sub>, H<sub>b</sub>, and H<sub>c</sub>, or cumulatively as H<sub>abc</sub>) present in N terminus. Syntaxin isoforms 1, 2, 3 and 4 are localized to the PM and each reportedly functions in insulin secretion (28, 76, 102-103). GLUT4 vesicle exocytosis uses only the PM-localized Syntaxin 4 isoform, although Syntaxin isoforms 2, 3, 5, 6, 7, 8, and 12 are reportedly present in adipocytes (32, 89, 91)

#### **1.5.4 Syntaxin 1**

Syntaxin 1 is a ~35 kDa polypeptide discovered in bovine brain extracts and later identified in pancreatic islets (70, 103-104). Deletion of Syntaxin 1 impairs docking of synaptic vesicles in chromaffin cells. Similarly, Syntaxin 1<sup>-/-</sup> knockout mouse islets have reduced first-phase secretion (105), showing it is essential for docking and fusion of RRP granules (28). Syntaxin 1 binds to other proteins, which can facilitate exocytosis under normal circumstances, but can be detrimental when Syntaxin 1 levels are too high. For example, when present in excess (106), Syntaxin 1 blocks the SUR subunit of K<sub>ATP</sub> channels and inhibits PM depolarization to attenuate insulin secretion (107). Syntaxin 1 also decreases the surface expression of these channels (108-109). While Syntaxin 1 binding to calcium channels presumably fosters fast exocytosis by localizing docked granules in the vicinity of initial calcium influx, Syntaxin 1 surfeit inhibits calcium influx (110). Indeed, over-expression of Syntaxin 1 in insulinoma cells and normal healthy islets reduces insulin secretion (111). Transgenic mice engineered to over-express Syntaxin 1 had impaired glucose and insulin tolerance and fasting hyperglycemia (104, 112). Moreover, a hemizygous mutation of Syntaxin 1 in humans, linked with Williams-Beuren

syndrome, leads to abnormal glucose homeostasis (109). Several SNPs for Syntaxin 1 have been identified, and associated with diabetes (113).

### **1.5.5 Syntaxins 2 and 3**

Syntaxins 2 and 3 are expressed in beta cells, and very recent work has implicated Syntaxin 3 in unusual forms of insulin granule exocytosis. Syntaxin 3 plays a role in secretory granule fusion to other secretory granules (SG-SG fusion) in beta cells leading to biphasic insulin release (76, 102). However, it is difficult to rely on the data, since insulin secretion under Syntaxin 3 depleted conditions was performed in clonal beta cells and not in primary islets. Also, TIRF microscopy was used to delineate that Syntaxin 3 is required for the recruitment of new coming granules. Given the discrepancies in TIRF microscopy methodologies, due to the differences in the distance measured from the PM, further analyses are required to discern Syntaxin 3 participation in SNARE mediated exocytosis.

### **1.5.6 Syntaxin 4**

Syntaxin 4 is a ~35 kDa, ubiquitously expressed protein known to have a function in pancreatic beta cells, muscle, adipose, kidney, postsynaptic density and mast cells (114-115). Syntaxin 4 plays a major role in the regulation of insulin secretion in pancreatic beta cells and glucose uptake in peripheral tissues to coordinately maintain glucose homeostasis. Islets from heterozygous Syntaxin 4 knockout mice had reduced biphasic insulin secretion, while islets isolated from transgenic mice with Syntaxin 4 over-expression had ~35% increased insulin release in both phases (76), indicating

Syntaxin 4's positive role in insulin secretion. Correspondingly, serum insulin content peaked within 5 minutes after glucose injection in Syntaxin 4 Tg mice compared to Wt mice, in which serum insulin levels peaked after 15-30 minutes (Oh, Stull, Mirmira and Thurmond, unpublished).

Syntaxin 4 is the only syntaxin isoform shown to have a role in GLUT4 vesicle exocytosis (116). While early studies suggested that Syntaxin 2 was expressed in 3T3-L1 adipocytes (116), Syntaxin 2 has yet to be implicated in GLUT4 vesicle exocytosis. Syntaxin 4 regulates the docking and fusion of GLUT4 vesicles. Syntaxin 4 heterozygous mice displayed significant insulin resistance owing to impaired GLUT4 accumulation in sarcolemmal and t-tubule membranes, consistent with reduced skeletal muscle and whole-body glucose uptake in these mice (76, 91). Similarly, Syntaxin 4 transgenic mice, over-expressing Syntaxin 4 by 3-5 fold exclusively in muscle and adipose had enhanced glucose uptake mediated by increased GLUT4 translocation in muscle (89); these mice were also protected against diet-induced insulin resistance (Oh and Thurmond, unpublished). In Syntaxin 4 heterozygous mice, Munc18c protein levels were also decreased even though levels of other SNARE proteins remained unchanged. In a consistent fashion, Munc18c levels were similarly increased in Syntaxin 4 over-expressing mice. These findings are consistent with other reports suggesting a chaperone-type relationship between Munc18-Syntaxin proteins (117).



### **1.5.7 SNAP**

SNAPs are 23–29 kDa proteins consisting of three isoforms SNAP23, SNAP25, and SNAP29. All three have similar sequence and structure. Each contains two alpha helical SNARE motifs, but no transmembrane domain, and therefore are not membrane-integrated like the syntaxins and VAMPs. The two SNARE motifs of the SNAPs are connected by a loop region, which contains palmitoylated cysteine residues that help anchor SNAPs to the PM (118). SNAP23 and SNAP25 proteins bind with the other SNAREs to regulate the docking and fusion of insulin granules and GLUT4 vesicles. SNAP25 is exclusively found in beta cells and neuronal cells (119), and is absent from muscle or adipose (120). In contrast, SNAP23 is ubiquitously expressed and detected in adipose, muscle, and beta cells (121). SNAP23 can compensate for the loss of SNAP25 in beta cells, and vice versa (122). Studies of SNAP25 or SNAP23 knockout must await the generation of inducible tissue-specific knockout mice, since classic knockout mice of the genes is embryonic lethal (123).

### **1.5.8 VAMP2**

VAMP2 is a ~18 kDa vesicle-associated SNARE protein from a family of seven isoforms. Each isoform contains a single C-terminal SNARE motif. While multiple VAMP isoforms have been investigated in regards to GLUT4 vesicle exocytosis, VAMP2 is the primary isoform involved in this process (63, 124-125). At the time of their discovery in adipocytes and muscle, VAMP2 and VAMP3 were both considered pertinent to this process. However subsequent studies with VAMP3 knockout mice indicated no defects in GLUT4 vesicle exocytosis or glucose homeostasis (126), thereby

arguing against a role for VAMP3. VAMP8 has recently gained attention in this role, although conflicting data regarding the relative importance of VAMP8 versus VAMP2 preclude a clear picture at this time (127). VAMP2, 3 and 8 are also expressed in beta cells where VAMP2 plays a predominant role in insulin exocytosis similar to the process in adipocytes and muscle (63).

## **1.6 SNARE ACCESSORY PROTEINS**

### **1.6.1 Munc18 proteins**

Sec1/Munc18 (SM) proteins are the most widely studied family of proteins that regulate membrane fusion by controlling SNARE complex formation. Homologues to the SM proteins include Sec-1 in *S. cerevisiae*, unc18 in *C. elegans*, and Rop in *D. melanogaster* (128-129). Three mammalian SM isoforms, Munc18-1, Munc18b, and Munc18c, having a high degree of sequence similarity have been identified. These isoforms are 66-68 kDa cytosolic proteins that have no transmembrane domain but are localized to the PM when complexed with their cognate syntaxin. A high degree of structural similarity exists between Munc18 isoforms; SM proteins form an arch-shaped clasp that holds specific syntaxins in multiple binding modes. Vps45 has recently been demonstrated to have a role in the delivery of GLUT4 into the specialized, insulin-regulated compartment (130) Additional SM proteins that are operative in intracellular fusion events exist (Vps33 and vps16) but will not be discussed as they are not thought to be required for insulin exocytosis or GLUT4 vesicle exocytosis events (131-132). Two isoforms, Munc18-1 and Munc18c, are associated with impaired insulin exocytosis and GLUT4 vesicle exocytosis and correlated with the T2D phenotype (80, 84, 133).

## 1.6.2 Munc18-1

Munc18-1 was originally cloned in neuronal tissues as a Syntaxin 1 binding partner and later identified in islet beta cells (134). Munc18-1 is expressed only in neuroendocrine cell types, and therefore is detectable in beta cells but not in fat or muscle cells. Munc18-1 (also known as Munc18a, N-Sec1, STXBP1 and Syntaxin binding protein) is known to bind plasma membrane syntaxin isoforms 1, 2, and 3 (134). Reduced levels of Munc18-1 are known to impair neurotransmitter release (135) and its depletion from beta cells results in defective docking of insulin granules and reduced insulin secretion (136). Over-expression of Munc18-1 in human islets selectively enhanced first-phase insulin secretion (136), demonstrating that Munc18-1 is an important protein for first-phase insulin release. Surprisingly, Munc18-1 over-expression drove the assembly of Syntaxin 4-based SNARE core complexes, rather than of Syntaxin 1-based complexes as would have been predicted based upon the specificity of SM-syntaxin pairing. The enhancement effect of Munc18-1 was shown to require Syntaxin 4, indicating that a novel cross-talk must exist between these protein complexes in the beta cell.

Two models have been developed to explain the interaction of Munc18-1 with Syntaxin 1. In one model, Munc18-1 holds its cognate syntaxin isoform, Syntaxin 1, in a 'closed' conformation (118, 137), which blocks Syntaxin 1 from 'opening' and interacting with the tertiary SNARE complex. It is proposed that domain 3A of Munc18-1 facilitates conversion of Syntaxin 1 from a closed to an open conformation (138). In the open conformation, the H<sub>abc</sub> domain unfolds, exposing Syntaxin 1's SNARE motif and allowing it to participate in SNARE core complex formation (139). The binding of

Munc18-1 to the linker region of Syntaxin 1 has been shown to stabilize this closed conformation of Syntaxin 1 (140). Further, more point mutations that keep Syntaxin 1 open abolish its interactions with Munc18-1 (141). In particular, Munc18-1 phosphorylation at Thr 574 by cyclin-dependent kinase 5 (CDK5) or at Ser 306 and Ser 313 by protein kinase C, reduces its affinity for Syntaxin 1 (142). In contrast, Munc18-1 phosphorylation at Thr 479 by Dryk-1 stimulates its binding to Syntaxin 1 (133, 143). While these events have yet to be investigated in beta cells, they do suggest post-translational modifications as an additional layer of complexity by which Munc18-1 may regulate insulin exocytosis. In the second model, Munc18-1 interacts with Syntaxin 1 in the open conformation. Munc18-1 would bind to a short region at the amino terminal of Syntaxin 1 allowing it to be compatible for SNARE complex formation under Munc18-1 bound conditions (144). It may be necessary for Munc18-1 to wrap around Syntaxin 1 to provide spatial organization of SNARE complex (145). Indeed, Munc18-1 can bind to the SNARE complex in beta cells, whereas Munc18c cannot, as detailed in the next section below.

### **1.6.3 Munc18c**

Munc18c is ubiquitously expressed, detected in beta cells, fat and skeletal muscle, and is the exclusive SM binding partner of Syntaxin 4 (146-147). Munc18c is an essential regulator in SNARE mediated exocytosis, by virtue of its role and requirement as a binding partner for Syntaxin 4. In adipocytes, beta cells, and muscle, Munc18c has been shown to bind Syntaxin 4 in a manner that is mutually exclusive of Syntaxin 4's interactions with SNAP23 and VAMP2 (148-149). In these cell types, Munc18c has been

shown to impact the ability of Syntaxin 4 to form SNARE core complexes similar to that of the Munc18-1-Syntaxin 1 complex. However, recent crystallographic evidence suggested that Syntaxin 4 was perpetually in an open conformation (150), distinct from the dual conformations detected for Munc18-1. Thus, while there is clear evidence of conservation of function with Syntaxin 4/Munc18c/SNARE complex formation and Syntaxin 1/Munc18-1/SNARE complexes, there appear to be significant departures that may ultimately impact how each set promotes insulin exocytosis.

Although Munc18c is now regarded as a required and positive factor for GLUT4 vesicle exocytosis and insulin exocytosis, based upon reduced function of each in Munc18c heterozygous knockout mice (151), Munc18c was initially labeled as an inhibitor of these processes based upon over-expression studies in clonal cells and *in vivo* (152). These data suggest that while Munc18c is required for these exocytosis processes, it is not limiting. This was confirmed in a study in which impaired GLUT4 translocation, seen under Munc18c over-expressed conditions, was reversed with Syntaxin 4 over-expression (153).

Munc18c specifically facilitates second-phase glucose-stimulated insulin secretion (GSIS) wherein Munc18c phosphorylation at Tyr 219 was identified as a crucial trigger for SNARE complex formation (154). Concurrent with this finding, Munc18c in 3T3-L1 adipocytes was found to be tyrosine phosphorylated at residue 521 (149), which occurred concomitant with dissociation of Syntaxin 4-Munc18c complex and the promotion of GLUT4 vesicle exocytosis. Insulin-stimulated phosphorylation of Munc18c

at both sites was found to be required for GLUT4 vesicle exocytosis via a knock-in approach (41). Further, this mechanism was shown to be conserved in primary mouse skeletal muscle. Very recently, the PTPIB phosphatase was shown to dephosphorylate Munc18c and reverse these actions (155). The ‘switch hypothesis’, whereby Munc18c undergoes stimulus-dependent tyrosine phosphorylation to release Syntaxin 4, promoting Syntaxin 4 incorporation into SNARE complexes, is illustrated in Fig. 1-4.

It had been presumed for years, based upon analogy to yeast orthologs of Munc18 and Syntaxin association/dissociation dynamic mechanisms, that downstream of AS160, a Rab-type protein would serve to dissociate Munc18c from Syntaxin 4 at the PM. This was predicted to facilitate the opening and accessibility of Syntaxin 4 to incoming VAMP2-laden GLUT4 vesicles. However, no such Rab protein has ever been definitively identified. Emerging evidence regarding a putative role for Munc18c phosphorylation in this mechanism led to investigations of protein kinase(s) that might circumvent the need for the unidentified Rab-like protein, and indeed, IR was found to carry out this role (41). Given this observation, it is conceivable that the function of a Rab-like protein downstream of AS160 to facilitate SNARE pairing may *not* be required in the process of GLUT4 vesicle translocation.

#### **1.6.4 Munc13**

Munc13 proteins are large, ranging from 100-200 kDa; there are four known isoforms (Munc13-1, -2, -3, -4, also referred to as Munc13 A-D). Except Munc13-4, other

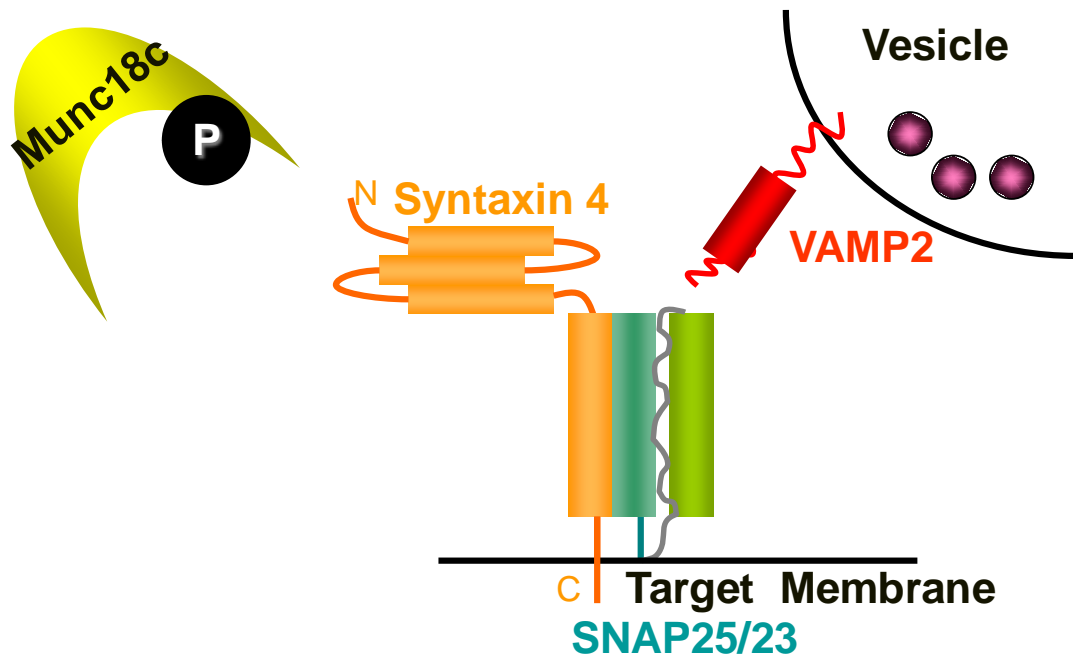


**Figure 1-4. The switch hypothesis model.** Doc2b functions as a switch to bind phosphorylated Munc18c facilitating the opening of Syntaxin 4. Once opened, Syntaxin 4 participates in SNARE complex formation, ultimately leading to exocytosis.

Munc13 isoforms contain three calcium/phospholipid binding domains, with one C1 domain and two C2 domains (156). Munc13 isoforms are not yet described to exist in muscle or fat cells (157). Of the numerous Munc13 isoforms implicated in synaptic exocytosis, only Munc13-1 is well characterized and defined in insulin secretion. The C2 domains of Munc13-1 mediate the binding of phorbol ester and diacylglycerol binding (158). Munc13-1 was originally identified in beta cells and islets as a RIM binding protein (157), and found to be limiting for insulin exocytosis, as evidenced by over-expression studies showing increased insulin secretion (157). Consistent with this, Munc13-1 heterozygous mice had impaired glucose tolerance and reduced insulin secretion (159). In addition, Munc13-1 binds to a novel domain present in Doc2 proteins, referred to as the Munc13-interacting domain (MID). Another isoform of Munc13, Munc13-4 was recently identified to bind Syntaxin 4 using *in vitro* liposome assays (160). Munc13-4 is also identified as a limiting factor in platelet exocytosis (161), suggesting it may carry importance in insulin exocytosis.

### **1.6.5 Doc2 proteins**

Doc2 proteins, so named for their inclusion of double C2 domains called C2A and C2B, are 45 kDa polypeptides first discovered in 1995 (162-163). They are soluble proteins lacking a transmembrane domain. The N-terminal MID region of Doc2 proteins is separated from the C2A domain by a short linker, with the C2B domain closest to the C-terminus (Fig. 1-5). Three different isoforms of Doc2 are known: Doc2alpha, Doc2beta, and Doc2gamma, commonly known as Doc2a, Doc2b and Doc2g. Doc2a is predominantly expressed in brain, while Doc2b is ubiquitously expressed in tissues



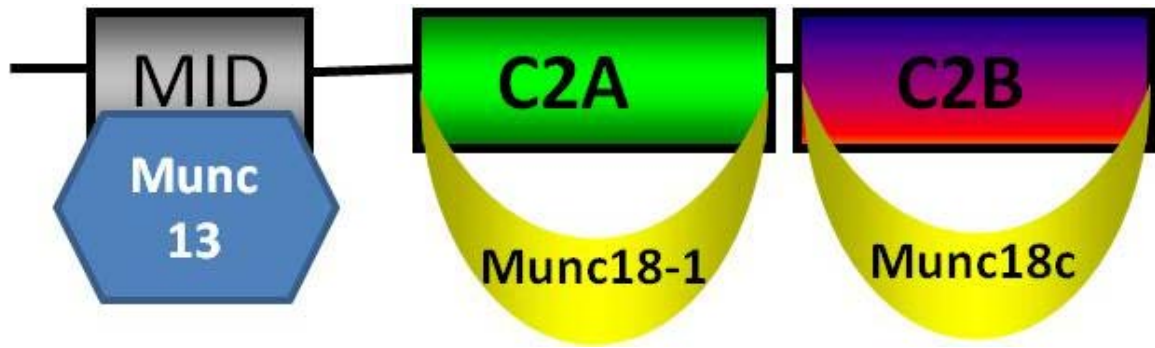


**Figure 1-5. Doc2b functions as a scaffold for Munc18-1 and Munc18c.** An unrelated Munc protein, Munc13-1, a priming factor, binds Doc2b via its MID domain. C2A domain binds Munc18-1 while C2B binds Munc18c.

including brain, kidney, adipose, muscle, and pancreas (164-165). Doc2g is found only in the heart, and its functions are poorly defined (166). Doc2b is 69% identical to Doc2a and 43% to Doc2g at the amino acid level (166). Both Doc2a and Doc2b bind to phospholipids in response to a calcium stimulus in neuronal cell types, and are known to bind to Munc18 proteins through their C2 domains (167). While Doc2a expression and function in beta cells, adipocytes or skeletal muscle has yet to be investigated, Doc2b is expressed and functional in these cell types, and is therefore the focus of the discussion detailed below.

#### **1.6.6 Doc2b**

Doc2b was first shown to bind Munc18-1 protein via its C2A domain in 1997, competing for the binding to Munc18-1 with Syntaxin 1 (164). Similarly, Doc2b was later identified as a binding partner for Munc18c (165), but via its C2B domain, but did compete with Syntaxin 4 for binding to Munc18c. However, these findings contrasted with subsequent *in vitro* studies that concluded Doc2b to be a syntaxin binding protein (168). Given the ability of Doc2b to bind these Munc18 isoforms via its different C2 domains, it will be important to determine if Doc2b serves as a scaffold to capture the transiently dissociating Munc18 proteins, as modeled in Fig. 1-5. Indeed, the stimulus-induced tyrosine phosphorylation of Munc18c diminishes its association with Syntaxin 4 in beta cells and adipocytes, and temporally correlates with an increase in Doc2b-Munc18c binding. Whether Doc2b preferentially binds to phosphorylated Munc18c or Munc18-1 remains untested.

Doc2b was originally identified as a putative calcium sensor in neurons, with the C2B domain shown as a requisite for calcium-induced Doc2b translocation to the PM (169). In contrast, the C2A domain of Doc2b binds liposomes containing phosphatidylcholine and phosphatidylserine in a calcium-dependent manner, which facilitates attachment to the PM (163). This binding of the C2A domain to the PM reduces the energy barrier by causing membrane curvature, which ultimately enhances vesicle fusion with the PM. Strikingly, Doc2b was very recently demonstrated to modulate exocytosis by a mechanism independent of calcium in neurons (170). Similarly, in clonal beta cell lines conflicting data regarding calcium-stimulated Doc2b translocation exist (167) and therefore requires examination in primary islet beta cells to gain evidence in a more physiologically relevant system.

Independent over-expression studies showed Doc2b to be a positive factor in Syntaxin 4-based insulin exocytosis and GLUT4 exocytosis events in cultured clonal beta cells and adipocytes, respectively (165, 168). Further, the RNAi-mediated depletion of Doc2b from clonal beta cells (165, 171) and from 3T3-L1 adipocytes in 2009 (168) suggested that Doc2b plays required roles in these processes (165, 171). The abundance of data implicates Doc2b as a key player in exocytosis events from multiple cell types, suggesting a universal function for Doc2 proteins, akin to that of the Munc18 proteins, in SNARE-mediated exocytosis events. However, the role of Doc2b to maintain whole body glucose homeostasis *in vivo* is yet to be tested.

## **1.7 RATIONALE**

The rationale for the studies in this dissertation is that understanding the role of Doc2b in maintaining whole body glucose homeostasis will further advance our knowledge of exocytotic processes involved in maintaining glucose homeostasis, and may unveil potential new therapeutic targets for the prevention and/or treatment of T2D. The central hypothesis of the proposed research was based upon the following evidence: 1) Doc2b is a positive regulator of SNARE complex formation in beta cells and adipocytes *in vitro*, 2) Increasing or decreasing Doc2b protein levels increases or decreases insulin secretion and GLUT4 vesicle exocytosis in cultured cells, respectively, and 3) Doc2b binds two SM proteins, Munc18-1 and Munc18c, both of which regulate different phases of insulin secretion. Thus, my central hypothesis is that Doc2b-Munc18 complexes maintain glucose homeostasis by simultaneously regulating insulin action in peripheral tissues and biphasic insulin secretion from pancreatic islet beta cells, and perturbations in the function of Doc2b lead to dysregulation of glucose homeostasis. To test my hypothesis I pursued two aims: 1) Establish the role of Doc2b-Munc18c complexes in the regulation of skeletal muscle insulin action using Doc2b knockout and regulatable Doc2b over-expressing transgenic mouse models, and 2) Elucidate how Doc2b-Munc18 complexes regulate biphasic insulin secretion using the two Doc2b genetic mouse models.

## **CHAPTER 2. MATERIALS AND METHODS**

## **2.1 MATERIALS**

The rabbit anti-Munc18c and rabbit anti-Syntaxin 4 antibodies were generated in-house as described (172-173). The rabbit anti-Syntaxin 4 (for immunoprecipitation), rabbit anti-SNAP23/ SNAP25 and mouse anti-Doc2b antibodies were purchased from Chemicon (Temecula, CA), Affinity Bioreagents (Golden, CO) and Abcam (Cambridge, MA), respectively (Table 2-1). The mouse anti-Munc18-1, mouse anti-VAMP2 and mouse anti-Syntaxin 1A antibodies were acquired from Synaptic Systems (Gottingen, Germany). Mouse anti-GFP antibody was acquired Clontech Laboratories. The rabbit anti-PY20, rabbit-AKT and rabbit-phosphoserine (p<sup>Ser 473</sup>)-specific AKT antibodies were purchased from Cell Signaling, Inc. (Beverly, MA). Goat anti-rabbit-HRP and goat anti-mouse-HRP secondary antibodies were purchased from Bio-Rad (Hercules, CA). Protein G+ agarose beads and goat anti-GLUT4 antibody were acquired from Santa Cruz (Santa Cruz, CA). The rat sensitive insulin radioimmunoassay kit was acquired from Millipore. Enhanced chemiluminescence (ECL) and Supersignal West Femto chemiluminescent reagents were purchased from Amersham Biosciences (Pittsburg, PA) and Thermo, respectively. The RNeasy mini kit was purchased from Qiagen (Valencia, CA). The Superscript First Strand cDNA synthesis kit was obtained from Invitrogen (Carlsbad, CA). Humulin R was obtained from Eli Lilly (Indianapolis, IN).

## **2.2 ANIMALS**

All studies involving mice followed the Guidelines for the use and care of laboratory Animals. All knockout Doc2b studies utilized male mice 4-6 months old.

Table 2-1 List of antibodies used

<b>Antibody Name</b>	<b>Host Species</b>	<b>kDa</b>	<b>Company</b>	<b>Cat#</b>	<b>Dilution</b>
AKT	Anti-rabbit	60	Cell signaling	9272	1:1000
p <sup>ser 473</sup> -AKT	Anti-rabbit	60	Cell signaling	9271	1:1000
Anti-phosphotyrosine (Clone 4G10)	Anti-mouse	n/a	Upstate cell signaling	05-321	1:1000
Anti-Phospho tyrosine (PY-20)	anti-rabbit	n/a	BD laboratories	00 778	1:1000
GAPDH	Anti-rabbit	37	Abcam	ab9485	1:2000
GFP (Clone JL-8)	Anti-mouse	n/a	Clontech	632380	1:1000
GFP	Anti-rabbit	n/a	Abcam	6556	For IP
GST	Anti-rabbit	n/a	ABR	PA1-982A	1:5000
GLUT4	Anti-goat	45	Santa Cruz	SC1608	1:500
Munc18-1	Anti-mouse	66	SySy	116 011	1:1000
Munc18c	Anti-rabbit	66	In-house	n/a	1:5000
Myc	Anti-mouse	n/a	Santa Cruz	SC 9e10	1:1000
PY-20	anti-rabbit	n/a	BD laboratories	00 778	1:1000

			BD		
SNAP23	Anti-rabbit	23	laboratories	pa1-738	1:1000
			BD		
SNAP25	Anti-rabbit	25	laboratories	610366	1:1000
Syntaxin-1A	Anti-mouse	34	SySy	110 111	1:1000
Syntaxin 4	Anti-rabbit	34	Chemicon	AB5330	for IP
Syntaxin 4	Anti-rabbit	34	In-House	n/a	1:5000
$\alpha$ -Tubulin	Anti-mouse	55	Sigma	T9026	1:5000
VAMP2	Anti-mouse	18	SySy	104 211	1:5000

---



Female mice 4-6 months old were used for Tg studies. Doc2b knockout mice were initially characterized for neuronal alterations (174), with breeders obtained from Dr. Matthijs Verhage of VU University in Amsterdam to establish a colony at Indiana University School of Medicine. The colony stock at VU consisted of mice backcrossed for more than 15 generations on the C57BL/6 J background and was carried further through an additional 2 generations upon arrival at the Indiana University School of Medicine Laboratory Animal Resources Center. Paired littermates from heterozygous crossings were used for experimentation, with genotypes determined by PCR on DNA from tail-biopsy specimens (primers, 5' to 3': RZ-cttgtcaatggccgatccc; mad 206-cggctacgagtcagacgactg; mav 102-cacacaagccaccaggagag), whereby the PCR product of the wild-type (Wt) allele was 650 bp and that of the targeted allele was 800 bp, as described (174).

The Puc-Combi-CMV plasmid used for generation of tetracycline-repressible Doc2b Tg mice was a gift from Dr. Ulli Certa (Hoffman Roche, Switzerland) (175). The full-length cDNA for Doc2b carrying an N-terminal Myc tag was inserted into the pCombi-CMV vector at the PmeI site. The construct was linearized by digestion with NotI and microinjected into the nucleus of pre-implantation embryos. These embryos were then transferred into the oviduct of pseudo-pregnant C57Bl6J female mice by the Indiana University, School of Medicine Transgenic Animal Facility. Thirty eight pups were screened for the presence of the transgene using PCR of genomic DNA, with four founders resulting. Of the four lines, F5170, the line with the highest expression (~ 3

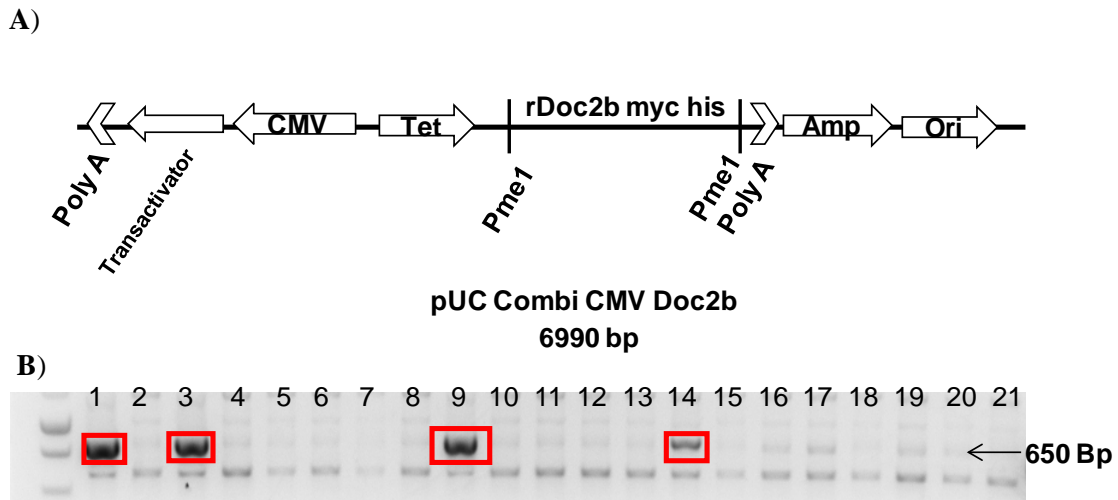


**Figure 2-1. Linear sequence schematic of Doc2b Myc his and genotyping analysis of Doc2b Transgenic mice.** (A) Doc2b Myc his cDNA was inserted into the pUC-Combi CMV vector. Doc2b insert was under the control of the bidirectional CMV promoter. Tetracycline administration sequesters the transactivator which inhibits the tet operon from driving the expression. (B) PCR genotyping of tail DNA with Doc2b primers was run on 2% agarose gel to identify Doc2b Tg founders. Four founders were identified among 38 pups that were initially screened. Lane 1- founder 5168, lane 3- founder 5170, lane 9- founder 5178, and lane 14- founder 5183.

fold) was selected for phenotypic characterization. Genotypes determined by PCR on DNA from tail-biopsy specimens (primers for Tg: 5' to 3': #3-ggcagaggacaagtcctgg; #9-agaggattgagcgttgccac; and #10-acgacgaggcttcaggatcataa. Primers for Wt: 5' to 3': O-ggaaagaaggcgaatggaag and F-tcactccagggtttcatcc), whereby the PCR product of the wild-type (Wt) allele was 500 bp and that of the Tg allele was 681 and 277 bp.

## **2.3 METHODS**

### **2.3.1 Tissue Homogenization**

For immunoblot analysis of protein content, tissues (100 mg frozen) were cut on dry ice. Tissues were homogenized using a Polytron PTA 10S homogenizer in 2 mL of NP40 detergent buffer (25 mM Tris, pH 7.4, 1% NP40, 10% glycerol, 50 mM sodium fluoride, 10 mM sodium pyrophosphate, 137 mM sodium chloride, 1 mM sodium vanadate, 1 mM phenylmethylsulfonyl fluoride, 10 µg/ml aprotinin, 1 µg/ml pepstatin and 5 µg/ml leupeptin). Lysates were centrifuged at 2000 x g for 5 minutes at 4 °C, and subsequent supernatants microcentrifuged at 13,500 x g for 20 minutes at 4 °C to clarify. Lysates were boiled for five minutes in leammli sample buffer (12% SDS, 37.5 mM Tris pH 6.8, 60% glycerol, 60 mM dithiothreitol and 0.02% bromophenol blue. Lysates for analysis of GLUT4 were left unboiled. Proteins were resolved on 10-12% SDS-PAGE followed by transfer to PVDF or nitrocellulose (for GLUT4) membrane for immunoblotting.

### **2.3.2 Islet RNA Isolation and Quantitative-PCR**

Total RNA from mouse islets was obtained using the RNeasy mini kit (Qiagen). RNA (2 µg) was reverse-transcribed with the Superscript First Strand cDNA synthesis kit (Invitrogen), and 1% of the product was used for Q-PCR. Doc2b primers used: forward 5'- ccagcaaggcaaataagctc; reverse 5'- attgggcttcagcttctca. GAPDH primers used: forward 5'-atggtgaaggtcgggtggaacg and reverse 5'-gttgatcatggatgaccttgccc. Q-PCR conditions: 50 °C for 2 minutes hold (UDG incubation), 95 °C for 2 minutes hold, then 40 cycles of 95 °C for 15 seconds and 60 °C for 30 seconds. The delta delta CT method was used for analyzing data and values were normalized to GAPDH for relative gene expression.

### **2.3.3 Intraperitoneal Glucose Tolerance Test and Insulin Tolerance Test**

Male Doc2b<sup>+/+</sup>, Doc2b<sup>+/-</sup> and Doc2b<sup>-/-</sup> mice (4-6 months old) were fasted for either 6 h (08:00-14:00) or 18 h (18:00-12:00) before IPGTT. Similarly, female Doc2b Tg and their littermate Wt mice (4-6 months) were fasted for 6 hours before IPGTT. Following sample collection of fasted blood from the tail, animals were given glucose (2 g/kg body weight) by intraperitoneal injection and blood glucose readings were taken at 30 minutes intervals over 120 minutes period for the IPGTT. Blood was collected from the tail vein and diluted in saline for measurement of blood glucose using the Hemocue glucometer (Mission Viejo, CA). For the ITT, mice were fasted for 6 h (08:00-14:00 h). Following sample collection of fasted blood, animals were injected intraperitoneally with Humulin R (0.75 U/kg body weight) and blood glucose readings were taken at 15, 30, 60 and 90 minutes after injection. Tetracycline (1 mg/ml) was administered in drinking water for a

week to Doc2b Tg and their Wt littermate mice to repress the Doc2b transgene levels, and IPGTT reported on the same mice.

#### **2.3.4 Skeletal Muscle Subcellular Fractionation**

Hindlimb skeletal muscle was subfractionated into PM and intracellular membrane components as described (89, 176). Doc2b<sup>-/-</sup> and Wt littermate male mice (4-6 months old) were used for knockout studies, while female Doc2b Tg and Wt littermate mice (4-6 months) were used for Tg studies. Mice were fasted overnight for 16 h, injected intraperitoneally with Humulin R (21 U/kg body weight) or vehicle. Mice were killed after 40 minutes of injection for dissection of the hindquarter muscles into homogenization buffer (20 mM HEPES pH 7.4, 250 mM Sucrose, 1 mM EDTA, 5 mM benzamidine, 10 µg/ml aprotinin, 5 µg/ml leupeptin, 1 µg/ml pepstatin, 1 mM phenylmethylsulfonyl fluoride) for Polytron homogenization and differential centrifugation to yield pellets containing t-tubule and sarcolemmal membrane fractions as described (89, 176). Homogenates were centrifuged at 2000 x g for 5 minutes at 4 °C, and supernatant then centrifuged at 9000 x g for 20 minutes at 4 °C. That supernatant was subsequently centrifuged at 180,000 x g for 90 minutes. Pellets containing t-tubule and sarcolemmal membrane fractions (named P1 and P2) were resuspended in 1% NP40 lysis buffer and proteins resolved by 10% SDS-PAGE for subsequent immunoblotting for GLUT4.

### **2.3.5 *In Vitro* Skeletal Muscle Glucose Uptake**

Extensor digitorum longus (EDL) muscles were excised By Dr. Joe Brozinick (Eli Lilly) and immediately placed into a 25 mL Erlenmeyer flask containing 2 mL of Krebs-Henseleit Buffer (KHB; 116 mM NaCl, 2.5 mM NaHCO<sub>3</sub>, 4.6 mM KCl, 32 mM mannitol, 8 mM glucose, 1.2 mM KH<sub>2</sub>PO<sub>4</sub> and 0.01% bovine serum albumin) for one hour at 29 °C in a shaking water bath. Each muscle was then transferred into a flask containing incubation media (KHB containing 13.3 nM insulin or saline) for 30 minutes. Then, muscles were transferred into a flask with label media (116 mM NaCl, 2.5 mM NaHCO<sub>3</sub>, 4.6 mM KCl, 39 mM mannitol, 1 mM 2-deoxy glucose, 1.2 mM KH<sub>2</sub>PO<sub>4</sub>, 0.01% bovine serum albumin, 5 mCi/mMol of <sup>3</sup>H-2-deoxyglucose (Perkin Elmer), 8 μCi/mMol of mannitol containing 13.3 nM insulin or saline) for 20 minutes for glucose uptake and freeze clamped as previously described (177). Weighed muscles were then homogenized with 1 N hydrochloric acid followed by neutralization with 1 N potassium hydroxide. 200 μl of the resulting sample was added to 4 ml of scintillation cocktail and disintegrations per minute were measured using a scintillation counter.

### **2.3.6 Isolation, Culture and Perfusion of Mouse Islets**

Pancreatic mouse islets were isolated as previously described (178), from 10-14 weeks old male mice for knockout studies and 10-14 weeks old female mice for Tg mice studies. Islets cultured overnight in CMRL media (Gibco) were hand-picked onto cytodex bead columns (Fisher), pre-incubated in Krebs-Ringer bicarbonate buffer (10 mM HEPES pH 7.4, 134 mM NaCl, 5 mM NaHCO<sub>3</sub>, 4.8 mM KCl, 1 mM CaCl<sub>2</sub>, 1.2 mM MgSO<sub>4</sub>, 1.2 mM KH<sub>2</sub>PO<sub>4</sub>) containing 2.8 mM glucose and 0.1% BSA for 30 minutes and

perfused for at a rate of 0.3 ml/minute. During stimulations, islets were perfused with 20 mM glucose for knockout studies and 16.7 mM glucose for transgenic studies. Following 20 minutes return to low glucose, islets were stimulated with 35 mM KCl, with fractions collected every 1-3 minutes. Insulin secreted into fractions and the corresponding islet lysate insulin content was quantified by sensitive radioimmunoassay (RIA; Millipore) and regular RIA kit respectively.

### **2.3.7 Cell Culture and Transient Transfection**

MIN6 beta cells were cultured in Dulbecco's modified Eagle's medium (DEEM with 25 mM glucose) supplemented with 15% fetal bovine serum, 100 units/ml penicillin, 100 µg/mL streptomycin, 292 µg/mL L-glutamine, and 50 µM beta-mercaptoethanol as described previously (179). MIN6 beta cells at 50-60% confluence were transfected with 40 µg of cesium chloride purified plasmid DNA per 10 cm<sup>2</sup> dish using Transfectin (Bio-Rad) to obtain ~40-70% transfection efficiency. After 48 h of incubation, cells were incubated for 2 hours in freshly prepared modified Krebs-Ringer bicarbonate buffer (MKRBB; 5 mM KCl, 120 mM NaCl, 15 mM Hepes pH 7.4, 24 mM NaHCO<sub>3</sub>, 1 mM MgCl<sub>2</sub>, 2 mM CaCl<sub>2</sub>, and 1 mg/ml BSA) and gassed (95% O<sub>2</sub>/5% CO<sub>2</sub>) for 30 minutes. Cells were harvested in 1% NP40 lysis buffer for use in immunoprecipitation or western blotting and in homogenization buffer for subcellular fractionation.

Rat L6 muscle cells stably expressing GLUT4 with an exofacial myc-epitope (gift from Amira Klip, Univ of Toronto) were cultured as previously described (180). Myoblasts were maintained in  $\alpha$ -MEM (Gibco) containing 5.5 mM glucose and 10% fetal

bovine serum (Fisher Scientific). Myoblasts were electroporated (0.20 kV and 960  $\mu$ Farad) with 150  $\mu$ g of cesium chloride purified GFP Doc2b DNA per 10  $\text{cm}^2$  dish. After electroporation, cells were allowed to adhere to plates for 48 hours. Cells were then washed with serum free  $\alpha$ -MEM and serum starved for 2 hours in the same medium followed by stimulation for 5 minutes with 100 nM insulin. Cells were harvested in 1% NP40 lysis buffer and detergent lysates used for immunoprecipitation.

### **2.3.8 Subcellular Fractionation of MIN6 Beta Cells**

MIN6 beta cells at 80-90% confluence were harvested into 1 mL of homogenization buffer (20 mM Tris, pH 7.4, 0.5 mM EDTA, 0.5 mM EGTA, 250 mM sucrose, 1 mM DTT, 1 mM sodium orthovanadate, 10  $\mu$ g/mL leupeptin, 4  $\mu$ g/mL aprotinin, 2  $\mu$ g/mL pepstatin, and 100  $\mu$ M phenylmethylsulfonyl fluoride). Cells were disrupted by 10 strokes of a 27 gauge needle, and homogenates were centrifuged at 900 x g for 10 minutes. Postnuclear supernatants were centrifuged at 5,500 x g, for 15 minutes and the subsequent supernatant centrifuged at 25,000 x g for 20 minutes to obtain the secretory granule fraction in the pellet. The supernatant was further centrifuged at 100,000 x g for 1 hour to obtain the cytosolic fraction. PM fractions were obtained by mixing the postnuclear pellets with 1 mL of Buffer A (0.25 M Sucrose, 1 mM  $\text{MgCl}_2$ , and 10 mM Tris, pH 7.4) and 2 mL of Buffer B (2 M sucrose, 1 mM  $\text{MgCl}_2$ , and 10 mM Tris, pH 7.4). The mixture was overlaid with Buffer A and centrifuged at 113,000 x g for 1 hour to obtain an interface containing the PM fraction. This interface was collected and diluted to 2 mL with the homogenization buffer for centrifugation at 3,000 x g for 10



minutes, and the resulting pellet was collected as the PM fraction. All pellets were resuspended in 1% NP40 lysis buffer to solubilize membrane proteins.

### **2.3.9 Co-immunoprecipitation**

PM fractions from MIN6 cells (1 mg) or cleared detergent lysates from L6 myoblasts (2.5 mg) were combined with mouse anti-Syntaxin 1 antibody or rabbit anti-Syntaxin 4 antibody for 2 hours at 4 °C, followed by a second incubation with protein G Plus-agarose beads for 2 hours. The resultant immunoprecipitates were subjected to 10% SDS-PAGE followed by transfer to PVDF membranes for immunoblotting.

For immunoprecipitation using skeletal muscle lysates, mice were fasted 4 h (08:00-12:00) and injected intraperitoneally with 10 U/kg body weight insulin or saline for 5 minutes, after which animals were killed for hindlimb excision and lysate preparation. Skeletal muscle lysate protein (4 mg) was used in rabbit anti-Munc18c or rabbit anti-Syntaxin 4 immunoprecipitation reactions.

### **2.3.10 Recombinant Proteins and Interaction Assays**

The GST-VAMP2 protein generated in *E. coli* BL21 bacteria was purified by glutathione-agarose affinity chromatography as described previously (173) for use in the Syntaxin accessibility assay. GST-VAMP2 protein linked to Sepharose beads was combined with 2 mg of L6 myoblast detergent cell lysate for 2 hours at 4 °C in NP40 lysis buffer, followed by three stringent washes with lysis buffer. The associated proteins

were resolved on 10–12% SDS-PAGE followed by transfer to PVDF membranes for immunoblotting of Syntaxin 4 and GST.

### **2.3.11 Statistical Analysis**

All data were evaluated for statistical significance using Student's *t* test for pairwise comparison of two groups (i.e. Doc2b<sup>+/-</sup> or Doc2b<sup>-/-</sup>, versus Doc2b<sup>+/+</sup> and Doc2b Tg versus Wt). Data are expressed as the mean  $\pm$  S.E.

## **CHAPTER 3. DOC2B IS A KEY EFFECTOR OF INSULIN SECRETION AND SKELETAL MUSCLE INSULIN SENSITIVITY**

**Portion of the text in this chapter is reproduced from:**

Ramalingam L, Oh E, Yoder SM., Brozinick JT, Kalwat MA, Groffen AJ., Verhage M, and Thurmond DC. (2012) Doc2b Is a Key Effector of Insulin Secretion and Skeletal Muscle Insulin Sensitivity. *Diabetes* 61, 2424-2432

Author contributions: Yoder SM generated data for Table 3-1. The rest of the data were generated by Ramalingam L.

### **3.1 INTRODUCTION**

Insulin secretion and GLUT4 recruitment events are highly regulated, maintained at very low levels in the absence of appropriate stimuli, and rapidly and robustly activated in response to stimuli. Maintenance and activation of exocytotic processes are regulated by the Munc18 proteins, which bind and facilitate the accessibility of Syntaxin to interact with its cognate SNARE partners (181-182). In homogenates of beta cells, adipocytes and skeletal muscle, Munc18c binds to Syntaxin 4 in the absence of stimuli, dissociating in response to stimuli whilst undergoing tyrosine phosphorylation (41, 154, 183).

Concurrent with its dissociation from Syntaxin 4, phosphorylated Munc18c switches its affinity towards binding to the protein Doc2b in MIN6 clonal beta cells (148). Elevation of calcium is reported to yield complexation of Doc2b with Syntaxin 4 as well (168). *In vitro*, Doc2b selectively binds to Munc18-1 via Doc2b-domain C2A, and binds to Munc18c via Doc2b-domain C2B (164-165). In MIN6 beta cell and 3T3-L1 adipocyte clonal cell studies, the RNAi-mediated reduction of Doc2b attenuates stimulus-induced insulin exocytosis and GLUT4 exocytosis events, respectively (165, 168, 171). By contrast, Doc2b over-expression in these cell types enhances stimulus-induced exocytosis but not basal exocytosis (165, 168, 171). Unlike Munc18c and Syntaxin 4, the relevance of Doc2b function for whole body glucose homeostasis remains untested. Moreover, although Doc2b mRNA abundance in islets of congenic obese mice was significantly reduced (184), Doc2b deficiency has yet to be correlated with T2D, such that its promise as a novel therapeutic target remains in question.

In this study we utilized classic Doc2b knockout mice to investigate the role of Doc2b in insulin granule exocytosis and insulin-stimulated GLUT4 vesicle translocation, culminating in a new *in vivo* model of glucose intolerance and insulin resistance. Mechanistically, islet perfusion studies revealed Doc2b to function in both phases of GSIS, implicating Doc2b to act on both types of Munc18 and Syntaxin-based SNARE complexes. Furthermore, skeletal muscle fractionation studies demonstrated a requirement for Doc2b in insulin-stimulated GLUT4 accumulation; Munc18-SNARE interactions in muscle fractions were found to be altered by Doc2b deletion. Strikingly, the disease phenotype of the Doc2b<sup>+/-</sup> mice was equally severe to that of the Doc2b<sup>-/-</sup> mice, suggesting this to be a haploinsufficiency worthy of future investigation in diabetes therapies.

## **3.2 RESULTS**

### **3.2.1 Doc2b Knockout Mice are Glucose Intolerant**

While the Doc2b<sup>-/-</sup> mice have been characterized for alterations in neuronal protein expression and synaptic vesicle trafficking function, such studies are lacking for evaluation of Doc2b function in tissues relevant to glucose homeostasis. Gene ablation in the heterozygous and homozygous knockout mice was confirmed by comparing Doc2b mRNA levels with Doc2b<sup>+/+</sup> (wild type, Wt) littermates in brain, skeletal muscle (whole hind limb), liver and fat (epididymal) by quantitative PCR (Fig. 3-1A).

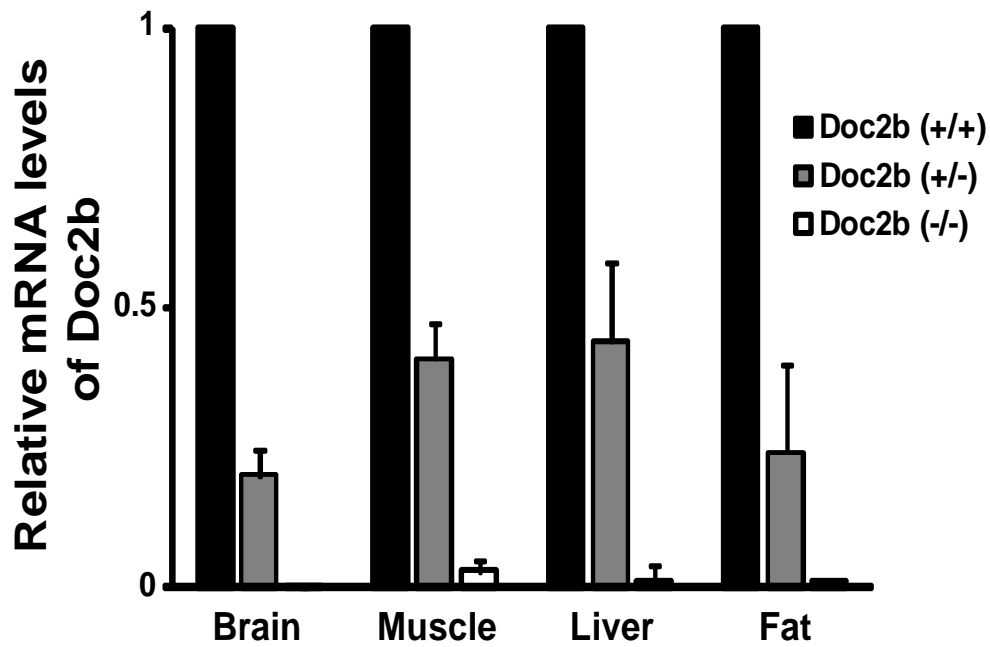


**Figure 3-1. mRNA expression in glucose homeostatic tissues from Doc2b<sup>+/-</sup> and Doc2b<sup>-/-</sup> knockout mice.** Brain, skeletal muscle (whole hindlimb), liver and fat (epididymal) were isolated from Doc2b<sup>+/+</sup>, Doc2b<sup>+/-</sup>, and littermate Doc2b<sup>-/-</sup> mice for use in quantitative PCR analysis; quantified relative to GAPDH from three sets of tissues.

Protein levels of Doc2b were reduced, in the absence of significant differences in other SNARE or Munc18 proteins implicated in insulin exocytosis, in islets isolated from Doc2b<sup>+/-</sup> and Doc2b<sup>-/-</sup> knockout mice, compared with the Doc2b<sup>+/+</sup> islets (Fig. 3-2A-B). The Doc2b antibody showed non-specific background, consistent with previous work (174). Doc2b levels were reduced in heart, skeletal muscle, liver and fat tissues of Doc2b<sup>+/-</sup> and Doc2b<sup>-/-</sup> mice, without alterations in abundance of Syntaxin 4, SNAP23, VAMP2 or Munc18c (Fig. 3-3A-B). Abundance of the glucose transporter GLUT4 protein was also unchanged in heart, skeletal muscle and fat from Wt or Doc2b-deficient mice (Fig. 3-3A-B).

To determine the effects of Doc2b deficiency upon whole-body glucose tolerance, 4-6 month old Doc2b<sup>+/+</sup>, Doc2b<sup>+/-</sup> and Doc2b<sup>-/-</sup> mice were subjected to IPGTTs. Glucose tolerance after either 18 h or 6 h fasting in Doc2b<sup>+/-</sup> and Doc2b<sup>-/-</sup> male mice was significantly impaired in comparison to Wt mice (Fig. 3-4A-B and Fig. 3-5). Doc2b<sup>-/-</sup> and Doc2b<sup>+/-</sup> mice showed similar fasting glucose levels compared with Wt mice (Table 3-1). Area under the curve (AUC) analysis confirmed Doc2b<sup>+/-</sup> and Doc2b<sup>-/-</sup> mice to be significantly less tolerant than Wt (Fig. 3-4B). These data suggest that full or partial depletion of Doc2b exerted a negative effect upon glucose tolerance *in vivo*. We next determined whether glucose intolerance was related to alterations in body weight or fasted serum metabolites commonly linked to aberrations in glucose metabolism. Table 3-1 shows serum triglycerides, cholesterol and non-esterified fatty acids (NEFAs) to be similar in Wt versus Doc2b<sup>+/-</sup> and Doc2b<sup>-/-</sup> mice. Table 3-2 shows body weights of Doc2b<sup>+/-</sup> and Doc2b<sup>-/-</sup> mice to be equivalent to that of Wt littermate mice. Tissue and

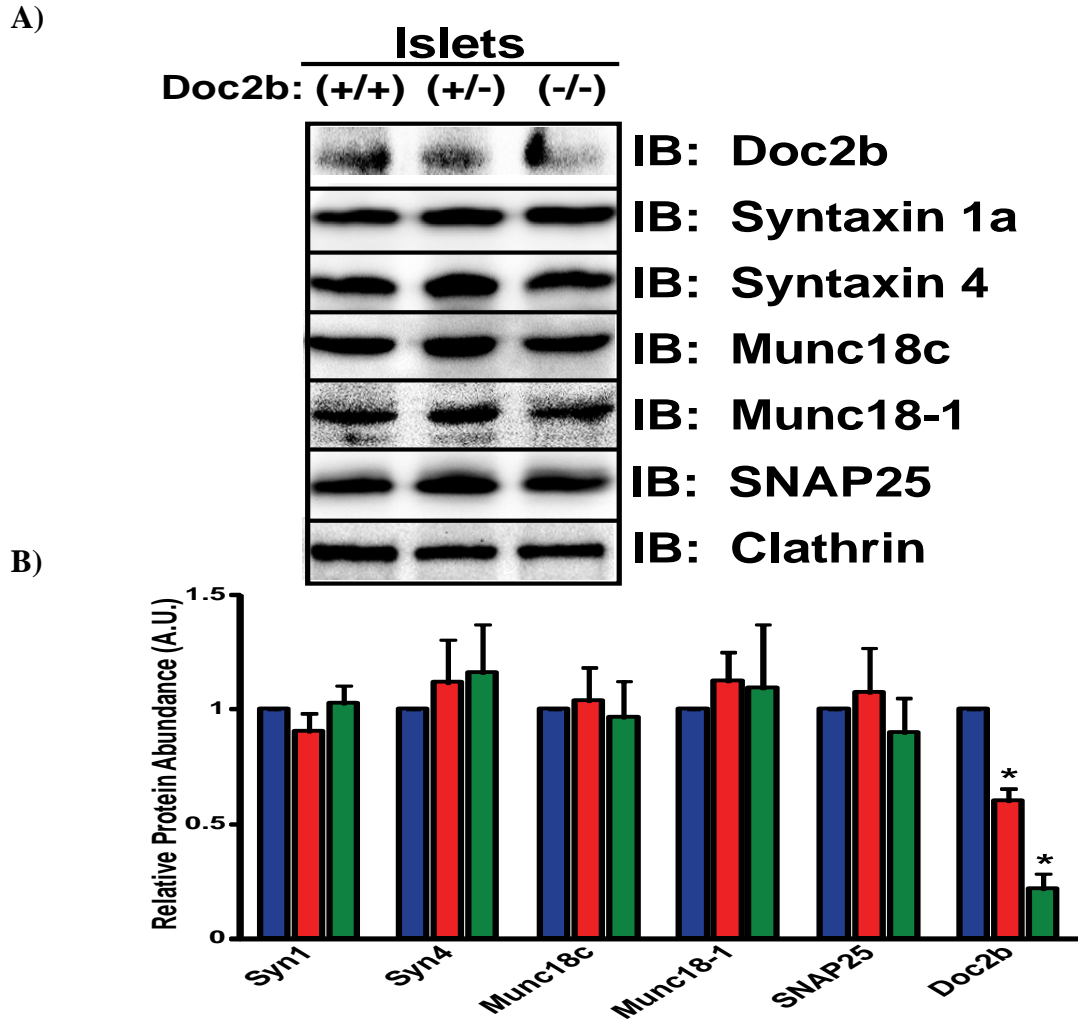
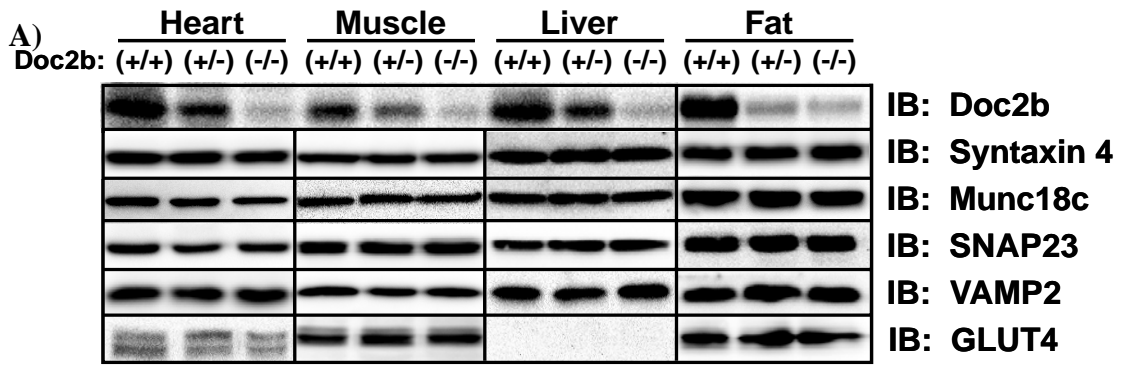


**Figure 3-2. Protein expression in islets from  $Doc2b^{+/-}$  and  $Doc2b^{-/-}$  knockout mice.**

**(A)** Islets were isolated from  $Doc2b^{+/+}$ ,  $Doc2b^{+/-}$ , and  $Doc2b^{-/-}$  knockout mice for analysis of SNARE protein expression. **(B)** Optical density scanning was used to quantify band intensities to derive the average  $\pm$  S.E. for each protein in each genotype (normalized to Wt=1) present in islets ( $n>3$ ).





**B)**

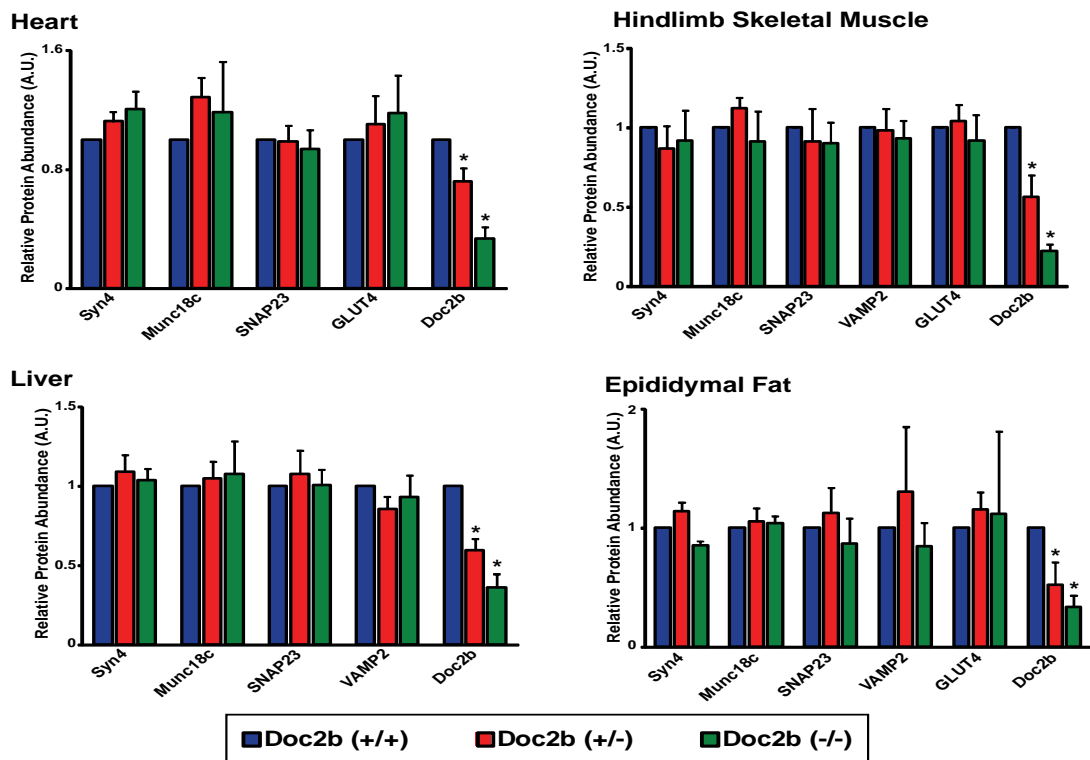
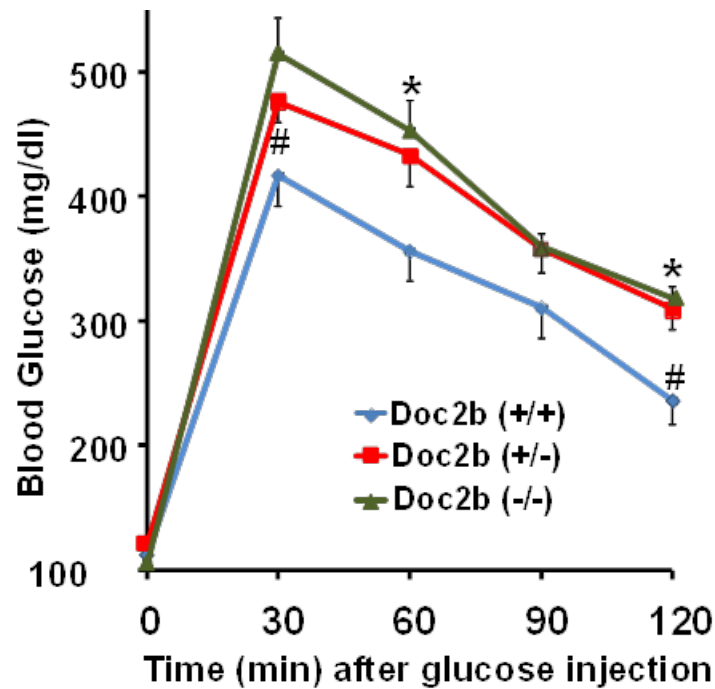


**Figure 3-3. Protein expression in glucose homeostatic tissues from *Doc2b*<sup>+/-</sup> and *Doc2b*<sup>-/-</sup> knockout mice. (A) Assessments of GLUT4, SNARE and SNARE accessory protein abundances were made by immunoblot for heart, skeletal muscle, liver and epididymal fat. (B) Quantification of the SNARE and its accessory proteins.**

A)



B)

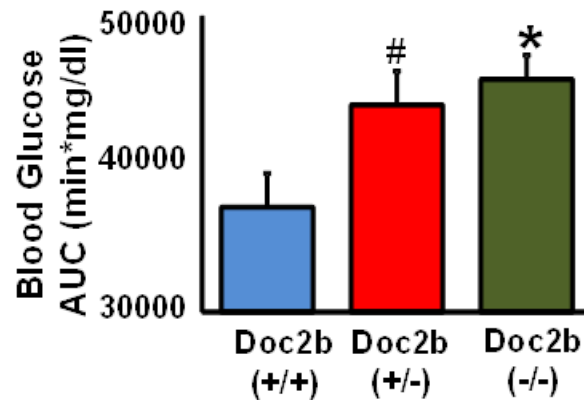


**Figure 3-4. Doc2b<sup>+/-</sup> and Doc2b<sup>-/-</sup> knockout mice are glucose intolerant.** (A) IPGTT of Doc2b<sup>+/-</sup>, Doc2b<sup>-/-</sup> and littermate Doc2b<sup>+/+</sup> mice was performed by intraperitoneal injection of D-glucose (2 g/kg body weight) into 4-6 month old male mice fasted for 18 h. (B) AUC data shown as the average  $\pm$  standard error (S.E.) from 7 sets of mice: \*P < 0.05, Wt versus Doc2b<sup>-/-</sup>; #P < 0.05, Wt versus Doc2b<sup>+/-</sup>.

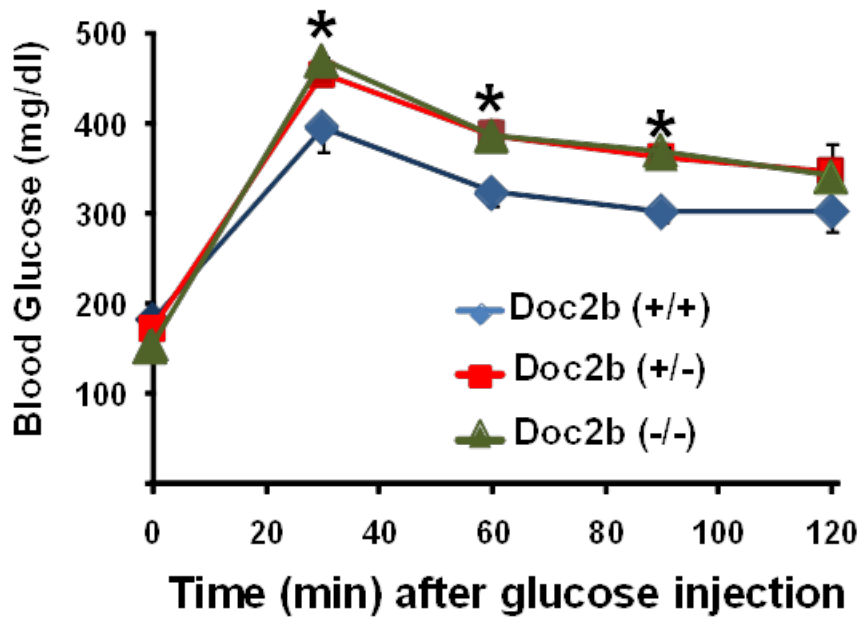


**Figure 3-5. Doc2b<sup>+/-</sup> and Doc2b<sup>-/-</sup> knockout mice are glucose intolerant after 6 hours fast.** Male Doc2b<sup>+/+</sup>, Doc2b<sup>+/-</sup> and Doc2b<sup>-/-</sup> mice (4-6 months old) were fasted for 6 h (08:00-14:00). Following sample collection of fasted blood, animals were given glucose (2 g /kg body weight) by intraperitoneal injection and blood glucose readings were taken at 30 minutes intervals over 120 minutes for IPGTT. Data represent the average  $\pm$  S.E.; \*P<0.05 (n=4 for Doc2b<sup>+/-</sup>, n=3 each for Doc2b<sup>+/+</sup> and Doc2b<sup>-/-</sup>).

**Table 3-1.** Fasting serum analytes of Doc2b<sup>+/+</sup>, Doc2b<sup>+/-</sup> and Doc2b<sup>-/-</sup> mice.

	<b>Doc2b<sup>+/+</sup></b>	<b>Doc2b<sup>+/-</sup></b>	<b>Doc2b<sup>-/-</sup></b>
<b>Glucose (mg/dl)</b>	112 ± 9	121 ± 5	105 ± 2
<b>Triglycerides (mg/dl)</b>	96.8 ± 15.6	107.2 ± 13.2	89.1 ± 9.3
<b>Cholesterol (mg/dl)</b>	123.2 ± 6.5	118.2 ± 8.9	128.5 ± 5.1
<b>NEFA (mmol/L)</b>	1.19 ± 0.11	1.33 ± 0.12	1.32 ± 0.04

Data represent the average ± S.E; no significant differences were detected amongst groups. Serum was collected from 18 h fasted Doc2b<sup>+/+</sup>, Doc2b<sup>+/-</sup> and Doc2b<sup>-/-</sup> male littermate mice at 4-6 months of age (n=7 for each genotype) for determination of parameters shown.

**Table 3-2.** Tissue weights normalized to body weight of Doc2b<sup>+/+</sup>, Doc2b<sup>+/-</sup> and Doc2b<sup>-/-</sup> mice.

	Doc2b <sup>+/+</sup>	Doc2b <sup>+/-</sup>	Doc2b <sup>-/-</sup>
<b>Body weight (g)</b>	28.3 ± 0.8	30.7 ± 0.9	30.7 ± 0.8
<b>Tissue (% body weight)</b>			
<i>Liver</i>	3.61 ± 0.23	2.85 ± 0.23	3.92 ± 0.10
<i>Lung</i>	0.65 ± 0.11	0.82 ± 0.08	0.81 ± 0.09
<i>Heart</i>	0.62 ± 0.18	0.79 ± 0.20	0.91 ± 0.07
<i>Fat</i>	2.66 ± 0.53	2.24 ± 0.49	2.20 ± 0.23
<i>Pancreas</i>	0.77 ± 0.11	0.56 ± 0.05	1.04 ± 0.06
<i>Kidney</i>	1.32 ± 0.07	1.17 ± 0.05	1.36 ± 0.10
<i>Muscle</i>	1.52 ± 0.14	1.22 ± 0.12	1.57 ± 0.12
<i>Spleen</i>	1.0 ± 0.48	0.9 ± 0.42	1.0 ± 0.23

Data represent the average ± S.E. Weights were collected from Doc2b<sup>+/+</sup>, Doc2b<sup>+/-</sup> and Doc2b<sup>-/-</sup> male littermate mice at 4-6 months of age (n=7 for Doc2b<sup>+/-</sup> and Doc2b<sup>-/-</sup>, n=5 for Doc2b<sup>+/+</sup>) for determination of parameters shown. No statistical differences were seen.

organ weights were also equivalent, both when normalized to body weight of the whole animal and to absolute tissue weight (3-3). By contrast, serum insulin levels taken 10 minutes post injection during the IPGTT were significantly reduced in the Doc2b<sup>-/-</sup> mice, but not in the Doc2b<sup>+/-</sup> or Wt mice (Fig. 3-6). These data indicate an insulin secretory defect.

### **3.2.2 Impaired Biphasic Insulin Secretion in Islets Isolated from Doc2b Knockout Mice**

To investigate the potential defect in islet beta cell glucose-stimulated insulin release, we isolated islets from male Doc2b<sup>+/+</sup>, Doc2b<sup>+/-</sup> and Doc2b<sup>-/-</sup> mice for perfusion analyses. *Ex vivo*, insulin secretion under basal conditions was similar amongst all three islet groups (Fig. 3-6A), similar to our findings of insulin content in fasted serum. Glucose stimulation (20 mM) elicited a 12-fold peak increase in insulin release from Wt islets during the initial phase, whereas Doc2b<sup>+/+</sup> and Doc2b<sup>-/-</sup> islets showed less response. During the second-phase, Doc2b<sup>+/-</sup> and Doc2b<sup>-/-</sup> islets secreted substantially less insulin (Fig. 3-7A-B). Consistent with impaired first-phase GSIS, KCl-stimulated insulin release was precipitously decreased as Doc2b expression decreased (Fig. 3-8A). Insulin content in Doc2b<sup>+/-</sup> and Doc2b<sup>-/-</sup> islets was comparable to that in Wt islets (Fig. 3-8B). These data indicated that Doc2b-depleted islets lacked function during both phases of GSIS, corroborating the deficient serum insulin content observed during the IPGTT in the Doc2b<sup>-/-</sup> mice. This is the first demonstration of Doc2b requirement in both phases of insulin secretion from islets.

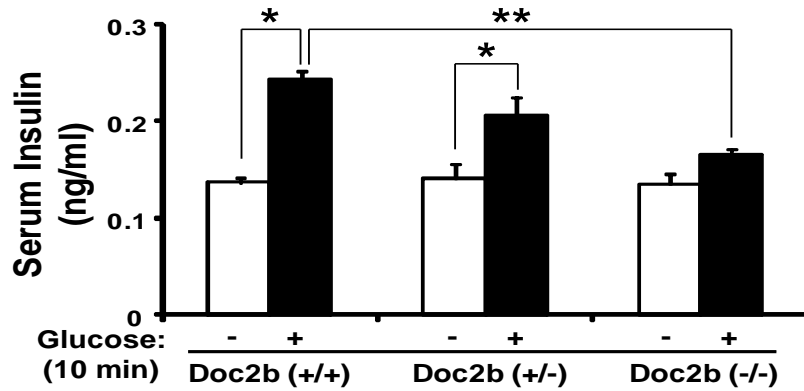


**Figure 3-6. Doc2b<sup>+/-</sup> and Doc2b<sup>-/-</sup> knockout mice have reduced serum insulin concentration post-glucose injection.** 10 minutes post-injection of glucose during the IPGTT, serum was collected and measured for insulin by RIA analysis. Data shown as the average ± standard error (S.E.) from sets of 4 mice: \*P< 0.05, versus pre-injected Wt; \*\*P< 0.05, stimulated Doc2b<sup>-/-</sup> versus Wt.

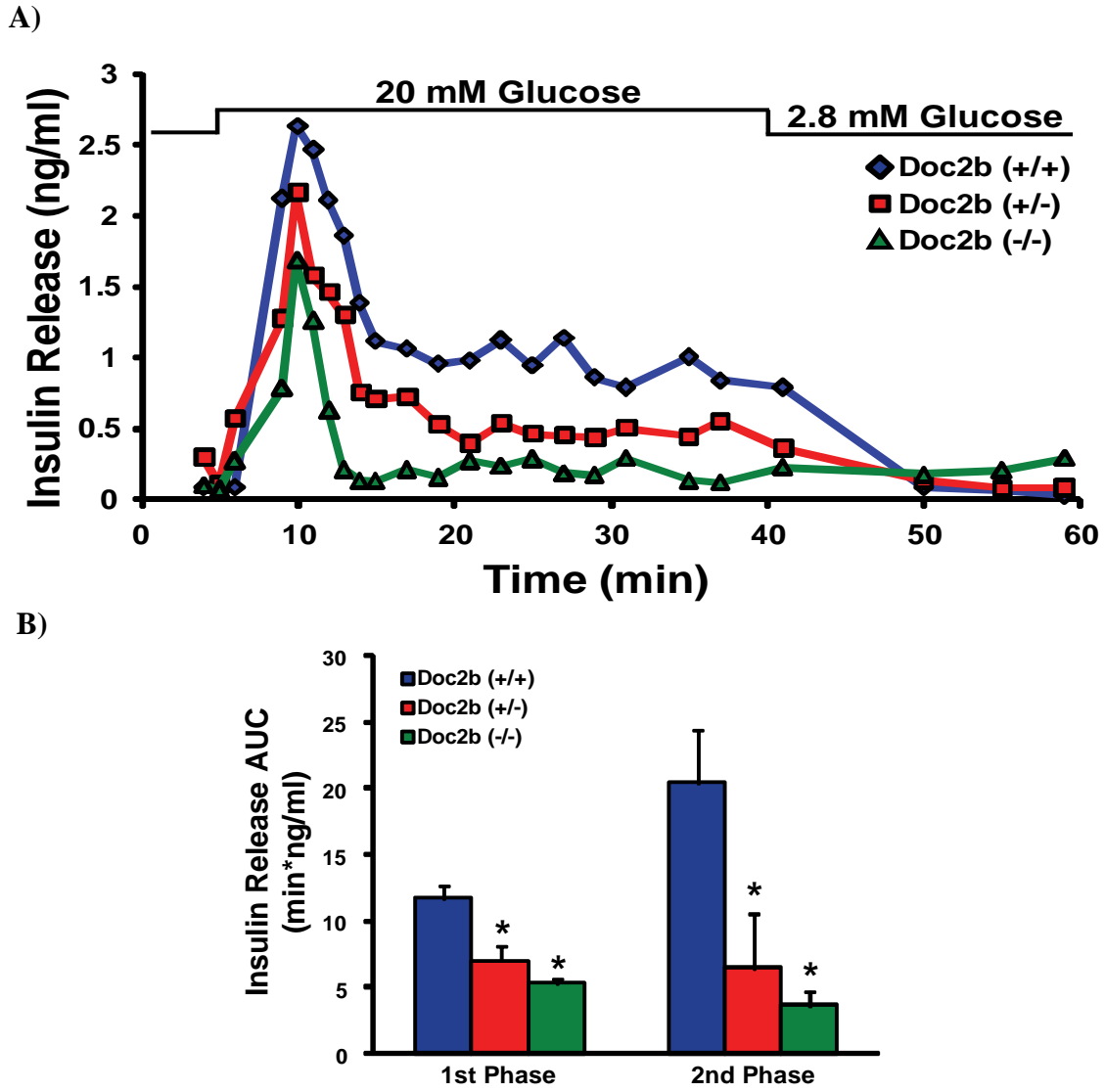


**Figure 3-7.  $Doc2b^{+/-}$  and  $Doc2b^{-/-}$  knockout mouse islets show reduced biphasic insulin release.** (A) Islets freshly isolated from  $Doc2b^{+/-}$ ,  $Doc2b^{-/-}$  and littermate  $Doc2b^{+/+}$  mice were cultured overnight and handpicked under a fluorescence microscope into groups of 40 and layered onto cytodex bead columns for perfusion. Islets were first pre-incubated for 30 minutes in low glucose (2.8 mM), followed by basal sample collection (1-10 min) at low glucose to establish a baseline. Glucose was then elevated to



20 mM for 35 min, then returned to low glucose for 20 min. Eluted fractions were collected at 1-3 min intervals at a flow rate of 0.3 ml/min and insulin secretion determined by RIA, as depicted in a representative experiment. **(B)** Quantitation of the AUC for first (11-17 min) and second (18-45 min) phase insulin secretion from islets, normalized to baseline; data are presented as average  $\pm$  S.E. of 4 sets of perfused islets, \* $P < 0.05$  versus Doc2b<sup>+/+</sup>.

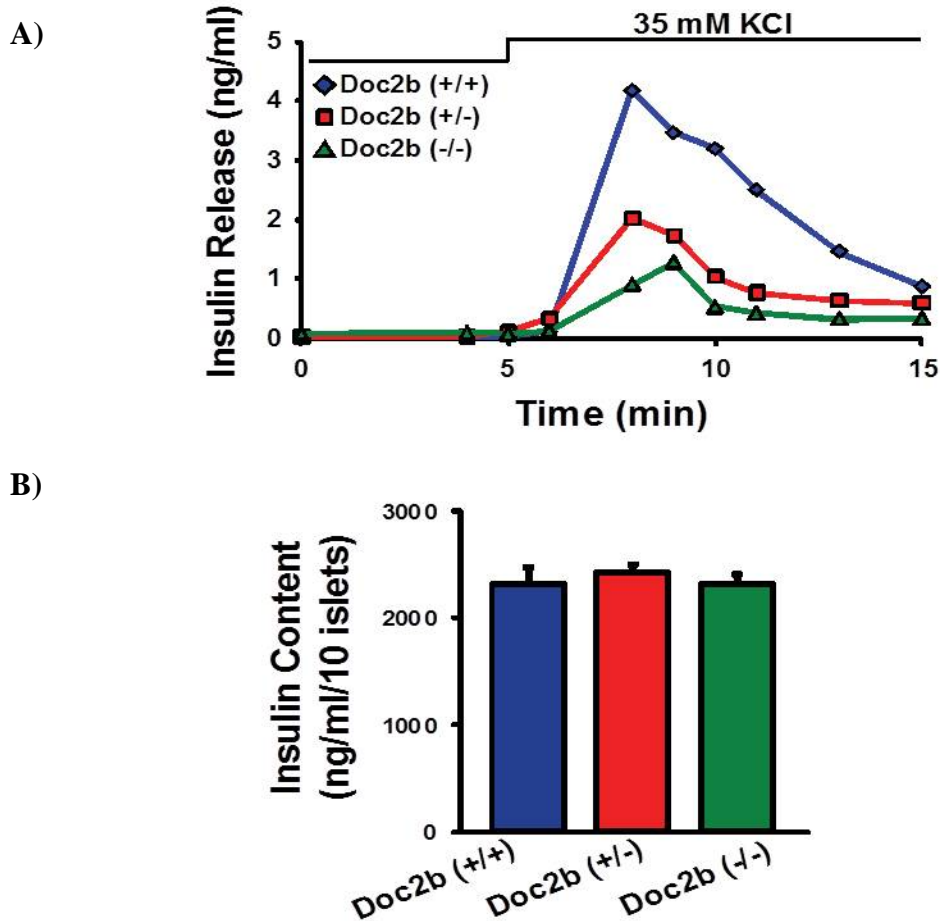


**Figure 3-8. Doc2b<sup>+/-</sup> and Doc2b<sup>-/-</sup> knockout mouse islets show reduced insulin release in response to KCl stimulation.** (A) Perfused islets from Fig. 3-7 following a 25 minutes rest under basal conditions, then stimulated with 35 mM KCl for 10 minutes, and finally returned to 2.8 mM glucose. (B) Average insulin content per 10 islets from Doc2b<sup>+/+</sup>, Doc2b<sup>+/-</sup> and Doc2b<sup>-/-</sup> littermate male mice used in perfusion studies above.

**Table 3-3.** Tissue weights of Doc2b<sup>+/+</sup>, Doc2b<sup>+/-</sup> and Doc2b<sup>-/-</sup> mice.

	<b>Doc2b<sup>+/+</sup></b>	<b>Doc2b<sup>+/-</sup></b>	<b>Doc2b<sup>-/-</sup></b>
<b>Tissue (g)</b>			
<i>Liver</i>	1.24 ± 0.11	1.03 ± 0.07	1.29 ± 0.09
<i>Lung</i>	0.22 ± 0.03	0.30 ± 0.03	0.23 ± 0.03
<i>Heart</i>	0.18 ± 0.05	0.29 ± 0.06	0.25 ± 0.02
<i>Fat</i>	0.78 ± 0.14	0.84 ± 0.18	0.56 ± 0.07
<i>Pancreas</i>	0.26 ± 0.03	0.21 ± 0.02	0.29 ± 0.02
<i>Kidney</i>	0.47 ± 0.08	0.43 ± 0.02	0.38 ± 0.03
<i>Muscle</i>	0.55 ± 0.11	0.45 ± 0.05	0.43 ± 0.03
<i>Spleen</i>	0.34 ± 0.13	0.32 ± 0.12	0.29 ± 0.07

Data represent the average ± S.E. Weights were collected from Doc2b<sup>+/+</sup>, Doc2b<sup>+/-</sup> and Doc2b<sup>-/-</sup> male littermate mice at 4-6 months of age (n=7 for Doc2b<sup>+/-</sup> and Doc2b<sup>-/-</sup>, n=5 for Doc2b<sup>+/+</sup>) for determination of parameters shown. No statistical differences were seen.

### 3.2.3 Impaired Insulin Sensitivity, and Skeletal Muscle Glucose Uptake and GLUT4 Translocation in Doc2b Knockout Mice

Whole body glucose intolerance could also be attributable to defects in insulin sensitivity, causing insulin resistance. To investigate this, 4-6 month old Doc2b<sup>+/+</sup>, Doc2b<sup>+/-</sup> and Doc2b<sup>-/-</sup> male mice were subjected to an ITT. As expected of Wt mice of this age and strain, insulin injection resulted in a sharp ~45% decline in blood glucose within 60 minutes (Fig. 3-9). By contrast, neither Doc2b<sup>+/-</sup> nor Doc2b<sup>-/-</sup> mice dropped below 70% of starting glucose levels, with levels back on the rise by 60 minutes post-injection. Analysis of AUC revealed a substantial difference in glucose levels during the ITT (in arbitrary units: Wt=5,971 ± 238; Doc2b<sup>+/-</sup>=7,019 ± 420; Doc2b<sup>-/-</sup>=7,210 ± 420), implicating a defect in the peripheral glucose uptake resulting from Doc2b depletion. Skeletal muscle GLUT4-mediated glucose uptake accounts for ~80% of whole body glucose clearance, and so largely controls the response in the ITT (see review: (185)). To assess insulin-stimulated GLUT4 translocation in skeletal muscle, sarcolemma/transverse tubule enriched fractions (referred to as P2 fractions) were prepared from insulin- or saline-injected mice as described previously (89, 91, 151, 176). A statistically significant nearly two-fold increase in GLUT4 protein accumulation into the P2 membrane fraction was detected from insulin-stimulated Wt mouse muscle (Fig. 3-10). Remarkably, no insulin-stimulated increase in GLUT4 accumulation was observed in Doc2b<sup>-/-</sup> mice. P2 fractions prepared from unstimulated Wt and Doc2b<sup>-/-</sup> mice showed similarly low levels of GLUT4 protein. Consistent with this, EDL muscle from Doc2b<sup>-/-</sup> mice showed a lack of insulin-stimulated <sup>3</sup>H-2-deoxyglucose uptake, in contrast to the nearly 2-fold increase seen in Wt EDL muscle (Fig. 3-11). Proximal insulin signaling in skeletal muscle and

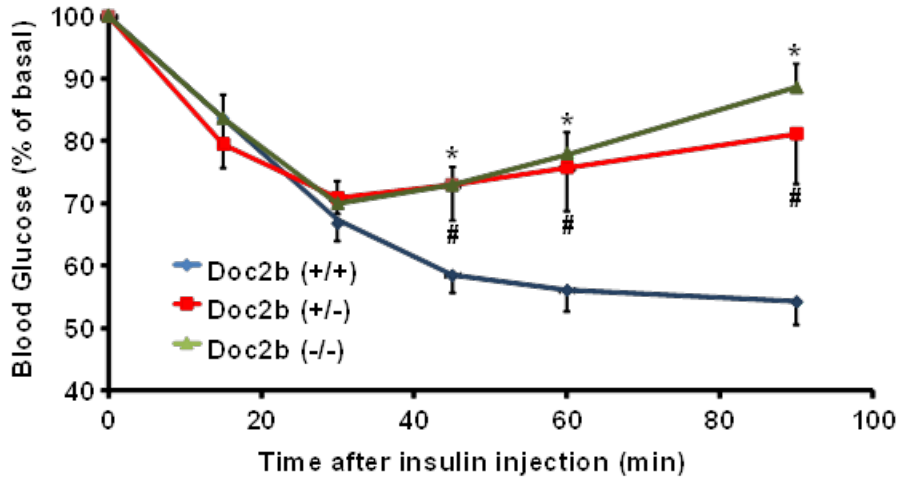


**Figure 3-9. Impaired insulin sensitivity in Doc2b-deficient mice.** Insulin tolerance testing (ITT) of Doc2b<sup>+/-</sup>, Doc2b<sup>-/-</sup> and littermate Doc2b<sup>+/+</sup> male mice (n=7) was performed by intraperitoneal injection of insulin (0.75 U/kg of body weight) into 4-6 month old male mice fasted for 6 h. Blood glucose was monitored before and at 15, 30, 60 and 90 minutes after injection as described in Methods. Data shown are presented as mean percent of basal blood glucose concentration  $\pm$  standard error (S.E.); \*P< 0.05 versus Wt mice.

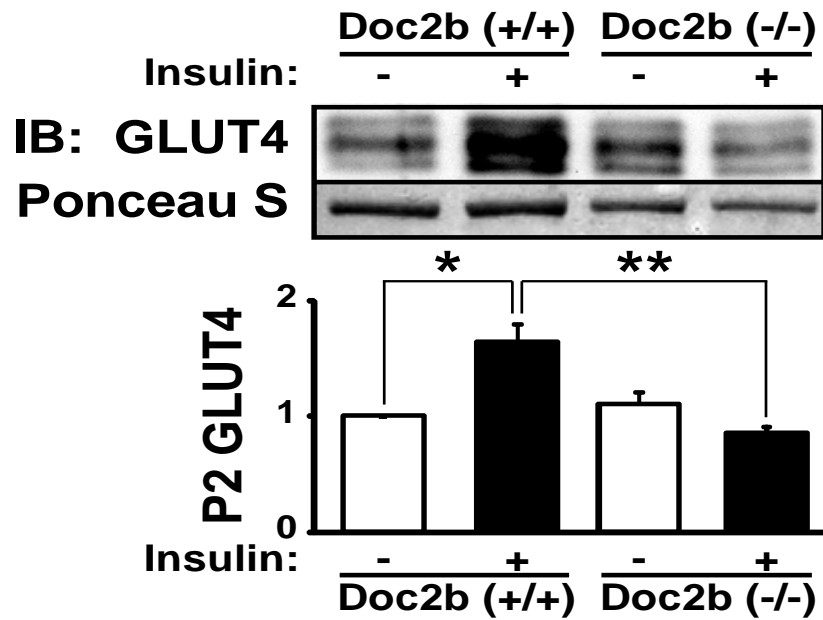


**Figure 3-10. Impaired insulin-stimulated GLUT4 translocation in skeletal muscle of Doc2b-deficient mice.** Littermate sets of male Wt or Doc2b<sup>-/-</sup> mice were fasted for 16 h and either left untreated or injected with 21 U/kg body weight of insulin as described in Methods. Hindquarter muscles were homogenized and centrifuged to partition muscle into sarcolemma/transverse tubule membrane and intracellular vesicular fractions. Proteins were resolved using SDS-PAGE for immunoblotting for GLUT4 (Ponceau S staining shows protein loading). Optical density quantitation of GLUT4 bands in three independent translocation assays is shown in the bar graph; \*P<0.05 compared to basal Wt, \*\*P<0.05 compared to insulin-stimulated Wt.

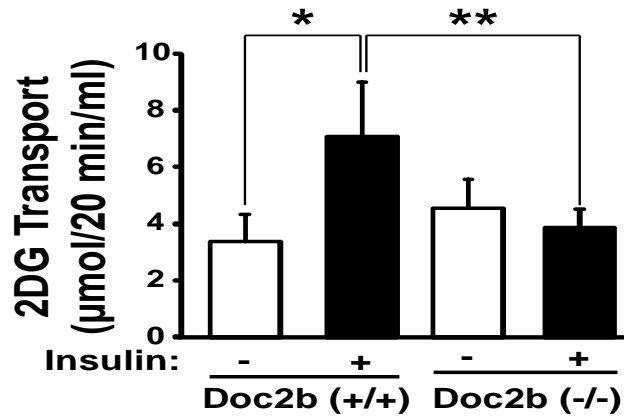


**Figure 3-11. Impaired Glucose uptake in Doc2b-deficient mice.** *In vitro*  $^3\text{H}$ -2-deoxyglucose uptake assay from EDL muscle of 6 pairs of Wt and Doc2b<sup>-/-</sup> male mice (for each mouse, one muscle was left in the basal state and one was treated with insulin. \*P<0.05 compared with basal Wt; \*\*P<0.05 compared with insulin-stimulated Wt.

and liver was unaffected, as determined by insulin-stimulated p<sup>S473</sup>-AKT phosphorylation and equivalent AKT expression (Fig. 3-12). Taken together these data demonstrate that insulin-stimulated GLUT4 externalization and glucose uptake is significantly impaired in skeletal muscle tissue of Doc2b<sup>-/-</sup> mice.

### **3.2.4 Altered SM and SNARE Complex Formations in Skeletal Muscle of the Doc2b Knockout Mice**

To date, all studies regarding the mechanistic role of Doc2b are from *in vitro* and cell culture model systems and results are controversial due to methodological differences (165, 168, 171). To resolve these issues we tested previously described Doc2b interactions using skeletal muscle of insulin-injected mice as a more physiologically relevant model system. Because calcium has been shown to trigger Doc2b association with Syntaxin 4 *in vitro* (17), we examined binding under calcium-deficient (2 mM EDTA) and calcium-supplemented (1 mM CaCl<sub>2</sub>) conditions. In Wt muscle lysates, Doc2b binding to Munc18c increased by ~60% in response to insulin stimulation; calcium addition to the lysis buffer failed to significantly alter either basal or insulin-stimulated binding events (Fig. 3-13). Similar results were obtained using basal or glucose-stimulated MIN6 cell lysates supplemented with calcium in the lysis buffer (Fig. 3-14). In skeletal muscle lysates, anti-Munc18c co-precipitated Syntaxin 4 regardless of calcium supplementation, while neither VAMP2 nor SNAP23 co-precipitated with Munc18c under any conditions (Fig. 3-15). Reciprocal anti-VAMP2 immunoprecipitation reactions showed no binding of Munc18c. Calcium supplementation did not impact SNARE complex formation: ratios of SNAP23/VAMP2 and Syntaxin 4/VAMP2,



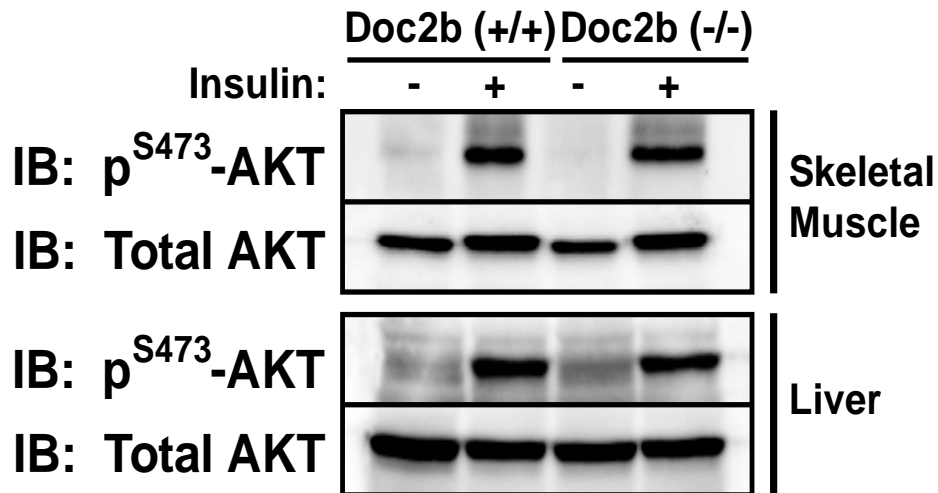


**Figure 3-12. No alterations in proximal insulin signaling in Doc2b deficient mice.** Skeletal muscle and liver homogenates were prepared from mice stimulated with or without insulin and proteins resolved on 10% SDS-PAGE for immunoblot analysis of AKT activation assessed by anti-p<sup>S473</sup>-AKT immunoblotting. Blots were stripped and reprobed for total AKT content. Data are representative of three independent sets of tissue homogenates.

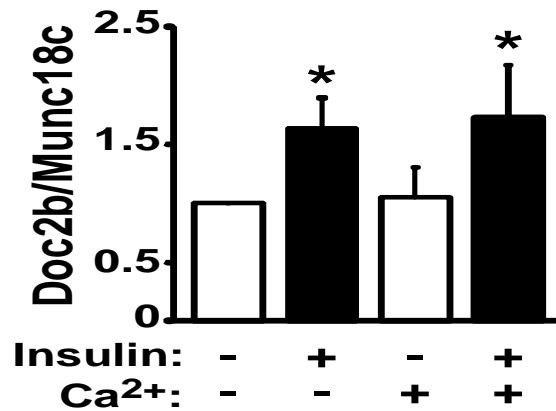
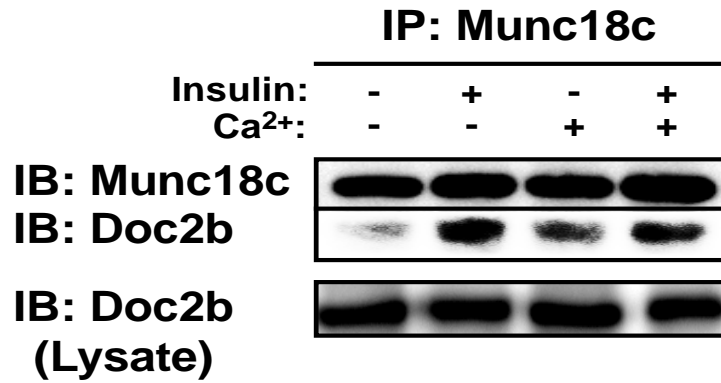


**Figure 3-13. Insulin-dependent but calcium-independent Doc2b-Munc18c association in mouse skeletal muscle.** The impact of insulin stimulation and/or calcium addition to lysis buffer upon association of Munc18c with Doc2b was assessed by co-immunoprecipitation reactions using hindlimb skeletal muscle extracts. Wt mice were injected with vehicle (saline) or insulin (10 U/kg body weight) for 5 minutes, homogenized in lysis buffers supplemented with either 2 mM EDTA or 1 mM CaCl<sub>2</sub>. Immunoprecipitated proteins were resolved on 10-12% SDS-PAGE for immunodetection of Munc18c and Doc2b. Equivalent abundance of proteins in the corresponding starting lysates was confirmed by immunoblot of Doc2b (Lysate).

## MIN6 $\beta$ -cells

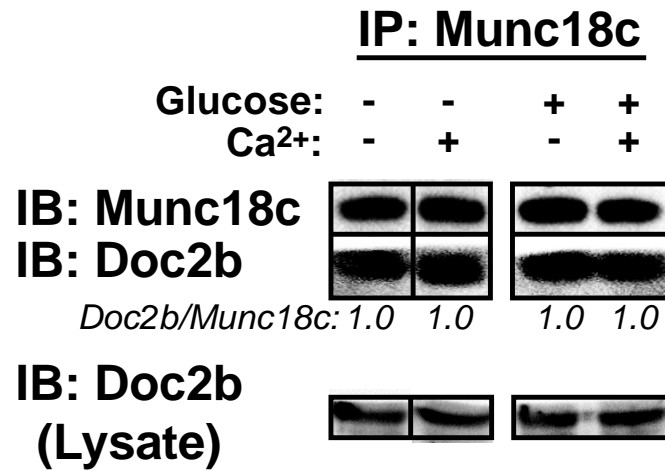


**Figure 3-14. Glucose-dependent but calcium-independent Doc2b-Munc18c association in MIN6 beta cells.** MIN6 cells were pre-incubated in glucose-free modified Krebs bicarbonate buffer 2 h followed by stimulated with glucose (20 mM) for 5 minutes. Cells were then harvested in 1% NP40 lysis buffer supplemented with 2 mM EDTA or 1 mM CaCl<sub>2</sub> and used in anti-Munc18c immunoprecipitation reactions. Precipitated proteins were resolved on 10% SDS-PAGE for immunodetection of Munc18c and Doc2b. Equivalent abundance of proteins in the corresponding starting lysates was confirmed by immunoblot (Lysate).

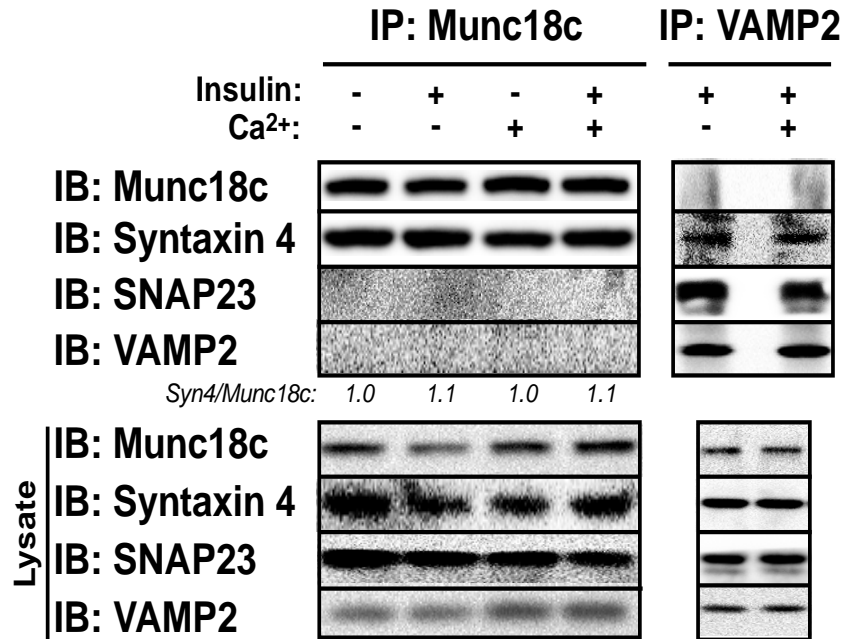


**Figure 3-15. Calcium-independent SNARE-Munc18c association in mouse skeletal muscle.** The impact of insulin stimulation and/or calcium addition to lysis buffer upon association of Munc18c with VAMP2, SNAP23 and Syntaxin 4 was assessed by co-immunoprecipitation reactions using hindlimb skeletal muscle extracts. Hindlimb muscle extracts from Wt mice injected with vehicle (saline) or insulin (10 U/kg body weight) for 5 minutes, homogenized in lysis buffers supplemented with either 2 mM EDTA or 1 mM CaCl<sub>2</sub>. Immunoprecipitated proteins were resolved on 10-12% SDS-PAGE for immunodetection of Munc18c, Doc2b, Syntaxin 4, SNAP23 and VAMP2. Equivalent abundance of proteins in the corresponding starting lysates was confirmed by immunoblot (Lysate).

normalized to 1.0 in the absence of calcium (2 mM EDTA) were measured to be  $0.8 \pm 0.2$  and  $0.8 \pm 0.2$ , respectively, in the presence of supplemental calcium (n=3 paired experiments,  $p>0.05$ ). Moreover, Syntaxin 4 failed to co-immunoprecipitate Doc2b, even under calcium-containing and insulin-stimulated conditions from skeletal muscle (Fig. 3-16A). Doc2b<sup>-/-</sup> muscle served as control for non-specific binding. Syntaxin 4 co-precipitated SNAP23 equivalently under all conditions, consistent with SNAP23 participation in binary and ternary SNARE complexes. Like Syntaxin 4, which was constitutively present containing and insulin-stimulated conditions from skeletal muscle (Fig. 3-16A), Doc2b abundance was unchanged by insulin in P2 fractions prepared 5 minutes post insulin injection, the time of peak tyrosine-phosphorylation of Munc18c and its association with Doc2b; and Doc2b translocation detected within 30 minutes post-insulin injection (Fig. 3-16B). These data suggest that in skeletal muscle lysate, Doc2b binds to Munc18c in an insulin sensitive manner, and fails to bind to Syntaxin 4 in response to insulin and/or added calcium.

We next sought to determine why GLUT4 accumulation in the target membranes of skeletal muscle was impaired in the Doc2b<sup>-/-</sup> mice by examining effects upon SM and SNARE protein complexation. In Wt extracts, insulin induced phosphorylation of Munc18c, as described previously (13), and was fully recapitulated in reactions using Doc2b<sup>-/-</sup> extracts (Fig. 3-17A), suggesting that Doc2b was not required for Munc18c to undergo insulin-stimulated tyrosine phosphorylation. Anti-Syntaxin 4 immunoprecipitation reactions using the same extracts revealed 40-50% more Munc18c binding to Syntaxin 4 in Doc2b<sup>-/-</sup> muscle (Fig. 3-17B), as compared with Wt muscle.

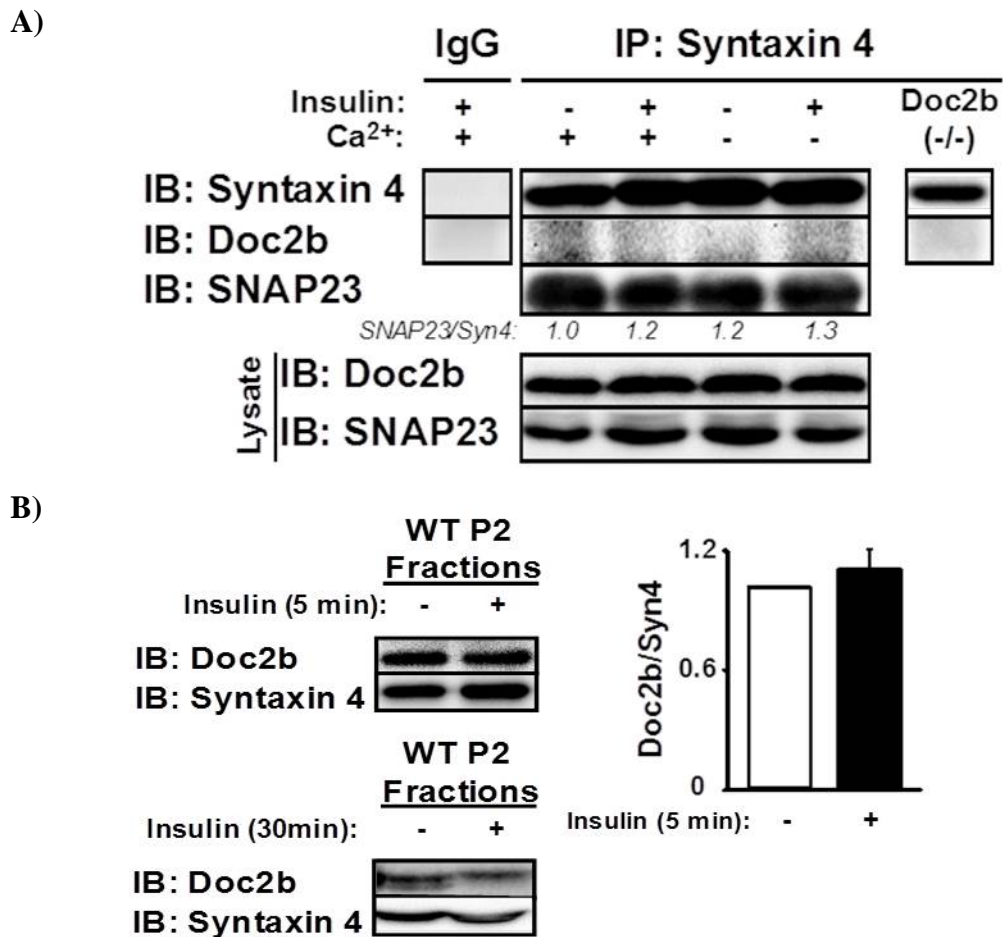


**Figure 3-16. Absence of Syntaxin 4-Doc2b association in mouse skeletal muscle. (A)** Muscle extracts used in Fig. 3-12 were subjected to anti-Syntaxin 4 immunoprecipitation for immunodetection of Doc2b, SNAP23 binding to Syntaxin 4. Control IgG and lysates from Doc2<sup>-/-</sup> mice were used in separate reactions as a control for non-specific banding occurring with the Doc2b antibody. **(B)** Evaluation of Doc2b protein recruitment to the PM fraction in response to insulin. P2 fraction extracts prepared from saline or insulin-stimulated Wt mice were subjected to SDS-PAGE for immunodetection of Doc2b and Syntaxin 4. Data are representative of three independent sets of homogenates or fractions.

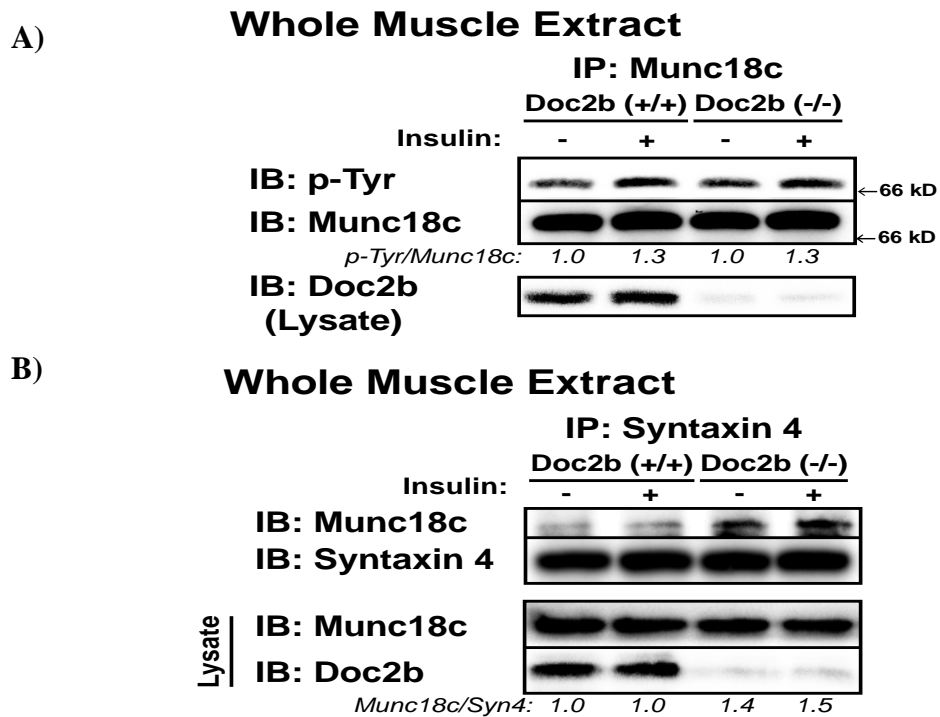


**Figure 3-17. Munc18c-Syntaxin 4 binding is increased in Doc2b<sup>-/-</sup> mouse skeletal muscle.** Male 4-6 month old Doc2b<sup>+/+</sup> and Doc2b<sup>-/-</sup> littermate mice were injected with insulin (10 U/kg body weight) for 5 minutes, then hindlimb muscles excised and detergent extracts prepared for use in (A) anti-Munc18c or (B) anti-Syntaxin 4 immunoprecipitation reactions. Immunoprecipitated proteins were resolved on 10% SDS-PAGE for immunodetection of Doc2b and tyrosine-phosphorylated Munc18c (using PY20 antibody), which was stripped and reblotted for total Munc18c, and Syntaxin 4. Vertical black lines indicate the splicing of lanes from the same gel. Optical density scanning was used to determine the ratio of phosphotyrosine-Munc18c/Munc18c and Munc18c/Syntaxin as indicated in the bar graphs.

Input lysates validated the absence of Doc2b in Doc2b<sup>-/-</sup> lysates and the otherwise comparable expression of Munc18c. Using sarcolemmal/transverse tubule (P2) membrane fractions from hindlimb muscles of insulin-stimulated Wt and Doc2b<sup>-/-</sup> mice, significant reductions of VAMP2 and SNAP23 binding to Syntaxin 4 in Doc2b<sup>-/-</sup> fractions were revealed (Fig. 3-18). Coordinately, Munc18c binding to Syntaxin 4 was elevated by 46% in Doc2b<sup>-/-</sup> fractions. Thus, our cumulative data suggest that ablation of insulin-stimulated GLUT4 vesicle translocation in Doc2b<sup>-/-</sup> muscles is underpinned by increased abundance of Munc18c-Syntaxin 4 complexes coordinate with diminished abundance of SNARE complexes.

### **3.3 DISCUSSION**

In this study we present the Doc2b<sup>+/-</sup> and Doc2b<sup>-/-</sup> mice as new *in vivo* models of metabolic dysregulation. The data reveal for the first time that Doc2b is a key effector for insulin-stimulated GLUT4 vesicle translocation in skeletal muscle, and for both phases of glucose-stimulated insulin secretion from pancreatic islets. Doc2b associates with Munc18c in an insulin-dependent manner, but Doc2b binding to Syntaxin 4 was not detected. Notably, Munc18c-Syntaxin 4 association was increased in the absence of Doc2b, suggesting that this increased association is inhibitory for the insulin-stimulated Syntaxin 4-mediated docking/fusion of GLUT4 vesicles. Strikingly, the disease phenotype of the Doc2b<sup>+/-</sup> knockout mice was almost equally severe to that of the Doc2b<sup>-/-</sup>, suggesting that Doc2b haploinsufficiency is worthy of future investigation in diabetes susceptibility.



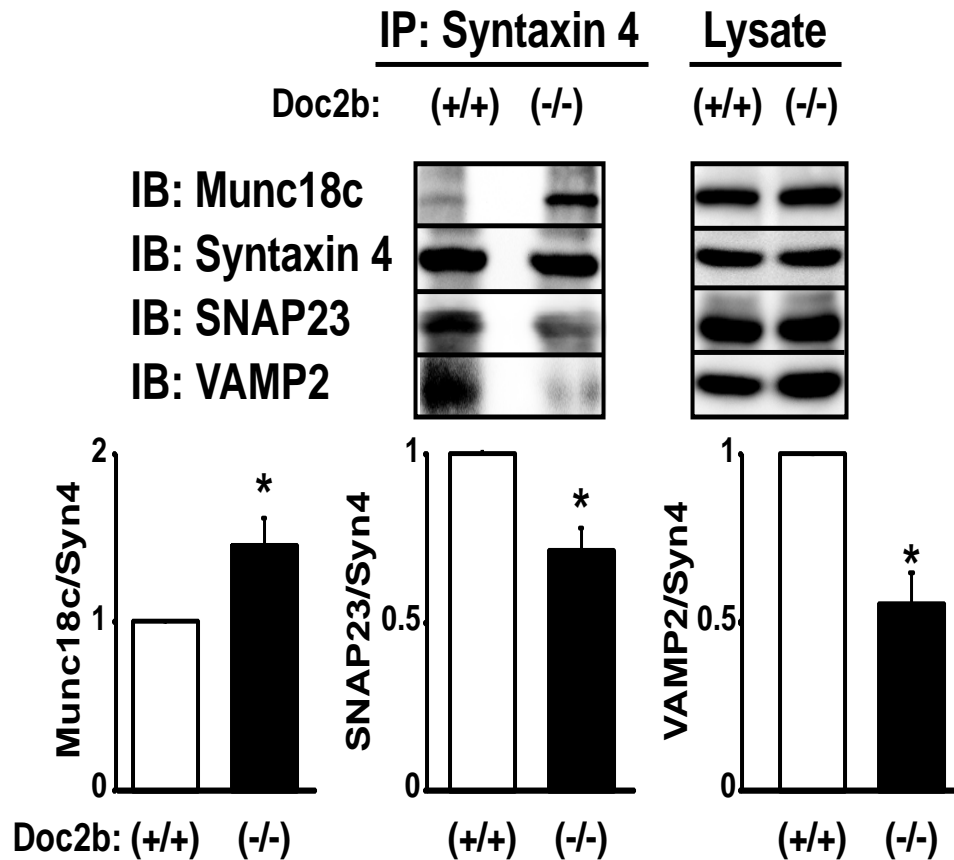


**Figure 3-18. Munc18c-Syntaxin 4 binding is increased in Doc2b<sup>-/-</sup> mouse skeletal muscle.** Male 4-6 month old Doc2b<sup>+/+</sup> and Doc2b<sup>-/-</sup> littermate mice were injected with insulin (10 U/kg body weight) for 5 minutes, then hindlimb muscles excised for Sarcolemmal/transverse tubule membrane fractions (P2) were used in anti-Syntaxin 4 immunoprecipitation reactions to capture binary and ternary SNARE complexes composed of VAMP2 and SNAP23, and Syntaxin 4-Munc18c complexes, all resolved on 12% SDS-PAGE for immunoblotting. Optical density quantitation of three independent pairs of Doc2b<sup>+/+</sup> and Doc2b<sup>-/-</sup> mouse muscle extracts is shown in the bar graph; \*P<0.05 compared to insulin-stimulated Wt.

### **3.3.1 Mechanism(s) of Doc2b-Dependent Insulin Granule and GLUT4 vesicle fusion events**

Unlike other secretory cell types, islet beta cells require multiple Munc18 and Syntaxin isoforms, otherwise sharing SNAP25/SNAP23 and VAMP2, for two distinct phases of glucose-stimulated insulin secretion. Syntaxin 1<sup>-/-</sup> null islets lack first-phase insulin release, while Munc18c and Syntaxin 4 are imperative for second-phase insulin release from islets (28, 76, 178); Munc18-1 null islet perfusion has yet to be reported, although Munc18-1 and Munc18-2 were recently implicated in fast calcium-dependent exocytosis in electrophysiological studies (186). Demonstrating here that Doc2b is required for both phases of insulin release from primary islets, we speculate that Doc2b regulates both Munc18-1-Syntaxin 1 as well as Munc18c-Syntaxin 4 dependent secretion mechanisms. The role of Doc2b in the first-phase went undetected in static incubation studies using stable Doc2b shRNA clonal beta cells (171), but is consistent with its role in Munc18-1-Syntaxin 1 driven exocytosis mechanisms in brain (174). The partial reduction of Doc2b in clonal beta cells may not have been sufficient to uncover the requirement for Doc2b in first-phase. Doc2b<sup>+/-</sup> islets retained more than 60% first-phase function (while losing ~75% second-phase), and total ablation of Doc2b was required to detect more than 50% loss of first-phase function. Our data does confirm the late phase deficit reported in stable Doc2b shRNA clonal beta cells (171). Strikingly, second-phase secretion was nearly abolished in Doc2b<sup>-/-</sup> islets. While our MIN6 beta cell studies support a mechanistic regulation of Munc18c-Syntaxin 4 and SNARE complexes analogous to our studies with these proteins in skeletal muscle, future beta cell studies

assessing the impact of Doc2b upon Munc18-1 or -2 with Syntaxin 1 are required, as well as assessment of all isoform binding interactions in primary beta cells.

Doc2b is present in skeletal muscle transverse tubule/sarcolemmal-enriched subcellular fractions under basal conditions, and does not translocate, in contrast to GLUT4, in response to insulin stimulation. This finding is consistent with similar observations in glucose-stimulated MIN6 beta cells, yet counter to calcium-stimulated translocation seen in other cell types (168-169). Doc2b is known to require very little calcium to translocate in neurons (35). Skeletal muscle may have baseline calcium already high enough to translocate Doc2b under resting conditions. Under such conditions, Doc2b can be considered constitutively active (167), which can explain the strong effects in the Doc2b<sup>-/-</sup> mice observed here, relative to effects previously observed in brain (174). In 3T3-L1 adipocytes, Doc2b is reported to bind to Syntaxin 4 only under high calcium buffer conditions (168). Therefore, we simulated those calcium conditions to investigate the physiological occurrence/relevance of this putative Doc2b-Syntaxin 4 complex in primary skeletal muscle. However, regardless of calcium levels in skeletal muscle extracts, Doc2b failed to co-precipitate in anti-Syntaxin 4 immunoprecipitation reactions, suggesting that such an interaction might not be a dominant factor in primary cells.

Concerning the mechanism of Doc2b actions in both insulin granule and GLUT4 vesicle exocytosis, several possibilities might be considered. One possibility is that Doc2b serves as a platform for transient interactions with Munc18 and Syntaxin.

According to this “switch hypothesis” model, derived from beta cell studies (148, 165), Munc18c becomes tyrosine phosphorylated in response to a stimulus, dissociates from Syntaxin 4, and switches its binding preference to Doc2b. Doc2b’s sequestration of Munc18c would facilitate Syntaxin 4’s participation in SNARE complexes to promote vesicle fusion. Such a model is consistent with 1) the insulin-stimulated association of Doc2b with Munc18c in skeletal muscle, and 2) the strong increase in Munc18c binding to Syntaxin 4, concurrent with the reduced binding of VAMP2 and SNAP23 to Syntaxin 4 in sarcolemmal/transverse tubule muscle membrane fractions, indicative of attenuated SNARE complex formation in the absence of Doc2b. Alternatively, Doc2b may facilitate fusion via a different or additional mechanism, by partially inserting into the plasma membrane upon calcium binding, and induce membrane deformations that assist merging vesicle- and plasma membrane. This property contributes to the exceptional *in vitro* fusogenic properties of Doc2b relative to all other C2-domain proteins studied (174).

While the disease phenotype of the Doc2b<sup>+/-</sup> knockout mice was almost equally severe to that of the Doc2b<sup>-/-</sup> mice, interpreting the relative contribution of insulin secretory defects versus insulin resistance is complex. For example, insulin content in the serum following the acute glucose challenge trended towards a decrease (p=0.08, n=6), intermediate between that of the Wt and Doc2b<sup>-/-</sup> mice, but did not reach statistical significance. However, since serum insulin content is not an absolute readout of insulin secretion, but rather is a net readout of pancreatic insulin release, hepatic insulin clearance, and insulin utilization by other tissues, use of the hyperglycemic clamp approach will be required for full assessment. Also noteworthy was that the initial drop

(15-30 minutes) in blood glucose in the ITT in the Doc2b<sup>-/-</sup> mice was similar to that of Wt mice, seemingly counter to the blunted glucose uptake into the EDL of the Doc2b<sup>-/-</sup> mice. However, the glucose uptake assay was performed *in vitro* using excised muscle, whereas the ITT is performed *in vivo*. *In vivo*, the insulin bolus will initiate a decrease in hepatic glucose output. Given that hepatic insulin signaling in the Doc2b<sup>-/-</sup> mice was normal, it would seem a likely contributor to the initial blood glucose drop.

### **3.4 CONCLUSIONS**

The data presented here demonstrate a key role for Doc2b in multiple exocytotic processes relevant to the maintenance of whole body glucose homeostasis, including insulin secretion and peripheral glucose clearance. We propose that Doc2b engages in stimulus-dependent association with Munc18c in skeletal muscle similar to that in beta cells; this implicates the mechanisms to be highly conserved, albeit the stimuli are cell-type specific. Furthermore, our data demonstrating the need for Doc2b in first-phase insulin release suggests that it may also participate as a scaffolding platform for Munc18-1 binding in the beta cell. Novel reagents based upon Doc2b may carry promise as dual insulin-sensitizing/insulin secretion enhancement approaches to combating a combinatorial disease like Type 2 diabetes.

**CHAPTER 4. DOC2B ENRICHMENT ENHANCES GLUCOSE HOMEOSTASIS  
VIA POTENTIATION OF INSULIN SECRETION AND PERIPHERAL INSULIN  
SENSITIVITY**

**The following text is currently in revision for publication:**

Ramalingam L, Oh E, Thurmond DC. Doc2b Enrichment Enhances Glucose Homeostasis via Potentiation of Insulin Secretion and Peripheral Insulin Sensitivity. *Diabetologia*

Author contributions: All data for figures were generated by Ramalingam L

## **4.1 INTRODUCTION**

Glucose-stimulated insulin secretion (GSIS) and insulin-stimulated glucose uptake into peripheral tissues are events mediated by similar exocytotic mechanisms involving soluble NSF attachment receptor (SNARE) proteins. Syntaxin proteins are regulated by specific high-affinity binding partners called Munc18 proteins (134, 146). Munc18c pairs exclusively with Syntaxin 4 and is a key regulator of both insulin-stimulated GLUT4 vesicle exocytosis as well as second-phase GSIS (146-147, 151, 178). Unexplained however, is why Syntaxin 4 should be necessary in both phases of GSIS, given that instead of binding to the first-phase isoform Munc18-1 it binds to Munc18c, and Munc18c is not involved in first-phase GSIS. This suggests that an additional “linking factor” might be required.

One possible linking factor is Doc2b (Double C2 domain protein). Support for Doc2b as a potentially limiting factor in GSIS and glucose uptake is based upon defects in Syntaxin 4 exocytosis events found in islets and skeletal muscle of Doc2b knockout mice (187), and a possible association between Doc2b deficiency and diabetes in rodents (184). Intriguingly, clonal beta cell and adipocytes over-expressing Doc2b reportedly show enhancements in GSIS and GLUT4 exocytosis (165, 168, 171). Taken together these data raise the possibility that intentional elevation of Doc2b could provide a means to rescue aberrations in insulin secretion and insulin action simultaneously.

As a first step towards testing this possibility, we generated regulatable Doc2b transgenic (Tg) mice using a targeting vector known to selectively drive expression in

pancreas, skeletal muscle, and adipose tissue (89, 152, 175). Indeed, elevated levels of Doc2b in these tissues *in vivo* resulted in improved glucose and insulin tolerance relative to wildtype (Wt) littermate mice. Mechanistically these improvements were underscored by enhanced SNARE complex formation and exocytosis function in Doc2b Tg islets and skeletal muscle, altogether consistent with the concept that Doc2b is limiting for these processes *in vivo*, and that Doc2b enrichment may provide the means to confer superior whole body glucose homeostasis.

## **4.2 RESULTS**

We generated tetracycline-repressible Tg mice using a targeting vector previously shown to drive expression primarily in pancreas, skeletal muscle, and adipose tissue (89, 152). Of the four founder lines, three transmitted the Doc2b gene, yet only one line exhibited greater than a 2-fold increase in Doc2b protein relative to endogenous expression in Wt littermates (Fig. 4-1A). No alterations in the levels of SNARE proteins such as Syntaxin 4, SNAP23, VAMP2 and Munc18c were detected. No transgene expression was detected in heart, liver, or spleen (Fig. 4-1B, no Myc staining). Doc2b protein levels in Tg islets were increased 3.1 fold over that in Wt islets, again with no alteration in expression of SNARE or Munc18 proteins (Fig. 4-2A). GLUT4 protein levels in heart, skeletal muscle and fat of Doc2b Tg mice were similar to that in Wt mice (Fig. 4-2B).



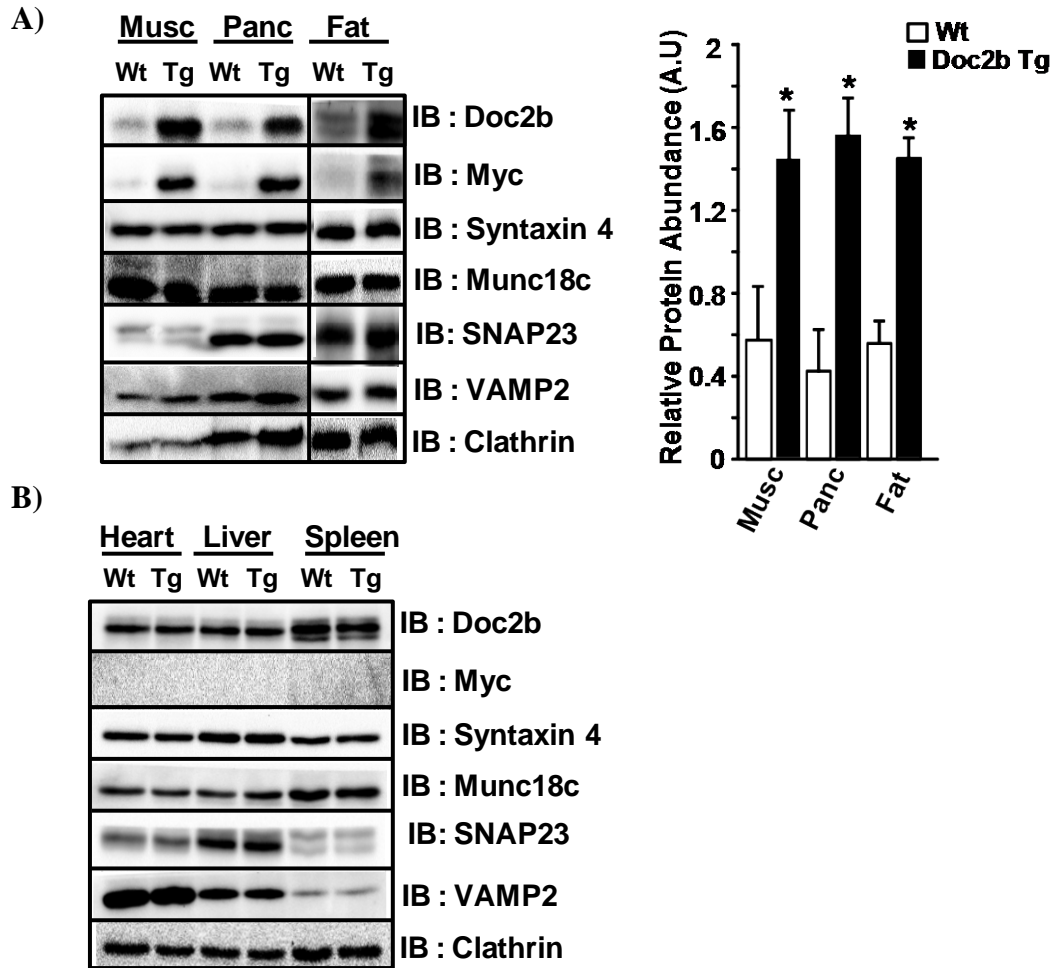
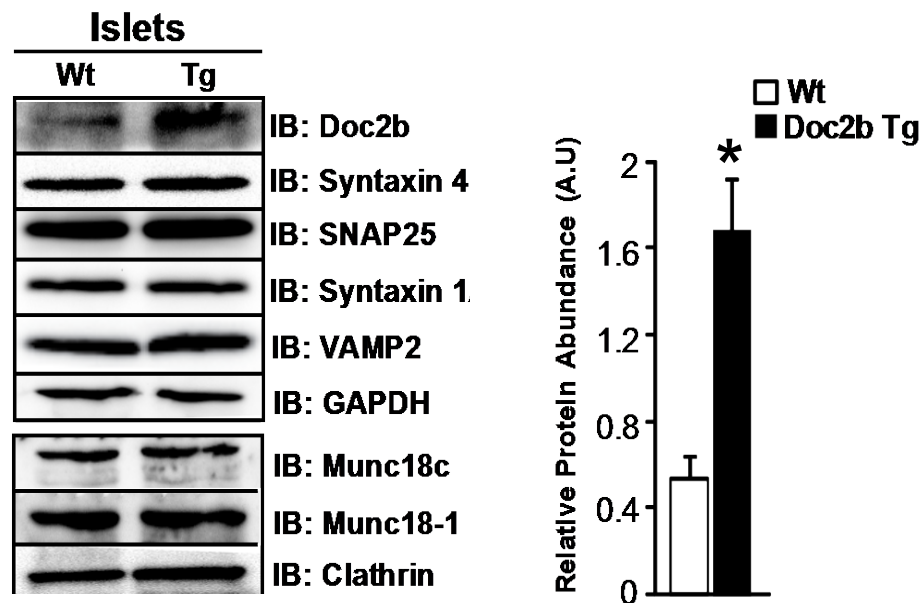


**Figure 4-1. Protein expression in tissues of Doc2b transgenic mice.** (A) Gastrocnemius skeletal muscle (Musc), Pancreas (Panc), and epigonadal fat were isolated from 3 pairs of Doc2b Tg and Wt littermate mice and immunoblotted for detection of SNARE and SNARE accessory proteins. Quantitation of Doc2b in each tissue is shown as the average  $\pm$  SE; \* $p < 0.05$  vs. Wt. (B) Heart, liver and spleen were similarly assessed for detection of SNARE and SNARE accessory proteins.

A)



B)

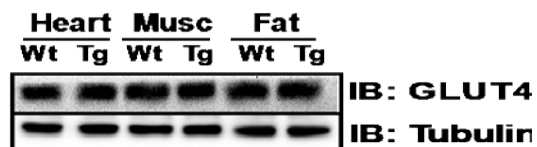


**Figure 4-2. Protein expression in islets and tissues of Doc2b transgenic mice. (A)** Isolated islets from Doc2b Tg and Wt mice were assessed for Doc2b and SNARE protein expression; quantitation of Doc2b is shown in the adjacent bar graph. **(B)** GLUT4 protein abundance was assessed in heart, skeletal muscle and fat in 3 pairs of Tg and Wt mice.

#### 4.2.1 Improved Glucose Tolerance in Doc2b Enriched Mice

To determine whether Doc2b expression in the select tissues was limiting for glucose homeostasis *in vivo*, IPGTT analyses were performed with the line of mice shown to exhibit >2.5-fold Doc2b over-expression (F5170). While fasting glycemia was unaltered, F5170 showed significantly lower blood glucose levels than Wt mice upon glucose challenge at all time points (Fig. 4-3A). AUC analysis quantified this to be a 44% improvement in glucose tolerance (Fig. 4-3B). The rapid drop in blood glucose correlated with significantly increased serum insulin content in the Doc2b Tg mice within the first 10 minutes post-glucose injection during the IPGTT (Fig. 4-3C). In addition, no differences in body or tissue weights were observed (Table 4-1). We also performed IPGTT assays with a second founder line, F5168, which over-expressed Doc2b only ~1.7-fold (and exhibited mosaic transgene expression), as a control for the presence of the transgene. No significant changes in glucose tolerance were observed in F5168 line compared to wild type littermates (Fig. 4-3D), hence F5170 was used for all further studies. Together, these data suggested that Doc2b enrichment to a level >2-fold simultaneously in skeletal muscle, fat and pancreas contributed to potentiated glucose tolerance perhaps via heightened insulin release and/or peripheral glucose uptake. To validate that the enhanced glucose tolerance of the Doc2b Tg mice was due to the presence of the transgene, Doc2b Tg and Wt mice examined in Fig. 4-4A studies were administered tetracycline (tet)-treated drinking water for 1 week to repress the transgene, after which the IPGTT was repeated. Glucose tolerance of the tet-treated Doc2b Tg mice was similar to that of Wt mice (Fig. 4-4A-B), as were the Doc2b protein levels (Fig. 4-4C-D).

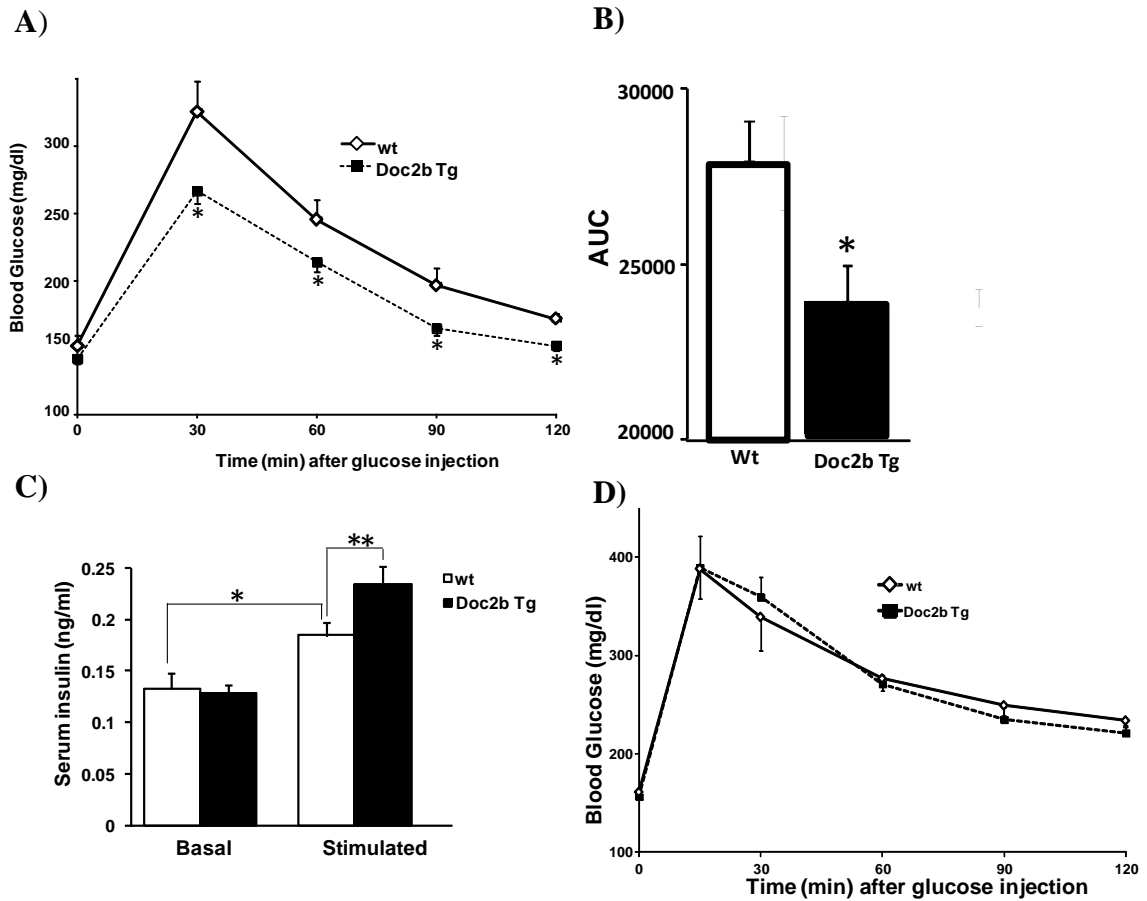


**Figure 4-3. Doc2b Tg mice have enhanced glucose tolerance.** (A) IPGTT of Doc2b F5170 Tg line and Wt littermate mice was performed in 4-6 months old female mice fasted for 6 hours. (B) AUC data are shown as the average  $\pm$  SE from 7 pair of mice; \* $P < 0.05$ , Doc2b Tg versus Wt. (C) Insulin content present in serum taken prior to and 10 minutes post-injection of glucose during the IPGTT. Data represent the average  $\pm$  SE from 6 pairs of mice; \* $P < 0.05$  vs. Wt basal; \*\*  $P < 0.05$  vs. Wt glucose-stimulated. (D) IPGTT of Doc2b F5168 line of mice. Data represent the average  $\pm$  SE from 5 pairs of mice.

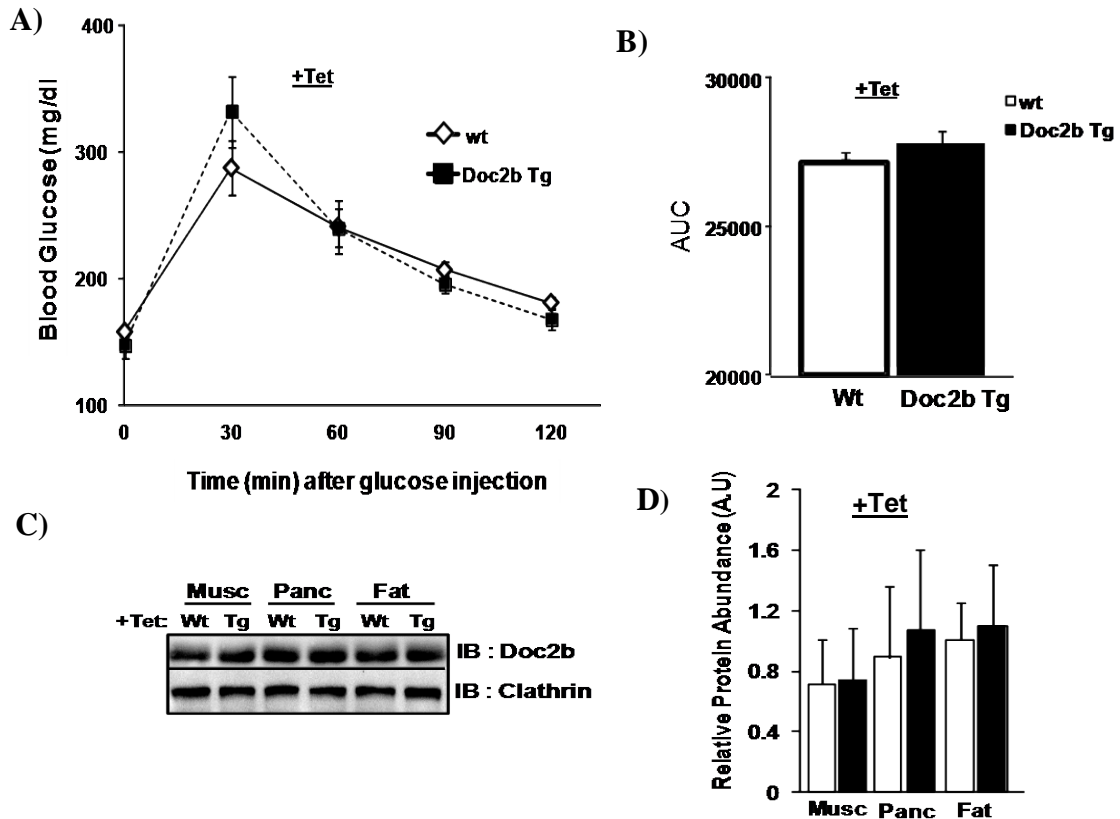


**Figure 4-4. Tetracycline-mediated repression of the Doc2b transgene reduces glucose tolerance to that of the Wt mice.** (A) Doc2b Tg and Wt female mice 4-6 months old were administered tetracycline (1 mg/ml) in the drinking water and IPGTT performed. (B) AUC analysis is shown as the average  $\pm$  SE from 7 pairs of mice. (C) Tissue extracts immunoblotted for Doc2b and Clathrin. Data are representative of at least 3 independent sets of tissues. (D) Quantitation of Doc2b in each tissue is shown as the average  $\pm$  SE from 4 pairs of mice.

**Table 4-1 Tissue weights of Doc2b Tg and Wt mice.**

<b>Tissue</b>	<b>Doc2b Wt</b>	<b>Doc2b Tg</b>
<b>Body wt (g)</b>	29.8 ± 4.60	29.5 ± 5.73
<b>Liver</b>	1.68 ± 0.05	1.62 ± 0.05
<b>Lung</b>	0.23 ± 0.04	0.28 ± 0.03
<b>Heart</b>	0.30 ± 0.04	0.25 ± 0.03
<b>Fat</b>	0.80 ± 0.07	0.78 ± 0.06
<b>Pancreas</b>	0.77 ± 0.05	0.56 ± 0.03
<b>Kidney</b>	0.55 ± 0.05	0.50 ± 0.06
<b>Muscle</b>	0.49 ± 0.04	0.55 ± 0.04
<b>Spleen</b>	0.19 ± 0.42	0.16 ± 0.40

Data represent the average ±Weights were collected from Doc2b Tg and Wt mice at 4-6 months for determination of parameters shown. No statistical differences were seen. (n=6 for Doc2b Tg and Wt mice).

These data confirmed that the enhanced glucose tolerant phenotype of the Doc2b Tg mice corresponded to the expression of the Doc2b transgene.

#### **4.2.2 Doc2b Enrichment Potentiates Biphasic GSIS.**

To determine if the increased serum insulin content of Doc2b Tg mice was related to increased islet function, we subjected islets to parallel perfusion analyses. Indeed, islets of Doc2b Tg mice exhibited a higher peak of first-phase insulin release as well as sustained elevation of second-phase release (Fig. 4-5A). AUC analysis quantified a 50% increase over that of Wt islets in the first-phase and a 250% increase in second-phase relative to Wt islets (Fig. 4-5B). Total insulin content was similar between Doc2b Tg and Wt islets (Fig. 4-5C). Basal insulin secretion was similar between Doc2b Tg and Wt islets (Fig. 4-5A), consistent with similar fasting serum insulin contents of the mice (Fig. 4-6C). These data suggested Doc2b to be limiting for each phase of GSIS and that its enrichment could enhance functional GSIS without aberrantly raising basal insulin release.

#### **4.2.3 Doc2b Tg Mice have Enhanced Insulin Sensitivity and cell Surface GLUT4 accumulation in Skeletal Muscle.**

We next assessed whether the beneficial effect of Doc2b enrichment on glucose tolerance was related to improved peripheral insulin sensitivity, by performing an ITT. Following insulin injection, blood glucose levels of the littermate Wt mice dropped by ~45% within 60 minutes, as is normal for the C57BL6/J strain (Fig. 4-6A). In Doc2b Tg mice, both the rate and extent of the reduction in glycemia was significantly enhanced

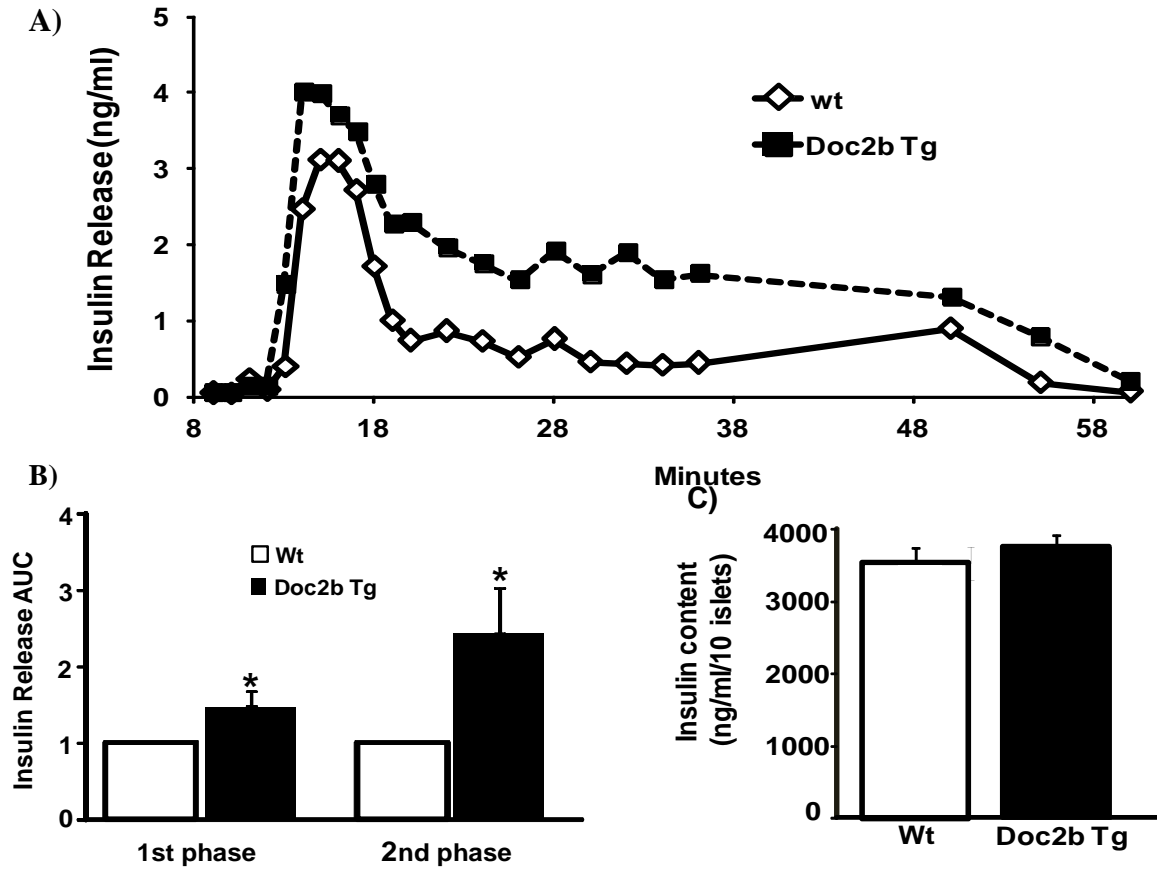


**Figure 4-5. Islets from Doc2b Tg mice exhibit potentiated biphasic insulin release.**

(A) Islets isolated from Doc2b Tg and littermate Wt mice were perfused in parallel at 2.8 mM glucose for 10 minutes, followed by 16.7 mM glucose for 35 min, then returned to low glucose for 20 minutes. Eluted fractions were collected and insulin secretion determined by RIA, as depicted in this representative pair of traces. (B) AUC for first (11-17 minutes) and second (18-45 minutes) phases of insulin secretion was quantified from islets, normalized to baseline. Data represent the average  $\pm$  SE of 3 independent sets



of perfused islets; \*P<0.05 versus Wt. (C) Average insulin content per 10 islets from Doc2b Tg and Wt littermates.

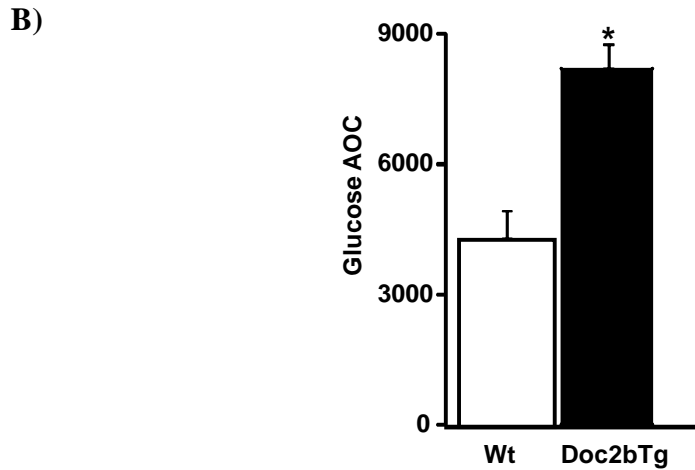
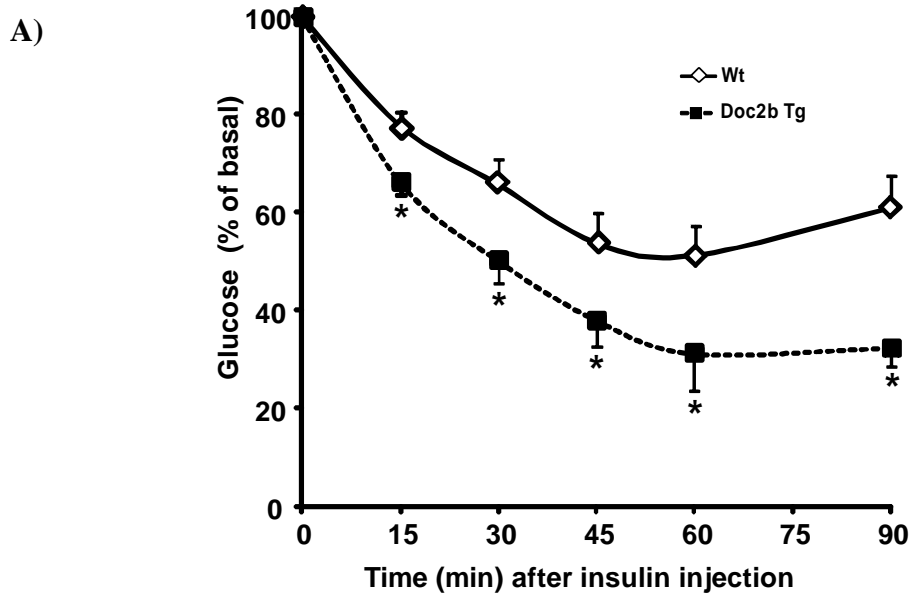


**Figure 4-6. Doc2b Tg mice exhibit enhanced insulin sensitivity.** (A) ITT of 7 pair of Doc2b Tg and littermate Wt female mice fasted for 6 h. Data are shown as the mean percent of starting basal blood glucose concentrations  $\pm$  SE; \*P < 0.05 versus Wt mice. (B) Area over the curve (AOC) data are shown as the average  $\pm$  SE from 7 pairs of mice; \*P < 0.05, Doc2b Tg versus Wt.

(Fig. 4-6A). Area over the ITT curve for the Doc2b Tg mice showed this to be a nearly 2 fold improvement in glycemia in the Doc2b Tg mice compared to Wt mice (Fig. 4-6B). These data indicated that Doc2b is limiting for peripheral insulin sensitivity.

The improved insulin sensitivity suggested that Doc2b may be limiting for insulin signalling or insulin-stimulated GLUT4 vesicle translocation to the cell surface membranes in skeletal muscle, given that skeletal muscle accounts for ~ 80% of glucose uptake in humans (188). To test this, t-tubule/sarcolemmal cell surface enriched membrane fractions (referred to as P2) were isolated from saline- or insulin-injected hindlimb skeletal muscle of Doc2b Tg and Wt mice. P2 fractions prepared from insulin-injected Wt mice showed the expected ~1.5-fold increase in GLUT4 accumulation relative to the unstimulated Wt mouse fraction (176). Remarkably, Doc2b Tg P2 fractions exhibited a ~2.4-fold increase in GLUT4 vesicle accumulation at the PM (Fig. 4-7A-B). Since AKT activation in Doc2b Tg skeletal muscle homogenates was similar to that of Wt mice (Fig. 4-7C), the beneficial action of Doc2b enrichment appeared to lie downstream of AKT activation. These data implicated enhanced insulin-stimulated GLUT4 vesicle accumulation at the PM as an underlying cause for the enhanced peripheral insulin sensitivity of the Doc2b Tg mice.

#### **4.2.4 Doc2b Enrichment Promotes SNARE Complex Formation in Beta Cells and Skeletal Myoblasts.**

Doc2b over-expression in clonal beta cells potentiate GSIS. This is based upon its ability to decrease Syntaxin 4-Munc18c association and increase Syntaxin 4-VAMP2

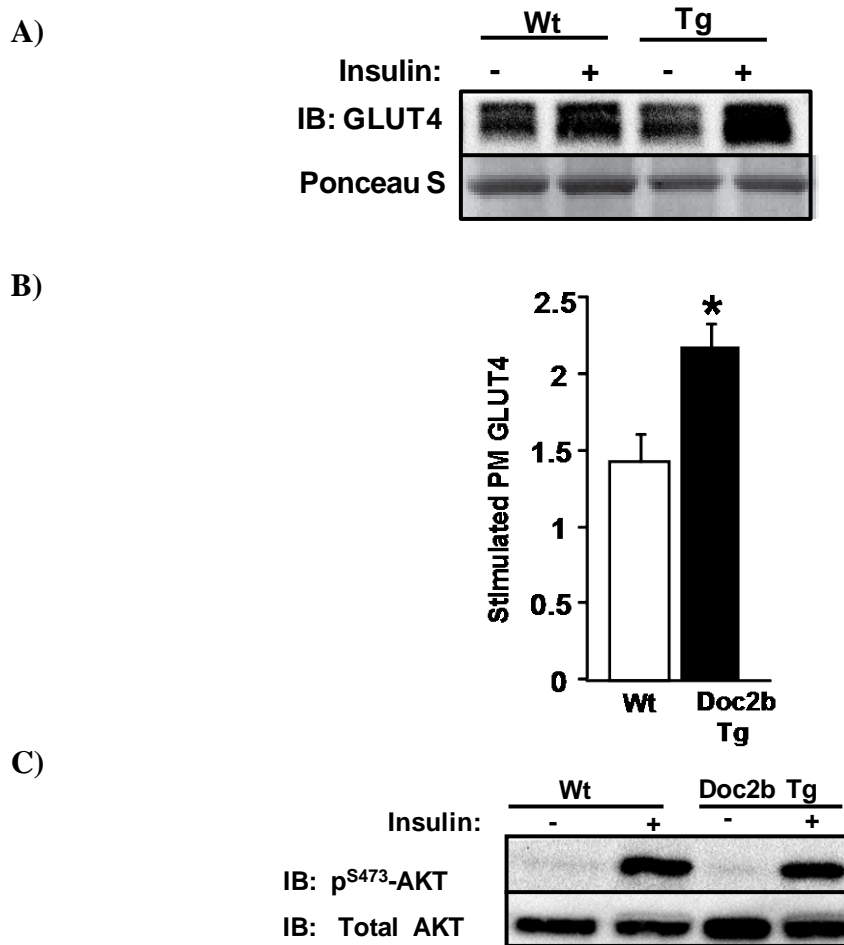


**Figure 4-7. Doc2b Tg mice show increased insulin-stimulated GLUT4 accumulation at the plasma membrane of skeletal muscle.** (A) Cell surface sarcolemma/transverse tubule membranes were obtained via subfractionation (176, 187) of hindquarter muscles from littermate mice, and GLUT4 abundance therein detected by immunoblot (Ponceau S shows protein loading). (B) Quantitation of GLUT4 accumulation in PM fractions, normalized to the unstimulated saline control in 3 sets of mice; \*P< 0.05 vs. Wt basal, \*\*P< 0.05 vs. Wt glucose-stimulated. (C) Whole skeletal muscle detergent homogenates from mice stimulated with insulin were immunoblotted for activated AKT (p<sup>S473</sup>-AKT).

binding, which promotes SNARE complex formation (165). Given the known role of Doc2b as a positive effector in clonal beta cells, and a Munc18-1 binding protein (164), we sought to determine if Doc2b might also impact Syntaxin 1 based SNARE-Munc18-1 interactions in MIN6 beta cells. Cells were transfected to over-express Doc2b, in effort to model that of the Doc2b Tg islet beta cells (which are insufficiently abundant for these biochemical assays). Indeed Doc2b over-expression increased Syntaxin 1-VAMP2-SNAP25 SNARE core complex formation, but did not alter Munc18-1 Syntaxin 1 association (Fig. 4-8A-B).

To determine how Doc2b enrichment in skeletal muscle of the Doc2b Tg mice might increase PM-localization of GLUT4, Munc18c-Syntaxin 4 binding and Syntaxin 4 activation/SNARE complex formation was studied in L6-GLUT4-myc myoblasts transfected to express exogenous GFP-tagged Doc2b (or GFP vector control). L6-GLUT4-myc skeletal myoblasts are the premiere clonal muscle cell line for recapitulating the events associated with GLUT4 vesicle exocytosis (189) and transfect with ~30-50% efficiency. Immunoprecipitation of Syntaxin 4 from insulin-stimulated GFP-Doc2b expressing L6 cells resulted in reduced Munc18c co-precipitation compared to GFP-vector expressing cells (Fig. 4-9A). Syntaxin 4 accessibility to VAMP2 was examined as an indicator of ability to form SNARE complexes, given the inability to obtain sufficient PM protein from transfected L6 cells for co-immunoprecipitation analyses. Syntaxin 4 accessibility to an exogenous GST-VAMP2 protein linked to sepharose beads from insulin-stimulated GFP-Doc2b expressing L6 myoblasts was enhanced by ~30% relative

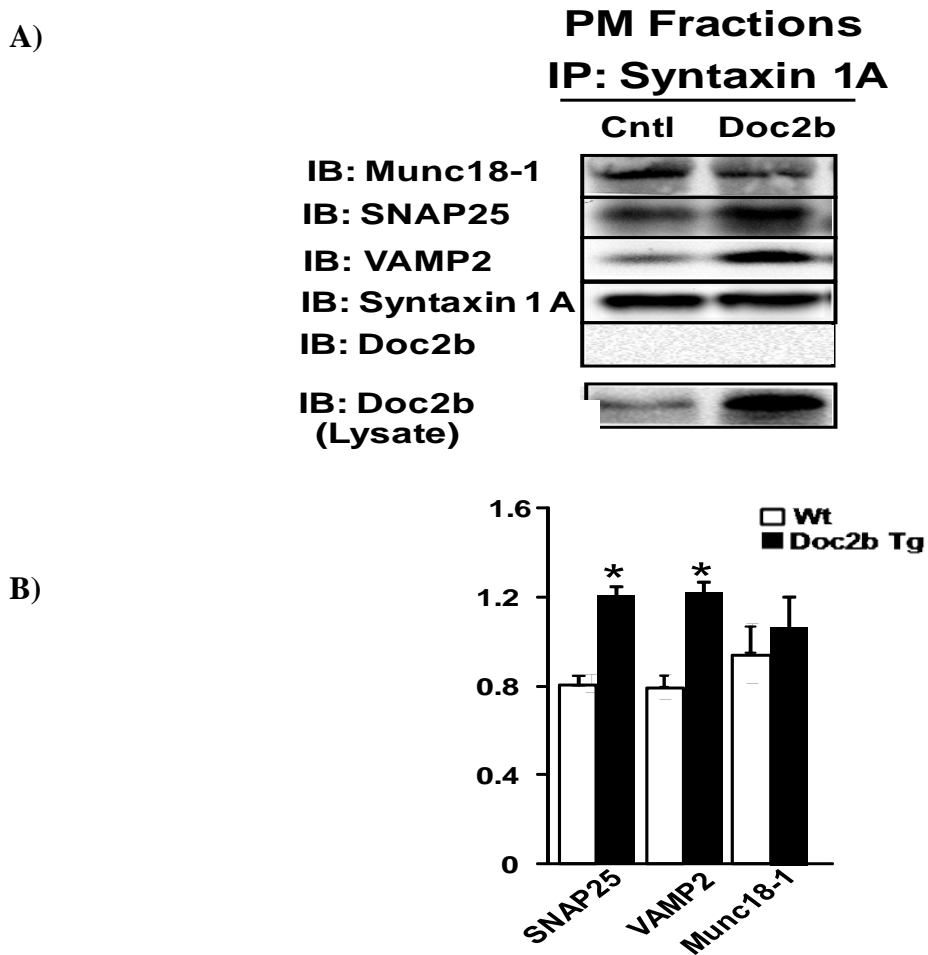
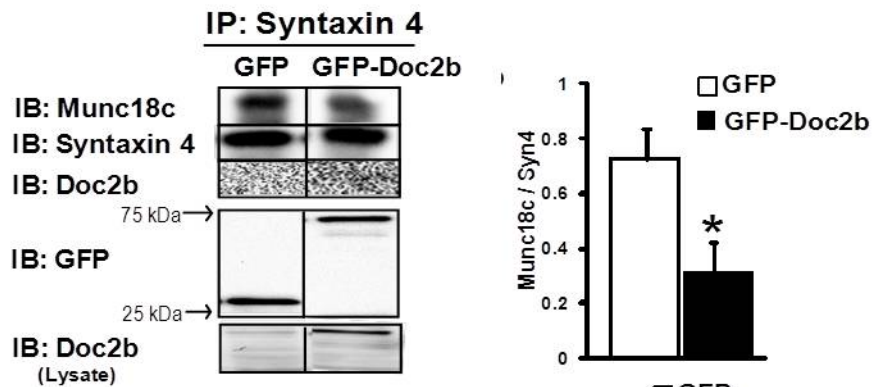


**Figure 4-8. Over-expression of Doc2b increases the abundance of SNARE complexes in the PM of MIN6 beta cells.** (A) MIN6 cells transfected to over-express Doc2b or vector control DNA were sub-fractionated as described (154). PM fractions were used in immunoprecipitation reactions with anti-Syntaxin1A antibody, and co-immunoprecipitated proteins were resolved on 12% SDS-PAGE for immunodetection of Munc18-1, SNAP25, VAMP2 and Doc2b. Doc2b protein over-expression was confirmed in lysates. (B) Quantitation is shown as the average  $\pm$  SE for 3 independent experiments; \* $P < 0.05$  vs. control transfected cells.

A)



B)

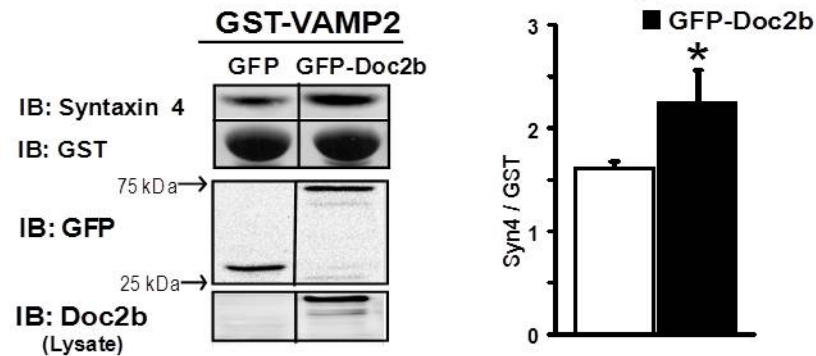


**Figure 4-9. Over-expression of Doc2b co-ordinately decreases Munc18c-Syntaxin 4 binding while increasing Syntaxin 4 activation in L6 GLUT4-myc myoblasts.** Detergent lysates prepared from L6 GLUT4-myc myoblasts transfected to express GFP-tagged Doc2b or GFP alone and stimulated with insulin were used in (A) anti-Syntaxin 4 immunoprecipitation reactions and co-precipitated Munc18c or Doc2b proteins detected by immunoblotting, or (B) GST-VAMP2 interaction assays for detection of the Syntaxin 4 present in lysates that is accessible to the exogenous GST-VAMP2 probe. Proteins were immunoblotted for Syntaxin 4 and GST. Quantitation is represented in the adjacent bar graph as the average  $\pm$  SE of the ratio of Syntaxin 4 normalized to GST-VAMP2 in 3 independent experiments; \*P<0.05 vs. GFP alone.

to cells expressing a similar amount of GFP control protein (Fig. 4-9B). Together, these results suggest that Doc2b is a limiting factor for Munc18c- Syntaxin 4 dissociation in skeletal muscle cells, and that the potentiation of Syntaxin 4 accessibility by increased expression of Doc2b may underlie the enhanced GLUT4 accumulation in PM fractions and insulin sensitivity of the Doc2b Tg mice.

### **4.3 DISCUSSION**

In this study, we tested the concept that Doc2b is limiting for glucose homeostasis, and that enriching Doc2b might provide a means to simultaneously improve insulin sensitivity and insulin secretion in an effort to enhance whole body glucose homeostasis *in vivo*. Using novel tetracycline-repressible Doc2b Tg mice, we show that increasing the expression of Doc2b by ~2-3 fold in pancreas results in potentiated insulin release during both first and second phases. This potentiated insulin release correlated with increased abundances of Syntaxin 1- and Syntaxin 4-based SNARE complexes assembled at the PM of beta cells. Increased expression of Doc2b in skeletal muscle substantially potentiated the accumulation of GLUT4 vesicles at the cell surface of sarcolemmal/t-tubule membranes, likely accounting for the improved insulin sensitivity in Doc2b Tg mice. Mechanistic studies performed in L6 myoblasts enriched with Doc2b demonstrated an increased abundance of Syntaxin 4 accessibility to the v-SNARE. These data provide the first *in vivo* proof of concept data for future research on Doc2b as a therapeutic target for treatment of pre- and T2D.



The enhanced glucose tolerance in the Doc2b Tg mice was found to be mediated by potentiation of both insulin secretion and peripheral insulin action. Increased serum insulin content in Doc2b Tg mice post-glucose injection is likely directly related to the improved glucose-stimulated biphasic insulin secretion of the islet beta cells. In our *ex vivo* islet studies, the second-phase was particularly robust, and it has been suggested that second-phase release communicates that quotient of insulin to the peripheral tissues, such as skeletal muscle. However Doc2b enrichment also potentiated the first-phase, and because the first-phase of insulin release rapidly impacts hepatic glucose output (190), it remains possible that the liver glucose output rate was reduced rapidly to contribute to the overall improvement of glucose tolerance. Another possibility is that the robustness of first-phase insulin release obviated the need for an extended second-phase. In addition, Doc2b Tg mice have significant enhancement in skeletal muscle insulin sensitivity and increased GLUT4 accumulation at the cell surface. As such, the skeletal muscle would require less insulin to accomplish its task, and the need for sustained insulin release during the second-phase may be reduced. Thus, this first Doc2b Tg mouse model provides the first proof of principle for the potential merit of Doc2b enrichment in glycemic control. Future studies utilizing skeletal muscle- and islet beta cell-specific Doc2b over-expression mouse models will facilitate delineation of the relative contributions of Doc2b enrichment in these tissues to maintenance of glucose homeostasis.

The positive effect of Doc2b enrichment upon peripheral insulin sensitivity and GLUT4 accumulation at the cell surface of skeletal muscle suggests that endogenous

Doc2b in skeletal muscle and/or fat is limiting for insulin-stimulated glucose clearance mechanisms. These *in vivo* and *ex vivo* skeletal muscle data validate an earlier report wherein Doc2b over-expression in 3T3-L1 adipocytes enhanced glucose uptake (168). Our data supports an indirect role for Doc2b in its potentiation of skeletal muscle insulin action at the level of SNARE complex formation, since Doc2b in skeletal muscle lysates failed to co-precipitate with Syntaxin 4 (187), and even over-expression of Doc2b in L6 myoblasts failed to drive an interaction of Doc2b with Syntaxin 4. However, these findings in primary skeletal muscle tissue do not recapitulate the binding interactions derived from *in vitro* mixing assays using recombinant Doc2b (191), and may suggest that these interactions are impacted by additional factors such as the particular cellular milieu, post-translational modifications of the proteins involved, and/or by calcium. For example, insulin triggers the tyrosine phosphorylation of Munc18c in skeletal muscle (41), enhancing the affinity of Munc18c for Doc2b nearly 2-fold while decreasing its affinity for Syntaxin 4 (148, 187). Thus, these data are congruent with a model whereby Doc2b would seemingly titrate out more Munc18c to make more cellular Syntaxin 4 accessible, generating more Syntaxin 4-based docking/fusion sites for incoming GLUT4 vesicles. Another possible manner by which Doc2b enrichment potentiates GLUT4 exocytosis is via its recently described role in calcium-induced plasma membrane curvature induction, *in vitro* (191). However, prior findings suggest that calcium-activated Doc2b actions in bona fide skeletal muscle may differ from that seen *in vitro*, or in neurons and adipocytes (167-168), and as such remains to be tested.

Like GLUT4 vesicle exocytosis, insulin granule exocytosis utilizes Syntaxin 4-based SNARE complexes. Our finding that the second-phase was enhanced to a greater degree than first-phase GSIS from the Doc2b Tg islets is consistent with our prior observation that Doc2b enrichment enhanced Syntaxin 4-SNARE complex formation in MIN6 beta-cells (165). Corroborating this concept, islets from Doc2b knockout mice showed a greater impairment in second versus first-phase GSIS (187). Since second-phase insulin exocytosis requires Munc18c and hinges upon Munc18c's ability to undergo glucose-induced tyrosine phosphorylation (41, 154), the requirement and the role of Doc2b may be linked indirectly to Syntaxin 4 in mechanism(s) similar to that described above for the skeletal muscle. Doc2b potentiation of first-phase GSIS was related to its ability to increase Syn-1 SNARE complexes similarly to Syntaxin 4-SNARE complexes suggesting Doc2b improves SNARE complexes formation in beta cells in a parallel fashion. However, Doc2b did not alter Syntaxin 1-Munc18-1 co-precipitation, indicating that dissociation of Munc18-1 from Syn-1 is different from Munc18c-Syntaxin 4 complex dissociation, consistent with prior data in beta cells (136, 154). Indeed, Doc2b has the ability to bind each Munc18 isoform via its distinct C2 domains: Munc18-1 binds to C2A (164) while Munc18c binds to C2B (165). In addition to binding Munc18 proteins, Doc2b also binds to Munc13-1 via an N-terminal domain that is dispensable for binding either Munc18 protein (165); Munc13-1 also participates in biphasic GSIS (159). As such, we speculate that Doc2b's role in potentiating GSIS involves its ability to serve as a "landing platform" for transient associations with Munc18 and possibly Munc13 proteins. Increasing the number of Doc2b platforms may provide increased capacity for 'landing.

In summary, the data presented show promise for the concept of Doc2b as a new therapeutic target for pre-clinical and T2D, demonstrate its use to be feasible and safe for betterment of glycaemic control *in vivo*, and provide insight into the mechanisms of Doc2b action into particular SNARE-mediated exocytosis events that may prove valuable in future drug design strategies.

***Acknowledgements:***

We are thankful to the Indiana University School of Medicine Transgenic Animal Facility for generating the Doc2b Tg mice. We are grateful to Dr. Alexander Groffen (VU University, Amsterdam) for the GFP-Doc2b plasmid. We would also like to thank Dr Elmendorf for aliquots of L6 myoblasts. We are grateful to the Indiana University School of Medicine Islet Core Facility for isolating islets for our studies. We would like to thank Angelina Hernandez for her technical help for generating the Doc2b Tg targeting vector.

## **CHAPTER 5. CONCLUDING REMARKS**

The objective of this dissertation was to elucidate the mechanisms by which Doc2b regulates glucose homeostasis by coordinating insulin action in peripheral tissues and biphasic insulin secretion from pancreatic islet beta cells. My dissertation work encompasses investigations of Doc2b as a requisite participant and as a limiting factor in the maintenance of whole body glucose homeostasis *in vivo*. Additionally, modifications in Doc2b levels can alter Munc18c-Syntaxin 4 mediated insulin secretion as well as insulin responsiveness in skeletal muscle. Here, I will discuss the primary issues addressed in each chapter of my dissertation, including how this work impacts the fields of beta cell biology, skeletal muscle biology and the regulation of whole body glucose homeostasis, with suggestions towards additional work needed in those specific areas. Additionally I propose future studies pertaining to post-translational control of SNARE complex formation, calcium regulation of Doc2b, and non-exocytotic roles for Doc2b and SNARE proteins, including their potential as therapeutics for the control of dysregulated glucose homeostasis.

Doc2b is a relatively understudied protein in beta cells and peripheral tissues for its role in maintenance of glucose homeostasis. Secretion of growth hormone is enhanced in PC-12 cells over-expressing Doc2b (192). Also, reduction in spontaneous release frequency is seen in the neurons of Doc2b (-/-) mice (174). These data implicated Doc2b as a key player in neuronal exocytotic events suggesting a universal function for Doc2b, akin to that of the SNARE proteins. Our lab has shown that Doc2b binds to Munc18c, more so when Munc18c is phosphorylated (148). My dissertation work supports these observations and extends our knowledge regarding roles for Doc2b beyond that as a

Munc18c binding partner to show the following: 1) Doc2b is required for insulin secretion and insulin action, 2) Doc2b is a primary regulator of the Munc18c- Syntaxin 4 binary complex, to facilitate SNARE complex formation and Syntaxin 4 activation in response to appropriate stimuli, and 3) Doc2b is limiting for insulin secretion and insulin action, such that its enrichment boosts these processes to benefit whole body glucose homeostasis. My finding that increased expression of Doc2b increases the abundance of SNARE complexes explains why Doc2b is limiting for the exocytotic events underlying insulin release and insulin action. These data contribute to our understanding how deficiencies in SNARE and SNARE associated proteins are associated with prediabetes development, and reveal for the first time the concept that Doc2b enrichment could provide a means of mitigating two primary aberrations underlying T2D development.

Using two different mouse models, a classic whole body Doc2b knockout model (Doc2b KO) and a pancreas, muscle, and adipose tissue-specific Doc2b over-expressing transgenic model (Doc2b Tg), I demonstrated that modifications in Doc2b levels can either severely impair or improve, respectively, whole body glucose homeostasis. Furthermore, the phenotype of the Doc2b Tg animal model suggests that Doc2b is a limiting factor in the exocytosis of insulin granules in the pancreatic beta cells and GLUT4-containing vesicles in the skeletal muscle. Doc2b KO mice, following an intraperitoneal glucose challenge, not only failed to mount an appropriate insulin secretory response but also were incapable of glucose uptake at the peripheral tissues, resulting in impaired glucose tolerance. On the other hand, the Doc2b Tg mice displayed enhanced glucose tolerance, mediated through the transient potentiation of both insulin



secretion and peripheral insulin action (specifically, at the skeletal muscle). This is consistent with the reports published in cultured cells that increasing/decreasing Doc2b protein levels increases/decreases insulin secretion and GLUT4 vesicle exocytosis, respectively (165, 168). The potentiation in insulin secretion in Doc2b Tg mice was due to an improvement in beta cell secretory function and not insulin content, since insulin content was similar between the Doc2b Tg and Wt mice. These data imply that sufficient insulin is present within the beta cells; however, the insulin granules are released in a more efficient manner.

Our lab has demonstrated that islets utilize Munc18c to sustain second-phase insulin release (178). Interestingly, islet beta cells also contain the Munc18-1 isoform, and over-expression of Munc18-1 in human islets selectively enhances first-phase insulin secretion (136). Given the ability of Doc2b to bind to both Munc18-1 and Munc18c isoforms via its different C2 domains, I have begun testing whether all three proteins could bind simultaneously in cultured cells and *in vitro* (Ramalingam and Thurmond, unpublished). Indeed, my preliminary studies show that the two different Munc18 proteins do not bind each other, and that neither Munc18 protein competes with the other for binding to Doc2b (Ramalingam and Thurmond, unpublished). Since my work and that of others shows the Munc18-Doc2b interactions to be transient and dynamic in response to stimuli, my data prompt the concept of Doc2b serving as a scaffold or ‘landing platform’ to assemble Munc18 proteins and facilitate their cognate syntaxin-mediated exocytosis events in islet beta cells, as part of the underlying mechanism of biphasic insulin release.

## **5.1 FUTURE STUDIES**

### **5.1.1 Post-translational modifications and SNARE complex formation**

SNARE proteins have been implicated in exocytosis for more than 20 years, and even though some crucial questions have been answered, detailed molecular basis of the steps leading to exocytotic release is not completely established. Moreover, components of the SNARE core machinery are not shared by all tissues, and the impact of stress upon the machinery, such as diabetogenic stresses associated with obesity and inflammation, remains untested. Using cell based approaches and animal tissues extracts, my research efforts have contributed to understanding that Doc2b function in SNARE-mediated exocytosis is regulated by tyrosine phosphorylation of Munc18c. Specifically, in response to a stimulus (e.g. glucose or insulin), Munc18c becomes tyrosine phosphorylated at Tyr 219 in beta cells and adipocytes, while at Tyr 521 in adipocytes and muscle (41, 154). This phosphorylation regulates Munc18c's interaction with Syntaxin 4 (148), and induces a switch in Munc18c's binding preference from Syntaxin 4 to Doc2b. A clear next step will be to elucidate the Doc2b-Munc18c interaction via mutation of these tyrosine residues, the potential for post-translational modification of Doc2b in insulin-secreting or -responsive cell types.

In addition, the insulin receptor was recently identified as the kinase for Munc18c phosphorylation in muscle, and very recent work has revealed the protein tyrosine phosphatase 1B to be the counterpart to IR in Munc18c phosphorylation (155). Hence, it is vital to perform Munc18c-Doc2b association studies in mice or cell lines depleted of IR and of protein tyrosine phosphatase 1B. If tyrosine phosphorylation at those specific

residues is important, it could be useful to develop phosphatase inhibitors for therapeutic purposes. Moreover, it will be important to study Munc18c-Doc2b interactions while Munc18c undergoes O-linked glycosylation (193). O-linked glycosylation of Munc18c was associated with insulin resistance in adipocytes, yet my pilot data in beta cells suggested that Munc18c glycosylation is a normal part of its function in GSIS. Thus, it is imperative that the sites of Munc18c glycosylation be identified and mutated for functional evaluation, because if Munc18c glycosylation prompts positive action in beta cells, it could be exploited to activate the Munc18c switch to Doc2b so that Syntaxin 4 can bind VAMP2. Another binding partner of Munc18c, Wnk-1 (With no K lysine) is a serine/threonine kinase implicated in insulin exocytosis. Wnk-1 binds Doc2b and Munc18c (Oh and Thurmond, unpublished). To gain further insight into the complex fusion process, it will be key to study if both Doc2b and Wnk-1 regulate Munc18c binding to Syntaxin 4. It will be intriguing if Doc2b switches its binding between Wnk-1 and Munc18c under stimulated versus basal conditions respectively, in beta cells. A third Munc18 isoform, Munc18b, is also expressed in beta cells and by virtue of its high degree of homology to Munc18-1, may also bind to Doc2b. Since Munc18b has been implicated in granule-granule fusion, via binding to Syntaxin 2/3 to purportedly supplement biphasic insulin secretion by increasing the number of newcomer granules at the PM (194), one could speculate that Doc2b utilizes a common regulatory mechanism similar to Munc18c with Syntaxin 4.

The binding switch from Syntaxin 4 to Doc2b of Munc18c temporally correlates with increased SNARE core complex formation, leading to exocytosis. Increased

Munc18c-Doc2b binding was observed under Doc2b-enriched conditions. Further, increased Munc18c-Doc2b binding also correlated with increased abundances of Syntaxin 4 available for VAMP2 binding. This elevation of PM-localized SNARE densities led to enhanced SNARE complex formation. The possible explanation is that increasing the SNARE densities would raise the probability of the SNARE complex formation, ultimately increasing the amount of vesicle exocytosis.

Apart from Munc18c, various other Doc2b binding partners have been identified in other tissues. In neuronal cells, Munc13-1 binds to Doc2b through its N terminal MID domain to promote vesicle release. Munc13-1 is an essential priming protein facilitating SNARE complex formation. The direct interaction between Munc13-1 and Doc2b is yet to be demonstrated in beta cells. It will be important to understand the requirement for this association in beta cells, as reduced Munc13-1 levels are known to inhibit biphasic insulin secretion. For example, Doc2b is required for Munc13-1 translocation to PM in chromaffin cells. Further Munc13-1 is known to directly interact with Syntaxin-1 and switch syntaxin from closed to open position; finding these events to hold in beta cells would strongly suggest Doc2b to operate in granule priming. Another isoform of Munc13, Munc13-4 was recently identified to bind Syntaxin 4 using *in vitro* liposome assays (160). Munc13-4 is also identified as a limiting factor in platelet exocytosis (161), suggesting it may carry importance in insulin exocytosis. An intriguing possibility is that the Munc13-Doc2b interaction acts as an extra signaling factor to promote fusion by activating syntaxins under stress-induced conditions like hyperglycemia. Diacylglycerol levels are increased under hyperglycemic conditions, and Munc13-1 is reported to

potentiate insulin secretion in the presence of diacylglycerol. Hence, I hypothesize that Doc2b could alter insulin secretion through Munc13, possibly independent of Munc18 proteins.

### **5.1.2 Regulation of Doc2b by calcium**

In 3T3-L1 adipocytes, Doc2b reportedly binds to Syntaxin 4, but only under high (1 mM) calcium buffer conditions (168). Doc2b-Syntaxin 4 binding is also detected *in vitro* under high calcium conditions. In contrast, I did not detect Doc2b-Syntaxin 4 interactions in skeletal muscle under similar calcium conditions. Doc2b is known to require very little calcium to translocate in neurons (35). As such, the *in vitro* studies performed uses full-length Syntaxin 4, which is known to exhibit non-specific “sticky” interactions owing to the presence of a transmembrane domain at the hydrophobic C-terminus, under conditions of very mild stringency (0.5% NP40 detergent), an interaction was detectable *in vitro*. The requirement for high calcium to see the interaction might be related to Doc2b’s two calcium binding domains. Previous studies in neuronal cells show that the translocation of Doc2b from the cytosol to PM requires micromolar amounts of calcium. In contrast, I have shown that Doc2b does not translocate under insulin-stimulated conditions in skeletal muscle extracts, but found already localized at the PM under resting conditions. Skeletal muscle may have baseline calcium already high enough to translocate Doc2b under resting conditions. Under such conditions, Doc2b can be considered constitutively active (167), which can explain the strong effects in the Doc2b<sup>-/-</sup> mice observed here, relative to effects previously observed in brain (174).

Supporting the concept of a calcium-independent role for Doc2b, a previous study in neuronal cells demonstrated that calcium is required only for binary complex formation between Syntaxin and SNAP25 but not for ternary complex (Syntaxin: SNAP25: VAMP2) (37). As such, Syntaxin 4 in muscle may be more accessible to form ternary complexes in a calcium-independent manner, contingent more upon the stimulus-induced phosphorylation and dissociation of Munc18c. Interestingly, no other protein with calcium binding domain, except Doc2b, is demonstrated to have a role in GLUT4 exocytosis, indicating that calcium may not have an important function in muscle, unlike neurons. Hence, it will be imperative to test whether calcium binds directly to Doc2b and triggers insulin action by studying the function of Doc2b mutants harboring point mutations in its 4 calcium binding sites, as done in neuronal cells (170).

Apart from Doc2b role in fusion, a few recent studies in neuronal cells have also focused on the role of Doc2b in membrane curvature. The C2A domain of Doc2b binds phospholipids in a calcium dependent manner and interacts with the PM (163). Further, mutation in the calcium binding residues in C2A affect fusion kinetics suggesting calcium may be necessary for inducing membrane curvature (191). A similar mechanism could possibly exist in beta cells since they express and utilize similar SNARE isoforms. Hence, it can be inferred that the C2B domain of Doc2b may have a role in translocation from cytosol to PM while the C2A domain has a role in its interaction with the PM.

### **5.1.3 Abundances of Doc2b and SNARE proteins.**

Doc2b transcript levels are significantly reduced in T2D mouse models, but mechanisms regulating Doc2b expression are, as of yet, unknown. MicroRNAs (miRNAs) may be one such mechanism. Similar to the findings from Regazzi and colleagues in which miRNA124 coordinately increased SNAP25 levels and elevated insulin release (195-196), it may be possible that miRNAs are also altering Doc2b levels, leading to changes in insulin secretion. Beyond miRNAs, other possible explanations for the reduced Doc2b expression associated with obesity and diabetes include proteosomal degradation, mRNA instability and impaired transcription. Evidence suggests that the SNARE proteins relevant to beta cell function are subject to proteosomal degradation, as well as miRNA targeting (82), indicating that Doc2b may be subject to similar processes. Identification of possible mechanisms that mediate Doc2b expression could be useful in deriving strategies to restore/enhance Doc2b levels to prevent and/or treat T2D. This would be a worthy avenue for future investigations, since restoring the levels of SNARE proteins in T2D islets is shown to enhance exocytotic function. Beyond improving beta cell function, there is a possibility that Doc2b could be involved in enhancing beta cell mass. Doc2b is expressed in the neuroepithelium by Embryonic Day 12 (E12), well before synaptic function is initiated at Embryonic Day 17 (E17), suggesting that Doc2b may have a role in the development of secretory cells. Coupled with data that demonstrates impaired blastocyst development in Syntaxin 4-depleted mouse lines, whether or not Doc2b has a role in beta cell development becomes an intriguing question to explore.

#### **5.1.4 Doc2b in whole body physiology and SNARE proteins as therapies**

Defects in both insulin secretion and action can lead to prediabetes and progression to T2D. Insulin secretion in beta cells and glucose transport in the peripheral tissues are mediated by similar exocytotic mechanisms, which utilize identical SNARE isoforms and Munc18 proteins. Since Doc2b was found to be a limiting factor for the exocytosis of insulin granules in beta cells and GLUT4 vesicles in skeletal muscle, the relative contribution of Doc2b enrichment in glucose homeostatic tissues needs to be further evaluated utilizing skeletal muscle- and islet beta cell-specific Doc2b over-expressing mouse models. Answering this question is essential, as our long term goal is to develop therapeutics that restore normoglycemia by targeting tissue-specific pathogenic effects. Of further interest is determining if over-expression of Doc2b affords protection against the development of glucose intolerance and insulin resistance under conditions of metabolic stress (e.g., high fat diet). The improvement in insulin secretion in Doc2b Tg mice is similar to improvements in Syntaxin 4 Tg mice. Since both Doc2b and Syntaxin 4 plays a role in granule docking/fusion, it would be exciting to explore the potential additive effect on insulin secretion in Syntaxin 4 and Doc2b double-transgenic mice. This is important to pursue since our lab has recently shown that islets of T2D humans are >40% deficient in Syntaxin 4 (Oh, Stull, Mirmira and Thurmond, manuscript submitted), such that Doc2b enrichment might be useful to more fully activate the residual Syntaxin 4 to improve GSIS function.

Doc2b is ubiquitously expressed, so one caveat to my studies is that I've not yet evaluated potential contributions from the fat, liver or alpha cells of the islet. Hence, it



will be important to perform a euglycemic-hyperinsulinemic clamp analysis to account for glucose output from the liver and glucose uptake in the peripheral tissues. Any impact of the liver would be indirect based upon current knowledge suggesting no exocytotic regulation for glucose output or insulin clearance mechanisms. It would be important to explore the role of Doc2b in islet alpha cells, given that SNARE mediated exocytosis occurs in alpha cells, hence alterations in Doc2b levels could affect glucagon secretion from the pancreatic alpha cells. The secreted glucagon could indirectly influence the glucose output. This could also assess the involvement of Doc2b in regulating glucagon secretion which influences glucose output. Glucose metabolism is also controlled to a certain extent by the brain. Since Doc2b is expressed in brain, its involvement in regulating glucose metabolism and leptin signaling in brain needs to be determined. Alternatively, a second Doc2a isoform that is functional in brain may also be expressed and functional in beta cells (it is notably neuroendocrine-cell specific), creating a brain-islet axis of metabolic control not yet investigated.

Currently, no studies regarding Doc2b have been reported in humans. Taking a step ahead, it will be interesting to check whether the phenotype of Doc2b Tg mice is recapitulated in healthy control and T2D human islets infected with Doc2b over-expressing adenovirus, or perhaps even peptides derived from Doc2b. Further, whether over-expression of Doc2b may also help preserve functional beta cell mass in T1D is of interest, since better insulin secretory function is observed in Doc2b over-expressing islets and Doc2b is implicated in cellular development. Due to the advancement in transplantation techniques, islets from Doc2b Tg mice can be transplanted into

streptozotocin-induced diabetic mice to delineate if Doc2b enrichment promotes islet function *in vivo* to restore euglycemia.

## **5.2 CONCLUSION**

Altogether, this research has extended our understanding of the molecular mechanisms by which Doc2b facilitate regulated exocytosis in insulin-secreting and insulin-responsive cell types to control glucose homeostasis. Given its nature as a soluble protein and its ability to enhance SNARE complex formation *in vivo*, Doc2b is an attractive therapeutic target for the prevention/treatment of T2D. The hope is that this discovery will bring clarification to the complex exocytotic processes in beta cells and muscle/adipose tissue. The greater anticipation is that one day this research may have some real consequence in the treatment and/or prevention of diabetes.

**APPENDIX: PERMISSION TO REPRODUCE PREVIOUSLY PUBLISHED  
MATERIAL**



**Confirmation Number: 11128746**  
**Order Date: 10/08/2013**

#### Customer Information

**Customer:** Latha Ramalingam  
**Account Number:** 3000705211  
**Organization:** Latha Ramalingam  
**Email:** lathrama@iupui.edu  
**Phone:** +1 (317)3746694  
**Payment Method:** Invoice

#### Order Details

##### Diabetes : a journal of the American Diabetes Association

Billing Status: N/A
------------------------

**Order detail ID:** 64071468  
**ISSN:** 1939-327X  
**Publication Type:** e-Journal  
**Volume:**  
**Issue:**  
**Start page:**  
**Publisher:** AMERICAN DIABETES ASSOCIATION]  
**Author/Editor:** American Diabetes Association ;  
Stanford University

**Permission Status:** **Granted**  
**Permission type:** Republish or display content  
**Type of use:** Republish in a thesis/dissertation  
**Order License Id:** 3244330952671

<b>Requestor type</b>	Academic institution
<b>Format</b>	Print, Electronic
<b>Portion</b>	chapter/article
<b>Number of pages in chapter/article</b>	10
<b>Title or numeric reference of the portion(s)</b>	entire article
<b>Title of the article or chapter the portion is from</b>	Doc2b is a Key Effector of Insulin Secretion and Skeletal Muscle Insulin Sensitivity
<b>Editor of portion(s)</b>	NA
<b>Author of portion(s)</b>	BA
<b>Volume of serial or monograph</b>	NA
<b>Issue, if republishing an article from a serial</b>	NA
<b>Page range of portion</b>	1-10
<b>Publication date of portion</b>	OCT 2012
<b>Rights for</b>	Main product
<b>Duration of use</b>	Life of current edition
<b>Creation of copies for the disabled</b>	no
<b>With minor editing privileges</b>	no
<b>For distribution to</b>	Worldwide
<b>In the following language(s)</b>	Original language of publication
<b>With incidental promotional use</b>	no
<b>Lifetime unit quantity of new product</b>	0 to 499

This is a License Agreement between Latha Ramalingam ("You") and Springer ("Springer") provided by Copyright Clearance Center ("CCC").

License Number 3244331263767

License date Oct 08, 2013

Licensed content publisher Springer

Licensed content  
publication

Cellular and Molecular Life Sciences

Licensed content title Novel roles for insulin receptor (IR) in adipocytes and skeletal muscle cells via new and unexpected substrates

Licensed content author Latha Ramalingam

Licensed content date Jan 1, 2012

Volume number 70

Issue number 16

Type of Use Thesis/Dissertation

Portion Full text

Number of copies 1

Author of this Springer  
article

Yes and you are a contributor of the new work

Order reference number

Title of your thesis /  
dissertation

Regulation of Glucose homeostasis by Doc2b and Munc18 proteins.

Expected completion date Jan 2014

Estimated size(pages) 100

Total 0.00 USD

## REFERENCES

1. Steyn, N. P., Lambert, E. V., and Tabana, H. (2009) Conference on "Multidisciplinary approaches to nutritional problems". Symposium on "Diabetes and health". Nutrition interventions for the prevention of type 2 diabetes. *Proc Nutr Soc* **68**, 55-70
2. Cherrington, A. D., Sindelar, D., Edgerton, D., Steiner, K., and McGuinness, O. P. (2002) Physiological consequences of phasic insulin release in the normal animal. *Diabetes* **51 Suppl 1**, S103-108
3. Meier, J. J., Veldhuis, J. D., and Butler, P. C. (2005) Pulsatile insulin secretion dictates systemic insulin delivery by regulating hepatic insulin extraction in humans. *Diabetes* **54**, 1649-1656
4. Rogers, S., and Silink, M. (1985) Residual insulin secretion in insulin dependent diabetes mellitus. *Arch Dis Child* **60**, 200-203.
5. Buchanan, T. A. (2003) Pancreatic beta-cell loss and preservation in type 2 diabetes. *Clin Ther* **25 Suppl B**, B32-46
6. Leibowitz, G., Kaiser, N. and Cerasi, E. (2011)  $\beta$ -Cell failure in type 2 diabetes. *Journal of Diabetes Investigation* **2**
7. Carnethon, M. R., De Chavez, P. J., Biggs, M. L., Lewis, C. E., Pankow, J. S., Bertoni, A. G., Golden, S. H., Liu, K., Mukamal, K. J., Campbell-Jenkins, B., and Dyer, A. R. (2012) Association of weight status with mortality in adults with incident diabetes. *JAMA* **308**, 581-590
8. Corkey, B. E. (2012) Diabetes: have we got it all wrong? Insulin hypersecretion and food additives: cause of obesity and diabetes? *Diabetes Care* **35**, 2432-2437
9. DeFronzo, R. A. (2009) Banting Lecture. From the triumvirate to the ominous octet: a new paradigm for the treatment of type 2 diabetes mellitus. *Diabetes* **58**, 773-795
10. Butler, A. E., Janson, J., Bonner-Weir, S., Ritzel, R., Rizza, R. A., and Butler, P. C. (2003) Beta-cell deficit and increased beta-cell apoptosis in humans with type 2 diabetes. *Diabetes* **52**, 102-110.
11. Nesher, R., and Cerasi, E. (2002) Modeling phasic insulin release: immediate and time-dependent effects of glucose. *Diabetes* **51**, S53-59.
12. Pimenta, W., Korytkowski, M., Mitrakou, A., Jenssen, T., Yki-Jarvinen, H., Evron, W., Dailey, G., and Gerich, J. (1995) Pancreatic beta-cell dysfunction as the primary genetic lesion in NIDDM. Evidence from studies in normal glucose-tolerant individuals with a first-degree NIDDM relative. *JAMA* **273**, 1855-1861
13. van Haeften, T. W., Dubbeldam, S., Zonderland, M. L., and Erkelens, D. W. (1998) Insulin secretion in normal glucose-tolerant relatives of type 2 diabetic subjects. Assessments using hyperglycemic glucose clamps and oral glucose tolerance tests. *Diabetes Care* **21**, 278-282
14. Ciaraldi, T. P., and Olefsky, J. M. (1980) Relationship between Deactivation of Insulin-stimulated Glucose Transport and Insulin Dissociation in Isolated Rat Adipocytes. *J. Biol. Chem.* **255**, 327-330
15. Kaiser, N., Yuli, M., Uckaya, G., Opreescu, A. I., Berthault, M. F., Kargar, C., Donath, M. Y., Cerasi, E., and Ktorza, A. (2005) Dynamic changes in  $\beta$ -cell mass and pancreatic

- insulin during the evolution of nutrition-dependent diabetes in psammomys obesus: impact of glycemic control. *Diabetes* **54**, 138-145
16. Sladek, R., Rocheleau, G., Rung, J., Dina, C., Shen, L., Serre, D., Boutin, P., Vincent, D., Belisle, A., Hadjadj, S., Balkau, B., Heude, B., Charpentier, G., Hudson, T. J., Montpetit, A., Pshezhetsky, A. V., Prentki, M., Posner, B. I., Balding, D. J., Meyre, D., Polychronakos, C., and Froguel, P. (2007) A genome-wide association study identifies novel risk loci for type 2 diabetes. *Nature* **445**, 881-885
  17. P, L. (1869) Contributions to the microscopic anatomy of the pancreas. *In Faculty of Medicine Berlin: University of Berlin*
  18. Orci, L., and Unger, R. H. (1975) Functional subdivision of islets of Langerhans and possible role of D cells. *Lancet* **2**, 1243-1244
  19. Wierup, N., Svensson, H., Mulder, H., and Sundler, F. (2002) The ghrelin cell: a novel developmentally regulated islet cell in the human pancreas. *Regul Pept* **107**, 63-69
  20. Cerasi, E., and Luft, R. (1967) The plasma insulin response to glucose infusion in healthy subjects and in diabetes mellitus. *Acta Endocrinol (Copenh)* **55**, 278-304
  21. Cobelli, C., Toffolo, G. M., Dalla Man, C., Campioni, M., Denti, P., Caumo, A., Butler, P., and Rizza, R. (2007) Assessment of beta-cell function in humans, simultaneously with insulin sensitivity and hepatic extraction, from intravenous and oral glucose tests. *Am J Physiol Endocrinol Metab* **293**, E1-E15
  22. Grodsky, G. M. (1972) A threshold distribution hypothesis for packet storage of insulin and its mathematical modeling. *J Clin Invest* **51**, 2047-2059
  23. Curry, D. L., Bennett, L. L., and Grodsky, G. M. (1968) Dynamics of insulin secretion by the perfused rat pancreas. *Endocrinology* **83**, 572-584.
  24. Proks, P., Eliasson, L., Ammala, C., Rorsman, P., and Ashcroft, F. M. (1996) Ca(2+)- and GTP-dependent exocytosis in mouse pancreatic beta-cells involves both common and distinct steps. *J Physiol* **496**, 255-264.
  25. Rorsman, P., and Renstrom, E. (2003) Insulin granule dynamics in pancreatic beta cells. *Diabetologia* **46**, 1029-1045
  26. Rorsman, P., Eliasson, L., Renstrom, E., Gromada, J., Barg, S., and Gopel, S. (2000) The Cell Physiology of Biphasic Insulin Secretion. *News Physiol. Sci.* **15**, 72-77
  27. Gembal, M., Gilon, P., and Henquin, J. C. (1992) Evidence that glucose can control insulin release independently from its action on ATP-sensitive K<sup>+</sup> channels in mouse B cells. *J Clin Invest* **89**, 1288-1295.
  28. Ohara-Imaizumi, M., Fujiwara, T., Nakamichi, Y., Okamura, T., Akimoto, Y., Kawai, J., Matsushima, S., Kawakami, H., Watanabe, T., Akagawa, K., and Nagamatsu, S. (2007) Imaging analysis reveals mechanistic differences between first- and second-phase insulin exocytosis. *J Cell Biol* **177**, 695-705
  29. Grodsky, G. M. (2000) Kinetics of insulin secretion: underlying metabolic events. In *Diabetes Mellitus: a fundamental and clinical text* (LeRoith, D., Taylor, S., and Olefsky, J., eds), Lippincott Williams & Wilkins, Philadelphia, PA
  30. Newgard, C. B., and McGarry, J. D. (1995) Metabolic coupling factors in pancreatic beta-cell signal transduction. *Annu Rev Biochem* **64**, 689-719
  31. McCulloch, L. J., van de Bunt, M., Braun, M., Frayn, K. N., Clark, A., and Gloyn, A. L. (2011) GLUT2 (SLC2A2) is not the principal glucose transporter in human pancreatic beta cells: implications for understanding genetic association signals at this locus. *Mol Genet Metab* **104**, 648-653

32. Jewell, J. L., Oh, E., and Thurmond, D. C. (2010) Exocytosis mechanisms underlying insulin release and glucose uptake: conserved roles for Munc18c and syntaxin 4. *AJP Regul Integr Comp Physiol* **298**, R517-531. Epub 2010 Jan 2016.
33. Thorens, B., Wu, Y. J., Leahy, J. L., and Weir, G. C. (1992) The loss of GLUT2 expression by glucose-unresponsive beta cells of db/db mice is reversible and is induced by the diabetic environment. *Journal of Clinical Investigation* **90**, 77-85
34. Cook, D. L., and Hales, C. N. (1984) Intracellular ATP directly blocks K<sup>+</sup> channels in pancreatic B-cells. *Nature* **311**, 271-273
35. Ashcroft, F. M., Harrison, D. E., and Ashcroft, S. J. (1984) Glucose induces closure of single potassium channels in isolated rat pancreatic beta-cells. *Nature* **312**, 446-448.
36. Berggren, P. O., Arkhammar, P., Islam, M. S., Juntti-Berggren, L., Khan, A., Kindmark, H., Kohler, M., Larsson, K., Larsson, O., Nilsson, T., and et al. (1993) Regulation of cytoplasmic free Ca<sup>2+</sup> in insulin-secreting cells. *Adv Exp Med Biol* **334**, 25-45
37. Takahashi, N., Hatakeyama, H., Okado, H., Noguchi, J., Ohno, M., and Kasai, H. (2010) SNARE conformational changes that prepare vesicles for exocytosis. *Cell Metabolism* **12**, 19-29.
38. Baron, V., Kaliman, P., Gautier, N., and Van Obberghen, E. (1992) The insulin receptor activation process involves localized conformational changes. *J Biol Chem* **267**, 23290-23294
39. Herrera, R., and Rosen, O. M. (1986) Autophosphorylation of the insulin receptor in vitro. Designation of phosphorylation sites and correlation with receptor kinase activation. *J Biol Chem* **261**, 11980-11985
40. White, M. F., Shoelson, S. E., Keutmann, H., and Kahn, C. R. (1988) A cascade of tyrosine autophosphorylation in the beta-subunit activates the phosphotransferase of the insulin receptor. *J Biol Chem* **263**, 2969-2980
41. Jewell, J. L., Oh, E., Ramalingam, L., Kalwat, M. A., Tagliabracci, V. S., Tackett, L., Elmendorf, J. S., and Thurmond, D. C. (2011) Munc18c phosphorylation by the insulin receptor links cell signaling directly to SNARE exocytosis. *J Cell Biol* **193**, 185-199
42. Suzuki, K., and Kono, T. (1980) Evidence that insulin causes translocation of glucose transport activity to the plasma membrane from an intracellular storage site. *Proc Natl Acad Sci USA* **77**, 2542-2545
43. Cushman, S. W., and Wardzala, L. J. (1980) Potential mechanism of insulin action on glucose transport in the isolated rat adipose cell. Apparent translocation of intracellular transport systems to the plasma membrane. *J Biol Chem* **255**, 4758-4762
44. Rea, S., and James, D. E. (1997) Moving GLUT4: the biogenesis and trafficking of GLUT4 storage vesicles. *Diabetes* **46**, 1667-1677
45. Baumann, C. A., Ribon, V., Kanzaki, M., Thurmond, D. C., Mora, S., Shigematsu, S., Bickel, P. E., Pessin, J. E., and Saltiel, A. R. (2000) CAP defines a second signalling pathway required for insulin-stimulated glucose transport [see comments]. *Nature* **407**, 202-207
46. Pessin, J. E., and Saltiel, A. R. (2000) Signaling pathways in insulin action: molecular targets of insulin resistance. *J Clin Invest* **106**, 165-169.
47. Liu, J., Kimura, A., Baumann, C. A., and Saltiel, A. R. (2002) APS facilitates c-Cbl tyrosine phosphorylation and GLUT4 translocation in response to insulin in 3T3-L1 adipocytes. *Mol Cell Biol* **22**, 3599-3609
48. Hu, J., Liu, J., Ghirlando, R., Saltiel, A. R., and Hubbard, S. R. (2003) Structural basis for recruitment of the adaptor protein APS to the activated insulin receptor. *Mol Cell* **12**, 1379-1389



49. Ribon, V., Printen, J. A., Hoffman, N. G., Kay, B. K., and Saltiel, A. R. (1998) A novel, multifunctional c-Cbl binding protein in insulin receptor signaling in 3T3-L1 adipocytes. *Mol Cell Biol* **18**, 872-879
50. Liu, J., Deyoung, S. M., Zhang, M., Dold, L. H., and Saltiel, A. R. (2005) The stomatin/prohibitin/flotillin/HflK/C domain of flotillin-1 contains distinct sequences that direct plasma membrane localization and protein interactions in 3T3-L1 adipocytes. *J Biol Chem* **280**, 16125-16134
51. Ribon, V., Hubbell, S., Herrera, R., and Saltiel, A. R. (1996) The product of the cbl oncogene forms stable complexes in vivo with endogenous Crk in a tyrosine phosphorylation-dependent manner. *Mol Cell Biol* **16**, 45-52
52. Knudsen, B. S., Feller, S. M., and Hanafusa, H. (1994) Four proline-rich sequences of the guanine-nucleotide exchange factor C3G bind with unique specificity to the first Src homology 3 domain of Crk. *J Biol Chem* **269**, 32781-32787
53. Chiang, S.-H., Baumann, C. A., Kanzaki, M., Thurmond, D. C., Macara, I. G., Pessin, J. E., and Saltiel, A. R. (2001) Insulin-Stimulated GLUT4 translocation requires the CAP-Dependent but PI 3-kinase-independent activation of the small GTP binding protein TC10. (*submitted*).
54. Watson, R. T., Shigematsu, S., Chiang, S. H., Mora, S., Kanzaki, M., Macara, I. G., Saltiel, A. R., and Pessin, J. E. (2001) Lipid raft microdomain compartmentalization of TC10 is required for insulin signaling and GLUT4 translocation. *J Cell Biol* **154**, 829-840
55. Chang, L., Adams, R. D., and Saltiel, A. R. (2002) The TC10-interacting protein CIP4/2 is required for insulin-stimulated Glut4 translocation in 3T3L1 adipocytes. *Proc Natl Acad Sci U S A* **99**, 12835-12840
56. Omata, W., Shibata, H., Li, L., Takata, K., and Kojima, I. (2000) Actin filaments play a critical role in insulin-induced exocytotic recruitment but not in endocytosis of GLUT4 in isolated rat adipocytes. *Biochem J* **346**, 321-328
57. Tsakiridis, T., Vranic, M., and Klip, A. (1994) Disassembly of the actin network inhibits insulin-dependent stimulation of glucose transport and prevents recruitment of glucose transporters to the plasma membrane. *J. Biol. Chem.* **269**, 29934-29942
58. Brozinick, J. T., Jr., Berkemeier, B. A., and Elmendorf, J. S. (2007) "Actin"ing on GLUT4: membrane & cytoskeletal components of insulin action. *Curr Diabetes Rev* **3**, 111-122
59. Kanzaki, M., and Pessin, J. E. (2001) Insulin-stimulated GLUT4 translocation in adipocytes is dependent upon cortical actin remodeling. *J Biol Chem* **276**, 42436-42444.
60. Sarabia, V., Ramlal, T., and Klip, A. (1990) Glucose uptake in human and animal muscle cells in culture. *Biochem Cell Biol* **68**, 536-542
61. Burdett, E., Beeler, T., and Klip, A. (1987) Distribution of glucose transporters and insulin receptors in the plasma membrane and transverse tubules of skeletal muscle. *Arch Biochem Biophys* **253**, 279-286
62. Hansen, P. A., Gulve, E. A., Marshall, B. A., Gao, J., Pessin, J. E., Holloszy, J. O., and Mueckler, M. (1995) Skeletal muscle glucose transport and metabolism are enhanced in transgenic mice overexpressing the Glut4 glucose transporter. *J Biol Chem* **270**, 1679-1684
63. Olson, A. L., Knight, J. B., and Pessin, J. E. (1997) Syntaxin 4, VAMP2, and/or VAMP3/cellubrevin are functional target membrane and vesicle SNAP receptors for insulin-stimulated GLUT4 translocation in adipocytes. *Mol Cell Biol* **17**, 2425-2435

64. Volchuk, A., Mitsumoto, Y., He, L., Liu, Z., Habermann, E., Trimble, W., and Klip, A. (1994) Expression of vesicle-associated membrane protein 2 (VAMP-2)/synaptobrevin II and cellubrevin in rat skeletal muscle and in a muscle cell line. *Biochem J* **304 ( Pt 1)**, 139-145
65. Tamori, Y., Hashiramoto, M., Araki, S., Kamata, Y., Takahashi, M., Kozaki, S., and Kasuga, M. (1996) Cleavage of vesicle-associated membrane protein (VAMP)-2 and cellubrevin on GLUT4-containing vesicles inhibits the translocation of GLUT4 in 3T3-L1 adipocytes. *Biochem Biophys Res Commun* **220**, 740-745
66. Williams, D., and Pessin, J. E. (2008) Mapping of R-SNARE function at distinct intracellular GLUT4 trafficking steps in adipocytes. *J Cell Biol* **180**, 375-387
67. Steegmaier, M., Yang, B., Yoo, J. S., Huang, B., Shen, M., Yu, S., Luo, Y., and Scheller, R. H. (1998) Three novel proteins of the syntaxin/SNAP-25 family. *J Biol Chem* **273**, 34171-34179.
68. Sollner, T., Bennett, M. K., Whiteheart, S. W., Scheller, R. H., and Rothman, J. E. (1993) A protein assembly-disassembly pathway in vitro that may correspond to sequential steps of synaptic vesicle docking, activation, and fusion. *Cell* **75**, 409-418
69. Weber, T., Zemelman, B. V., McNew, J. A., Westermann, B., Gmachl, M., Parlati, F., Sollner, T. H., and Rothman, J. E. (1998) SNAREpins: minimal machinery for membrane fusion. *Cell* **92**, 759-772
70. Bennett, M. K., Garcia-Ararras, J. E., Elferink, L. A., Peterson, K., Fleming, A. M., Hazuka, C. D., and Scheller, R. H. (1993) The syntaxin family of vesicular transport receptors. *Cell* **74**, 863-873
71. Oyler, G. A., Higgins, G. A., Hart, R. A., Battenberg, E., Billingsley, M., Bloom, F. E., and Wilson, M. C. (1989) The identification of a novel synaptosomal-associated protein, SNAP-25, differentially expressed by neuronal subpopulation. *J Cell Biol* **109**, 3039-3052
72. Trimble, W. S., Cowan, D. M., and Scheller, R. H. (1988) Vamp-1: A synaptic vesicle-associated integral membrane protein. *Proc Natl Acad Sci, USA* **85**, 4538-4542
73. Ungar, D., and Hughson, F. M. (2003) SNARE protein structure and function. *Annu Rev Cell Dev Biol* **19**, 493-517
74. Fasshauer, D., Otto, H., Eliason, W. K., Jahn, R., and Brunger, A. T. (1997) Structural changes are associated with soluble N-ethylmaleimide-sensitive fusion protein attachment protein receptor complex formation. *J Biol Chem* **272**, 28036-28041
75. Sollner, T., Whiteheart, S. W., Brunner, M., Erdjument-Bromage, H., Geromanos, S., Tempst, P., and Rothman, J. E. (1993) SNAP receptors implicated in vesicle targeting and fusion. *Nature* **362**, 318-324
76. Spurlin, B. A., and Thurmond, D. C. (2006) Syntaxin 4 Facilitates Biphasic Glucose-Stimulated Insulin Secretion from Pancreatic {beta}-Cells. *Mol Endocrinol* **20**, 183-193
77. Regazzi, R., Wollheim, C. B., Lang, J., Theler, J. M., Rossetto, O., Montecucco, C., Sadoul, K., Weller, U., Palmer, M., and Thorens, B. (1995) VAMP-2 and cellubrevin are expressed in pancreatic beta-cells and are essential for Ca(2+)-but not for GTP gamma S-induced insulin secretion. *Embo J* **14**, 2723-2730
78. Bai, L., Wang, Y., Fan, J., Chen, Y., Ji, W., Qu, A., Xu, P., James, D. E., and Xu, T. (2007) Dissecting multiple steps of GLUT4 trafficking and identifying the sites of insulin action. *Cell Metab* **5**, 47-57.
79. Cheatham, B., Volchuk, A., Kahn, C. R., Wang, L., Rhodes, C. J., and Klip, A. (1996) Insulin-stimulated translocation of GLUT4 glucose transporters requires SNARE-complex proteins. *Proc Natl Acad Sci USA* **93**, 15169-15173

80. Ostenson, C. G., Gaisano, H., Sheu, L., Tibell, A., and Bartfai, T. (2006) Impaired gene and protein expression of exocytotic soluble N-ethylmaleimide attachment protein receptor complex proteins in pancreatic islets of type 2 diabetic patients. *Diabetes* **55**, 435-440.
81. Chan, C. B., MacPhail, R. M., Sheu, L., Wheeler, M. B., and Gaisano, H. Y. (1999) Beta-cell hypertrophy in fa/fa rats is associated with basal glucose hypersensitivity and reduced SNARE protein expression. *Diabetes* **48**, 997-1005
82. Andersson, S. A., Olsson, A. H., Esguerra, J. L., Heimann, E., Ladenvall, C., Edlund, A., Salehi, A., Taneera, J., Degerman, E., Groop, L., Ling, C., and Eliasson, L. (2012) Reduced insulin secretion correlates with decreased expression of exocytotic genes in pancreatic islets from patients with type 2 diabetes. *Mol Cell Endocrinol* **364**, 36-45
83. Nagamatsu, S., Nakamichi, Y., Yamamura, C., Matsushima, S., Watanabe, T., Ozawa, S., Furukawa, H., and Ishida, H. (1999) Decreased expression of t-SNARE, syntaxin 1, and SNAP-25 in pancreatic beta-cells is involved in impaired insulin secretion from diabetic GK rat islets: restoration of decreased t-SNARE proteins improves impaired insulin secretion. *Diabetes* **48**, 2367-2373
84. Bergman, B. C., Cornier, M. A., Horton, T. J., Bessesen, D. H., and Eckel, R. H. (2008) Skeletal muscle munc18c and syntaxin 4 in human obesity. *Nutr Metab (Lond)* **5**, 21.
85. Mayer, A., Wickner, W., and Haas, A. (1996) Sec18p (NSF)-driven release of Sec17p (alpha-SNAP) can precede docking and fusion of yeast vacuoles. *Cell* **85**, 83-94
86. Sudhof, T. C., and Rothman, J. E. (2009) Membrane fusion: grappling with SNARE and SM proteins. *Science* **323**, 474-477.
87. Jahn, R., and Scheller, R. H. (2006) SNAREs--engines for membrane fusion. *Nat Rev Mol Cell Biol* **7**, 631-643.
88. Barg, S., Knowles, M. K., Chen, X., Midorikawa, M., and Almers, W. (2010) Syntaxin clusters assemble reversibly at sites of secretory granules in live cells. *Proc Natl Acad Sci U S A* **107**, 20804-20809
89. Spurlin, B. A., Park, S. Y., Nevins, A. K., Kim, J. K., and Thurmond, D. C. (2004) Syntaxin 4 transgenic mice exhibit enhanced insulin-mediated glucose uptake in skeletal muscle. *Diabetes* **53**, 2223-2231.
90. Saito, T., Okada, S., Yamada, E., Ohshima, K., Shimizu, H., Shimomura, K., Sato, M., Pessin, J. E., and Mori, M. (2003) Syntaxin 4 and Synip (syntaxin 4 interacting protein) regulate insulin secretion in the pancreatic beta HC-9 cell. *J Biol Chem* **278**, 36718-36725. Epub 32003 Jul 36719.
91. Yang, C., Coker, K. J., Kim, J. K., Mora, S., Thurmond, D. C., Davis, A. C., Yang, B., Williamson, R. A., Shulman, G. I., and Pessin, J. E. (2001) Syntaxin 4 heterozygous knockout mice develop muscle insulin resistance. *J Clin Invest* **107**, 1311-1318.
92. Canaves, J. M., and Montal, M. (1998) Assembly of a ternary complex by the predicted minimal coiled-coil-forming domains of syntaxin, SNAP-25, and synaptobrevin. A circular dichroism study. *J Biol Chem* **273**, 34214-34221
93. Lin, R. C., and Scheller, R. H. (1997) Structural organization of the synaptic exocytosis core complex. *Neuron* **19**, 1087-1094
94. Nicholson, K. L., Munson, M., Miller, R. B., Filip, T. J., Fairman, R., and Hughson, F. M. (1998) Regulation of SNARE complex assembly by an N-terminal domain of the t-SNARE Sso1p. *Nat Struct Biol* **5**, 793-802
95. Sutton, R. B., Fasshauer, D., Jahn, R., and Brunger, A. T. (1998) Crystal structure of a SNARE complex involved in synaptic exocytosis at 2.4 Å resolution [see comments]. *Nature* **395**, 347-353

96. Pobbati, A. V., Stein, A., and Fasshauer, D. (2006) N- to C-terminal SNARE complex assembly promotes rapid membrane fusion. *Science* **313**, 673-676
97. Fasshauer, D., Antonin, W., Subramaniam, V., and Jahn, R. (2002) SNARE assembly and disassembly exhibit a pronounced hysteresis. *Nat Struct Biol* **9**, 144-151
98. Zhou, P., Bacaj, T., Yang, X., Pang, Z. P., and Sudhof, T. C. (2013) Lipid-Anchored SNAREs Lacking Transmembrane Regions Fully Support Membrane Fusion during Neurotransmitter Release. *Neuron* **80**, 470-483
99. Montecucco, C., Schiavo, G., and Pantano, S. (2005) SNARE complexes and neuroexocytosis: how many, how close? *Trends Biochem Sci* **30**, 367-372
100. Stein, A., Weber, G., Wahl, M. C., and Jahn, R. (2009) Helical extension of the neuronal SNARE complex into the membrane. *Nature* **460**, 525-528
101. Shi, L., Shen, Q. T., Kiel, A., Wang, J., Wang, H. W., Melia, T. J., Rothman, J. E., and Pincet, F. (2012) SNARE proteins: one to fuse and three to keep the nascent fusion pore open. *Science* **335**, 1355-1359
102. Zhu, D., Koo, E., Kwan, E., Kang, Y., Park, S., Xie, H., Sugita, S., and Gaisano, H. Y. (2013) Syntaxin-3 regulates newcomer insulin granule exocytosis and compound fusion in pancreatic beta cells. *Diabetologia* **56**, 359-369
103. Wheeler, M. B., Sheu, L., Ghai, M., Bouquillon, A., Grondin, G., Weller, U., Beaudoin, A. R., Bennett, M. K., Trimble, W. S., and Gaisano, H. Y. (1996) Characterization of SNARE protein expression in beta cell lines and pancreatic islets. *Endocrinology* **137**, 1340-1348
104. Nagamatsu, S., Fujiwara, T., Nakamichi, Y., Watanabe, T., Katahira, H., Sawa, H., and Akagawa, K. (1996) Expression and functional role of syntaxin 1/HPC-1 in pancreatic beta cells. Syntaxin 1A, but not 1B, plays a negative role in regulatory insulin release pathway. *J Biol Chem* **271**, 1160-1165
105. de Wit, H., Cornelisse, L. N., Toonen, R. F., and Verhage, M. (2006) Docking of secretory vesicles is syntaxin dependent. *PLoS One* **1**, e126
106. Leung, Y. M., Kang, Y., Gao, X., Xia, F., Xie, H., Sheu, L., Tsuk, S., Lotan, I., Tsushima, R. G., and Gaisano, H. Y. (2003) Syntaxin 1A binds to the cytoplasmic C terminus of Kv2.1 to regulate channel gating and trafficking. *J Biol Chem* **278**, 17532-17538
107. Pasyk, E. A., Kang, Y., Huang, X., Cui, N., Sheu, L., and Gaisano, H. Y. (2004) Syntaxin-1A binds the nucleotide-binding folds of sulphonylurea receptor 1 to regulate the KATP channel. *J Biol Chem* **279**, 4234-4240
108. Chen, P. C., Bruederle, C. E., Gaisano, H. Y., and Shyng, S. L. (2011) Syntaxin 1A regulates surface expression of beta-cell ATP-sensitive potassium channels. *Am J Physiol Cell Physiol* **300**, C506-516
109. Cherniske, E. M., Carpenter, T. O., Klaiman, C., Young, E., Bregman, J., Insogna, K., Schultz, R. T., and Pober, B. R. (2004) Multisystem study of 20 older adults with Williams syndrome. *Am J Med Genet A* **131**, 255-264
110. Kang, Y., Huang, X., Pasyk, E. A., Ji, J., Holz, G. G., Wheeler, M. B., Tsushima, R. G., and Gaisano, H. Y. (2002) Syntaxin-3 and syntaxin-1A inhibit L-type calcium channel activity, insulin biosynthesis and exocytosis in beta-cell lines. *Diabetologia* **45**, 231-241.
111. Nagamatsu, S., Nakamichi, Y., Yamaguchi, K., Sawa, H., and Akagawa, K. (1997) Overexpressed syntaxin 1A/HPC-1 inhibits insulin secretion via a regulated pathway, but does not influence glucose metabolism and intracellular Ca<sup>2+</sup> in insulinoma cell line beta TC3 cells. *Biochem Biophys Res Commun* **231**, 89-93

112. Lam, P. P., Leung, Y. M., Sheu, L., Ellis, J., Tsushima, R. G., Osborne, L. R., and Gaisano, H. Y. (2005) Transgenic mouse overexpressing syntaxin-1A as a diabetes model. *Diabetes* **54**, 2744-2754.
113. Tsunoda, K., Sanke, T., Nakagawa, T., Furuta, H., and Nanjo, K. (2001) Single nucleotide polymorphism (D68D, T to C) in the syntaxin 1A gene correlates to age at onset and insulin requirement in Type II diabetic patients. *Diabetologia* **44**, 2092-2097
114. Hou, J. C., and Pessin, J. E. (2007) Ins (endocytosis) and outs (exocytosis) of GLUT4 trafficking. *Curr Opin Cell Biol* **19**, 466-473. Epub 2007 Jul 2017.
115. Brant, A. M., Jess, T. J., Milligan, G., Brown, C. M., and Gould, G. W. (1993) Immunological analysis of glucose transporters expressed in different regions of the rat brain and central nervous system. *Biochem Biophys Res Commun* **192**, 1297-1302
116. Timmers, K. I., Clark, A. E., Omatsu-Kanbe, M., Whiteheart, S. W., Bennett, M. K., Holman, G. D., and Cushman, S. W. (1996) Identification of SNAP receptors in rat adipose cell membrane fractions and in SNARE complexes co-immunoprecipitated with epitope-tagged N-ethylmaleimide-sensitive fusion protein. *Biochem J* **320**, 429-436
117. Yu, H., Rathore, S. S., Lopez, J. A., Davis, E. M., James, D. E., Martin, J. L., and Shen, J. (2013) Comparative studies of Munc18c and Munc18-1 reveal conserved and divergent mechanisms of Sec1/Munc18 proteins. *Proc Natl Acad Sci U S A* **110**, E3271-3280
118. Misura, K. M., Gonzalez, L. C., Jr., May, A. P., Scheller, R. H., and Weis, W. I. (2001) Crystal structure and biophysical properties of a complex between the N-terminal SNARE region of SNAP25 and syntaxin 1a. *J Biol Chem* **276**, 41301-41309
119. Sadoul, K., Lang, J., Montecucco, C., Weller, U., Regazzi, R., Catsicas, S., Wollheim, C. B., and Halban, P. A. (1995) SNAP-25 is expressed in islets of Langerhans and is involved in insulin release. *J Cell Biol* **128**, 1019-1028
120. Ravichandran, V., Chawla, A., and Roche, P. A. (1996) Identification of a novel syntaxin- and synaptobrevin/VAMP-binding protein, SNAP-23, expressed in non-neuronal tissues. *J Biol Chem* **271**, 13300-13303
121. Kawanishi, M., Tamori, Y., Okazawa, H., Araki, S., Shinoda, H., and Kasuga, M. (2000) Role of SNAP23 in insulin-induced translocation of GLUT4 in 3T3-L1 adipocytes. Mediation of complex formation between syntaxin4 and VAMP2. *J Biol Chem* **275**, 8240-8247
122. Sadoul, K., Berger, A., Niemann, H., Weller, U., Roche, P. A., Klip, A., Trimble, W. S., Regazzi, R., Catsicas, S., and Halban, P. A. (1997) SNAP-23 is not cleaved by botulinum neurotoxin E and can replace SNAP-25 in the process of insulin secretion. *J Biol Chem* **272**, 33023-33027
123. Washbourne, P., Thompson, P. M., Carta, M., Costa, E. T., Mathews, J. R., Lopez-Bendito, G., Molnar, Z., Becher, M. W., Valenzuela, C. F., Partridge, L. D., and Wilson, M. C. (2002) Genetic ablation of the t-SNARE SNAP-25 distinguishes mechanisms of neuroexocytosis. *Nat Neurosci* **5**, 19-26
124. Nagamatsu, S., Nakamichi, Y., Watanabe, T., Matsushima, S., Yamaguchi, S., Ni, J., Itagaki, E., and Ishida, H. (2001) Localization of cellubrevin-related peptide, endobrevin, in the early endosome in pancreatic beta cells and its physiological function in exo-endocytosis of secretory granules. *J Cell Sci* **114**, 219-227
125. Rossetto, O., Gorza, L., Schiavo, G., Schiavo, N., Scheller, R. H., and Montecucco, C. (1996) VAMP/synaptobrevin isoforms 1 and 2 are widely and differentially expressed in nonneuronal tissues. *J Cell Biol* **132**, 167-179.

126. Yang, C., Mora, S., Ryder, J. W., Coker, K. J., Hansen, P., Allen, L. A., and Pessin, J. E. (2001) VAMP3 null mice display normal constitutive, insulin- and exercise-regulated vesicle trafficking. *Mol Cell Biol* **21**, 1573-1580.
127. Zhu, D., Zhang, Y., Lam, P. P., Dolai, S., Liu, Y., Cai, E. P., Choi, D., Schroer, S. A., Kang, Y., Allister, E. M., Qin, T., Wheeler, M. B., Wang, C. C., Hong, W. J., Woo, M., and Gaisano, H. Y. (2012) Dual role of VAMP8 in regulating insulin exocytosis and islet beta cell growth. *Cell Metab* **16**, 238-249
128. Katagiri, H., Terasaki, J., Murata, T., Ishihara, H., Ogihara, T., Inukai, K., Fukushima, Y., Anai, M., Kikuchi, M., Miyazaki, J., Yazaki, Y., and Oka, Y. (1995) A novel isoform of syntaxin-binding protein homologous to yeast Sec1 expressed ubiquitously in mammalian cells. *J Biol Chem* **270**, 4963-4966
129. Garcia, E. P., Gatti, E., Butler, M., Burton, J., and De Camilli, P. (1994) A rat brain Sec1 homologue related to Rop and UNC18 interacts with syntaxin. *Proc Natl Acad Sci USA* **91**, 2003-2007
130. Roccisana, J., Sadler, J. B., Bryant, N. J., and Gould, G. W. (2013) Sorting of GLUT4 into its insulin-sensitive store requires the Sec1/Munc18 protein mVps45. *Mol Biol Cell* **24**, 2389-2397
131. Shanks, S. G., Carpp, L. N., Struthers, M. S., McCann, R. K., and Bryant, N. J. (2012) The Sec1/Munc18 protein Vps45 regulates cellular levels of its SNARE binding partners Tlg2 and Snc2 in *Saccharomyces cerevisiae*. *PLoS One* **7**, e49628
132. Graham, S. C., Wartosch, L., Gray, S. R., Scourfield, E. J., Deane, J. E., Luzio, J. P., and Owen, D. J. (2013) Structural basis of Vps33A recruitment to the human HOPS complex by Vps16. *Proc Natl Acad Sci U S A* **110**, 13345-13350
133. Fujita, Y., Sasaki, T., Fukui, K., Kotani, H., Kimura, T., Hata, Y., Sudhof, T. C., Scheller, R. H., and Takai, Y. (1996) Phosphorylation of Munc-18/n-Sec1/rbSec1 by protein kinase C: its implication in regulating the interaction of Munc-18/n-Sec1/rbSec1 with syntaxin. *J Biol Chem* **271**, 7265-7268
134. Hata, Y., Slaughter, C. A., and Sudhof, T. C. (1993) Synaptic vesicle fusion complex contains unc-18 homologue bound to syntaxin. *Nature* **366**, 347-351
135. Verhage, M., Maia, A. S., Plomp, J. J., Brussaard, A. B., Heeroma, J. H., Vermeer, H., Toonen, R. F., Hammer, R. E., van den Berg, T. K., Missler, M., Geuze, H. J., and Sudhof, T. C. (2000) Synaptic assembly of the brain in the absence of neurotransmitter secretion. *Science* **287**, 864-869.
136. Oh, E., Kalwat, M. A., Kim, M. J., Verhage, M., and Thurmond, D. C. (2012) Munc18-1 regulates first-phase insulin release by promoting granule docking to multiple syntaxin isoforms. *J Biol Chem* **287**, 25821-25833
137. Dulubova, I., Yamaguchi, T., Wang, Y., Sudhof, T. C., and Rizo, J. (2001) Vam3p structure reveals conserved and divergent properties of syntaxins. *Nat Struct Biol* **8**, 258-264
138. Han, G. A., Bin, N. R., Kang, S. Y., Han, L., and Sugita, S. (2013) Domain 3a of Munc18-1 plays a crucial role at the priming stage of exocytosis. *J Cell Sci* **126**, 2361-2371
139. Dulubova, I., Sugita, S., Hill, S., Hosaka, M., Fernandez, I., Sudhof, T. C., and Rizo, J. (1999) A conformational switch in syntaxin during exocytosis: role of munc18. *Embo J* **18**, 4372-4382
140. Dulubova, I., Yamaguchi, T., Arac, D., Li, H., Huryeva, I., Min, S. W., Rizo, J., and Sudhof, T. C. (2003) Convergence and divergence in the mechanism of SNARE binding by Sec1/Munc18-like proteins. *Proc Natl Acad Sci U S A* **100**, 32-37

141. Bar-On, D., Nachliel, E., Gutman, M., and Ashery, U. (2011) Dynamic conformational changes in munc18 prevent syntaxin binding. *PLoS Comput Biol* **7**, e1001097
142. Fletcher, A. I., Shuang, R., Giovannucci, D. R., Zhang, L., Bittner, M. A., and Stuenkel, E. L. (1999) Regulation of exocytosis by cyclin-dependent kinase 5 via phosphorylation of Munc18. *J Biol Chem* **274**, 4027-4035
143. Park, J. H., Jung, M. S., Kim, Y. S., Song, W. J., and Chung, S. H. (2012) Phosphorylation of Munc18-1 by Dyrk1A regulates its interaction with Syntaxin 1 and X11alpha. *J Neurochem* **122**, 1081-1091
144. Yamaguchi, T., Dulubova, I., Min, S. W., Chen, X., Rizo, J., and Sudhof, T. C. (2002) Sly1 binds to Golgi and ER syntaxins via a conserved N-terminal peptide motif. *Dev Cell* **2**, 295-305
145. Dulubova, I., Khvotchev, M., Liu, S., Huryeva, I., Sudhof, T. C., and Rizo, J. (2007) Munc18-1 binds directly to the neuronal SNARE complex. *Proc Natl Acad Sci U S A* **104**, 2697-2702
146. Tellam, J. T., Macaulay, S. L., McIntosh, S., Hewish, D. R., Ward, C. W., and James, D. E. (1997) Characterization of Munc-18c and syntaxin-4 in 3T3-L1 adipocytes. Putative role in insulin-dependent movement of GLUT-4. *J Biol Chem* **272**, 6179-6186
147. Thurmond, D. C., Kanzaki, M., Khan, A. H., and Pessin, J. E. (2000) Munc18c function is required for insulin-stimulated plasma membrane fusion of GLUT4 and insulin-responsive amino peptidase storage vesicles. *Mol Cell Biol* **20**, 379-388
148. Jewell, J. L., Oh, E., Bennett, S. M., Meroueh, S. O., and Thurmond, D. C. (2008) The tyrosine phosphorylation of Munc18c induces a switch in binding specificity from syntaxin 4 to Doc2beta. *J Biol Chem* **283**, 21734-21746.
149. Latham, C. F., Lopez, J. A., Hu, S. H., Gee, C. L., Westbury, E., Blair, D. H., Armishaw, C. J., Alewood, P. F., Bryant, N. J., James, D. E., and Martin, J. L. (2006) Molecular dissection of the Munc18c/syntaxin4 interaction: implications for regulation of membrane trafficking. *Traffic* **7**, 1408-1419
150. Christie, M. P., Whitten, A. E., King, G. J., Hu, S. H., Jarrott, R. J., Chen, K. E., Duff, A. P., Callow, P., Collins, B. M., James, D. E., and Martin, J. L. (2012) Low-resolution solution structures of Munc18:Syntaxin protein complexes indicate an open binding mode driven by the Syntaxin N-peptide. *Proc Natl Acad Sci U S A* **109**, 9816-9821
151. Oh, E., Spurlin, B. A., Pessin, J. E., and Thurmond, D. C. (2005) Munc18c heterozygous knockout mice display increased susceptibility for severe glucose intolerance. *Diabetes* **54**, 638-647.
152. Spurlin, B. A., Thomas, R. M., Nevins, A. K., Kim, H. J., Kim, Y. J., Noh, H. L., Shulman, G. I., Kim, J. K., and Thurmond, D. C. (2003) Insulin resistance in tetracycline-repressible Munc18c transgenic mice. *Diabetes* **52**, 1910-1917.
153. Cheatham, B. (2000) GLUT4 and company: SNAREing roles in insulin-regulated glucose uptake. *Trends Endocrinol Metab* **11**, 356-361
154. Oh, E., and Thurmond, D. C. (2006) The stimulus-induced tyrosine phosphorylation of Munc18c facilitates vesicle exocytosis. *J Biol Chem* **281**, 17624-17634. Epub 12006 Apr 17625.
155. Bakke, J., Bettaieb, A., Nagata, N., Matsuo, K., and Haj, F. G. (2013) Regulation of the SNARE-interacting protein Munc18c tyrosine phosphorylation in adipocytes by protein-tyrosine phosphatase 1B. *Cell Commun Signal* **11**, 57

156. Li, W., Ma, C., Guan, R., Xu, Y., Tomchick, D. R., and Rizo, J. (2011) The crystal structure of a Munc13 C-terminal module exhibits a remarkable similarity to vesicle tethering factors. *Structure* **19**, 1443-1455
157. Sheu, L., Pasyk, E. A., Ji, J., Huang, X., Gao, X., Varoqueaux, F., Brose, N., and Gaisano, H. Y. (2003) Regulation of insulin exocytosis by Munc13-1. *J Biol Chem* **278**, 27556-27563. Epub 22003 May 27513.
158. Brose, N., Hofmann, K., Hata, Y., and Sudhof, T. C. (1995) Mammalian homologues of *Caenorhabditis elegans* unc-13 gene define novel family of C2-domain proteins. *J Biol Chem* **270**, 25273-25280
159. Kwan, E. P., Xie, L., Sheu, L., Nolan, C. J., Prentki, M., Betz, A., Brose, N., and Gaisano, H. Y. (2006) Munc13-1 deficiency reduces insulin secretion and causes abnormal glucose tolerance. *Diabetes* **55**, 1421-1429
160. Boswell, K. L., James, D. J., Esquibel, J. M., Bruinsma, S., Shirakawa, R., Horiuchi, H., and Martin, T. F. (2012) Munc13-4 reconstitutes calcium-dependent SNARE-mediated membrane fusion. *J Cell Biol* **197**, 301-312
161. Ren, Q., Wimmer, C., Chicka, M. C., Ye, S., Ren, Y., Hughson, F. M., and Whiteheart, S. W. (2010) Munc13-4 is a limiting factor in the pathway required for platelet granule release and hemostasis. *Blood* **116**, 869-877
162. Sakaguchi, G., Orita, S., Maeda, M., Igarashi, H., and Takai, Y. (1995) Molecular cloning of an isoform of Doc2 having two C2-like domains. *Biochem Biophys Res Commun* **217**, 1053-1061
163. Kojima, T., Fukuda, M., Aruga, J., and Mikoshiba, K. (1996) Calcium-dependent phospholipid binding to the C2A domain of a ubiquitous form of double C2 protein (Doc2 beta). *J Biochem* **120**, 671-676
164. Verhage, M., de Vries, K. J., Roshol, H., Burbach, J. P., Gispen, W. H., and Sudhof, T. C. (1997) DOC2 proteins in rat brain: complementary distribution and proposed function as vesicular adapter proteins in early stages of secretion. *Neuron* **18**, 453-461
165. Ke, B., Oh, E., and Thurmond, D. C. (2007) Doc2beta is a novel Munc18c-interacting partner and positive effector of syntaxin 4-mediated exocytosis. *J Biol Chem* **282**, 21786-21797.
166. Fukuda, M., and Mikoshiba, K. (2000) Doc2gamma, a third isoform of double C2 protein, lacking calcium-dependent phospholipid binding activity. *Biochem Biophys Res Commun* **276**, 626-632
167. Groffen, A. J., Friedrich, R., Brian, E. C., Ashery, U., and Verhage, M. (2006) DOC2A and DOC2B are sensors for neuronal activity with unique calcium-dependent and kinetic properties. *J Neurochem* **97**, 818-833
168. Fukuda, N., Emoto, M., Nakamori, Y., Taguchi, A., Miyamoto, S., Uraki, S., Oka, Y., and Tanizawa, Y. (2009) DOC2B: a novel syntaxin-4 binding protein mediating insulin-regulated GLUT4 vesicle fusion in adipocytes. *Diabetes* **58**, 377-384. Epub 2008 Nov 2025.
169. Groffen, A. J., Brian, E. C., Dudok, J. J., Kampmeijer, J., Toonen, R. F., and Verhage, M. (2004) Ca(2+)-induced recruitment of the secretory vesicle protein DOC2B to the target membrane. *J Biol Chem* **279**, 23740-23747. Epub 22004 Mar 23721.
170. Pang, Z. P., Baca, T., Yang, X., Zhou, P., Xu, W., and Sudhof, T. C. (2011) Doc2 supports spontaneous synaptic transmission by a Ca(2+)-independent mechanism. *Neuron* **70**, 244-251



171. Miyazaki, M., Emoto, M., Fukuda, N., Hatanaka, M., Taguchi, A., Miyamoto, S., and Tanizawa, Y. (2009) DOC2b is a SNARE regulator of glucose-stimulated delayed insulin secretion. *Biochem Biophys Res Commun* **384**, 461-465. Epub 2009 May 2003.
172. Thurmond, D. C., Ceresa, B. P., Okada, S., Elmendorf, J. S., Coker, K., and Pessin, J. E. (1998) Regulation of insulin-stimulated GLUT4 translocation by munc18c in 3T3L1 adipocytes. *J Biol Chem* **273**, 33876-33883
173. Wiseman, D. A., Kalwat, M. A., and Thurmond, D. C. (2011) Stimulus-induced S-nitrosylation of syntaxin 4 impacts insulin granule exocytosis. *J Biol Chem* **286**, 16344-16354
174. Groffen, A. J., Martens, S., Diez Arazola, R., Cornelisse, L. N., Lozovaya, N., de Jong, A. P., Goriounova, N. A., Habets, R. L., Takai, Y., Borst, J. G., Brose, N., McMahon, H. T., and Verhage, M. (2010) Doc2b is a high-affinity Ca<sup>2+</sup> sensor for spontaneous neurotransmitter release. *Science* **327**, 1614-1618
175. Schultze, N., Burki, Y., Lang, Y., Certa, U., and Bluethmann, H. (1996) Efficient control of gene expression by single step integration of the tetracycline system in transgenic mice. *Nat Biotechnol* **14**, 499-503
176. Zhou, M., Sevilla, L., Vallega, G., Chen, P., Palacin, M., Zorzano, A., Pilch, P. F., and Kandror, K. V. (1998) Insulin-dependent protein trafficking in skeletal muscle cells. *Am J Physiol* **275**, E187-E196
177. Brozinick, J. T., Jr., McCoid, S. C., Reynolds, T. H., Nardone, N. A., Hargrove, D. M., Stevenson, R. W., Cushman, S. W., and Gibbs, E. M. (2001) GLUT4 overexpression in db/db mice dose-dependently ameliorates diabetes but is not a lifelong cure. *Diabetes* **50**, 593-600
178. Oh, E., and Thurmond, D. C. (2009) Munc18c Depletion Selectively Impairs the Sustained Phase of Insulin Release. *Diabetes* **58**, 1165-1174
179. Thurmond, D. C., Gonelle-Gispert, C., Furukawa, M., Halban, P. A., and Pessin, J. E. (2003) Glucose-Stimulated Insulin Secretion Is Coupled to the Interaction of Actin with the t-SNARE (Target Membrane Soluble N-Ethylmaleimide-Sensitive Factor Attachment Protein Receptor Protein) Complex. *Mol Endocrinol* **17**, 732-742
180. Walker, P. S., Ramlal, T., Sarabia, V., Koivisto, U. M., Bilan, P. J., Pessin, J. E., and Klip, A. (1990) Glucose transport activity in L6 muscle cells is regulated by the coordinate control of subcellular glucose transporter distribution, biosynthesis, and mRNA transcription. *J Biol Chem* **265**, 1516-1523
181. Toonen, R. F., and Verhage, M. (2007) Munc18-1 in secretion: lonely Munc joins SNARE team and takes control. *Trends Neurosci* **30**, 564-572
182. Lang, T., and Jahn, R. (2008) Core proteins of the secretory machinery. *Handb Exp Pharmacol*, 107-127
183. Umahara, M., Okada, S., Yamada, E., Saito, T., Ohshima, K., Hashimoto, K., Yamada, M., Shimizu, H., Pessin, J. E., and Mori, M. (2008) Tyrosine phosphorylation of Munc18c regulates platelet-derived growth factor-stimulated glucose transporter 4 translocation in 3T3L1 adipocytes. *Endocrinology* **149**, 40-49. Epub 2007 Oct 2004.
184. Keller, M. P., Choi, Y., Wang, P., Davis, D. B., Rabaglia, M. E., Oler, A. T., Stapleton, D. S., Argmann, C., Schueler, K. L., Edwards, S., Steinberg, H. A., Chaibub Neto, E., Kleinhanz, R., Turner, S., Hellerstein, M. K., Schadt, E. E., Yandell, B. S., Kendziorski, C., and Attie, A. D. (2008) A gene expression network model of type 2 diabetes links cell cycle regulation in islets with diabetes susceptibility. *Genome Res* **18**, 706-716

185. Foster, L. J., and Klip, A. (2000) Mechanism and regulation of GLUT-4 vesicle fusion in muscle and fat cells. *Am J Physiol Cell Physiol* **279**, C877-890.
186. Mandic, S. A., Skelin, M., Johansson, J. U., Rupnik, M. S., Berggren, P. O., and Bark, C. (2011) Munc18-1 and Munc18-2 proteins modulate beta-cell Ca<sup>2+</sup> sensitivity and kinetics of insulin exocytosis differently. *J Biol Chem* **286**, 28026-28040
187. Ramalingam, L., Oh, E., Yoder, S. M., Brozinick, J. T., Kalwat, M. A., Groffen, A. J., Verhage, M., and Thurmond, D. C. (2012) Doc2b Is a Key Effector of Insulin Secretion and Skeletal Muscle Insulin Sensitivity. *Diabetes* **61**, 2424-2432
188. Ferrannini, E., Simonson, D. C., Katz, L. D., Reichard, G., Jr., Bevilacqua, S., Barrett, E. J., Olsson, M., and DeFronzo, R. A. (1988) The disposal of an oral glucose load in patients with non-insulin-dependent diabetes. *Metabolism* **37**, 79-85
189. Wang, Q., Khayat, Z., Kishi, K., Ebina, Y., and Klip, A. (1998) GLUT4 translocation by insulin in intact muscle cells: detection by a fast and quantitative assay. *FEBS Lett* **427**, 193-197
190. Edgerton, D. S., Lautz, M., Scott, M., Everett, C. A., Stettler, K. M., Neal, D. W., Chu, C. A., and Cherrington, A. D. (2006) Insulin's direct effects on the liver dominate the control of hepatic glucose production. *J Clin Invest* **116**, 521-527
191. Yu, H., Rathore, S. S., Davis, E. M., Ouyang, Y., and Shen, J. (2013) Doc2b promotes GLUT4 exocytosis by activating the SNARE-mediated fusion reaction in a calcium- and membrane bending-dependent manner. *Mol Biol Cell* **24**, 1176-1184
192. Orita, S., Sasaki, T., Komuro, R., Sakaguchi, G., Maeda, M., Igarashi, H., and Takai, Y. (1996) Doc2 enhances Ca<sup>2+</sup>-dependent exocytosis from PC12 cells. *J Biol Chem* **271**, 7257-7260
193. Chen, G., Liu, P., Thurmond, D. C., and Elmendorf, J. S. (2003) Glucosamine-induced insulin resistance is coupled to O-linked glycosylation of Munc18c. *FEBS Lett* **534**, 54-60
194. Lam, P. P., Ohno, M., Dolai, S., He, Y., Qin, T., Liang, T., Zhu, D., Kang, Y., Liu, Y., Kauppi, M., Xie, L., Wan, W. C., Bin, N. R., Sugita, S., Olkkonen, V. M., Takahashi, N., Kasai, H., and Gaisano, H. Y. (2013) Munc18b is a major mediator of insulin exocytosis in rat pancreatic beta-cells. *Diabetes* **62**, 2416-2428
195. Lovis, P., Gattesco, S., and Regazzi, R. (2008) Regulation of the expression of components of the exocytotic machinery of insulin-secreting cells by microRNAs. *Biol Chem* **389**, 305-312
196. Bagge, A., Dahmcke, C. M., and Dalgaard, L. T. (2013) Syntaxin-1a is a direct target of miR-29a in insulin-producing beta-cells. *Horm Metab Res* **45**, 463-466

## CURRICULUM VITAE

**Latha Ramalingam**

### EDUCATION

- PhD** Indiana University, Indianapolis IN 2008-2014  
Department of Biochemistry and Molecular Biology  
Project: Regulation of glucose homeostasis by Doc2b and SM proteins  
Mentor: Dr. Debbie Thurmond  
GPA: 3.7/4.00
- MTech** Vellore Institute of Technology, Vellore, India 2005-2007  
School of Biotechnology  
  
GPA: 9.30/10.0
- B.Pharm** Sri Ramachandra Medical College, Chennai, India 2001-2005  
School of Pharmacy  
GPA: 7.42/10

### RESEARCH EXPERIENCE

- Doctoral Research** 2009-2014t  
Indiana University, Indianapolis, IN  
Advisor: Dr. Debbie C Thurmond
- Currently investigating molecular mechanisms underlying regulation of insulin secretion and insulin action by Doc2b and SNARE proteins using pancreatic beta cells, muscle cells and in vivo mouse models.
- Graduate Research** 2006-2007  
Vellore Institute of Technology, Vellore, India  
Mentor: Dr. Asit Ranjan Ghosh.
- Development of a DGAT assay to screen drugs for metabolic syndrome
- Undergraduate Research** 2005  
Sri Ramachandra Medical College, Chennai, India  
Advisor: Dr. Chitra
- Reverse phase HPLC for estimation of haemostatic agents Ethamsylate and Tranexamic acid

## **FUNDING, AWARDS and FELLOWSHIPS**

Peggy Gibson Award	2012
American Heart Association Predoctoral Fellowship	2012 to 2014
Sigma Xi, second place, Graduate Student Research Competition	2011
Graduate Student Office Travel Fellowship	2008
University Fellowship, Indiana University School of Medicine	2008
University Fellowship, Vellore Institute of Technology	2006

## **PUBLICATIONS**

- Jewell JL, Oh E, **Ramalingam L**, Kalwat MA, Tagliabracci VS, Tackett L, Elmendorf JS, Thurmond DC. Munc18c phosphorylation by the insulin receptor links cell signaling directly to SNARE exocytosis. *J Cell Biol.* 2011 Apr 4;193(1):185-99
- **Ramalingam L**, Oh E, Yoder SM, Kalwat MA, Verhage M, Groffen AJ, Thurmond DC. Doc2b is a key effector of insulin secretion and skeletal muscle insulin sensitivity. *Diabetes.* 2012 Oct;61(10):2424-32.
- **Ramalingam L**, Oh E, Thurmond DC. Multifunctional roles of insulin receptor. *Cell Mol Life Sci.* 2012 Oct 10
- **Ramalingam L**, Oh E, Thurmond DC. Enhanced Insulin sensitivity, insulin secretion in Doc2b Tg mice. 2013 (in revision).
- **Ramalingam L**, Lu J, Thurmond DC. Doc2b role in SNARE scaffold. (in preparation)

## **PRESENTED ABSTRACTS**

- **Ramalingam L**, Oh E, Verhage M, Groffen AJ, Thurmond DC. “Impaired glucose tolerance, insulin sensitivity and biphasic insulin release in Doc2b knockout mice.” American Diabetes Association, 71<sup>st</sup> Annual Scientific Sessions 2011. *Selected for Guided Audio Tour*
- **Ramalingam L**, Jewell JL, Thurmond DC “Regulation of O-linked Glycosylation of Munc18c in beta cells.” Biochemistry Retreat, Indianapolis, IN 2010.

- **Ramalingam L,** Rajan C. “Reverse phase HPLC for estimation of hemostatic agents Ethamsylate and Tranexamic acid.” 47<sup>th</sup> Indian Pharmaceutical Congress, India, 2005.
- **Ramalingam L,** Chamundeshwari D. “Determination of toxicity of an Ayurvedic liver tonic -Heparsil.” 46<sup>th</sup> Indian Pharmaceutical Congress, India, 2004.